

INVESTIGATING THE STRUCTURAL AND MECHANISTIC PARAMETERS
OF TWO RADICAL SAM ENZYMES, SPORE PHOTOPRODUCT
LYASE AND HYDE

by

Shourjo Ghose

A dissertation submitted in partial fulfillment
of the requirements for the degree

of

Doctor of Philosophy

in

Biochemistry

MONTANA STATE UNIVERSITY
Bozeman, Montana

May 2013

©COPYRIGHT

by

Shourjo Ghose

2013

All Rights Reserved

APPROVAL

of a dissertation submitted by

Shourjo Ghose

This dissertation has been read by each member of the dissertation committee and has been found to be satisfactory regarding content, English usage, format, citation, bibliographic style, and consistency and is ready for submission to The Graduate School.

Dr. Joan B. Broderick

Approved for the Department of Chemistry and Biochemistry

Dr. Mary J. Cloninger

Approved for The Graduate School

Dr. Ronald W. Larsen

STATEMENT OF PERMISSION TO USE

In presenting this dissertation in partial fulfillment of the requirements for a doctoral degree at Montana State University, I agree that the Library shall make it available to borrowers under rules of the Library. I further agree that copying of this dissertation is allowable only for scholarly purposes, consistent with “fair use” as prescribed in the U.S. Copyright Law. Requests for extensive copying or reproduction of this dissertation should be referred to ProQuest Information and Learning, 300 North Zeeb Road, Ann Arbor, Michigan 48106, to whom I have granted “the right to reproduce and distribute my dissertation in and from microform along with the non-exclusive right to reproduce and distribute my abstract in any format in whole or in part.”

Shourjo Ghose

May 2013

DEDICATION

This work is dedicated to my dearest wife Neelambari Joshi and my parents, whose support in times tough has guided me through this adventure. I also wish to dedicate this work to all those teachers in high school who persevered and nurtured within me that innate curiosity of a child and kept alive the flame of inquisitiveness which has proven to be invaluable in earning this PhD.

ACKNOWLEDGEMENTS

I would like to express my gratitude to my advisor Dr. Joan Broderick, who has guided me throughout my graduate career. She has indeed been a source of inspiration and wisdom in all matters scientific or otherwise.

I would also like to acknowledge my graduate committee members, Dr. John Peters, Dr. Brian Bothner, Dr. Martin Teintze, Dr. Edward Dratz , and Dr. Kristin Ruppel. I would like to thank Dr. Brain Bothner for providing me the opportunity to work as a technician in the Mass spectrometry and proteomics facility, which proved to be invaluable in achieving the results summarized in this dissertation. Additionally, I would like to thank Dr. Jonathan Hilmer for mentoring me at the facility and providing me incredible insight in the use of LCMS in biochemistry.

I would like to thank Dr. Tilak Chandra, Dr. Sunshine Silver and Dr. Egidijus Zilinskas for their help and insight in getting started on the SPL project. I would like to give my thanks to Dr. Eric Shepard for our long discourses regarding the hydrogenase project and life in Montana in general. Finally I would like to thank all my colleagues at the Broderick laboratory who have helped me realize my dreams and help me maximize my potential: Kaitlin Duschene, Amanda Byer, Rachel Udelhoven, Nicholas Boswell, Adam Crain, Krista Schisler, Benjamin Duffus, Jeremiah Betz.

TABLE OF CONTENTS

1. INTRODUCTION	1
Iron Sulfur Clusters in Proteins.....	1
Radical SAM Superfamily of Enzymes	4
Mechanistic Insights into Radical SAM Enzymes.....	5
Structural Insights into Radical SAM Enzymes	8
Spore Photoproduct Lyase	10
DNA Damage and Repair	12
Bacterial Spores and the Role of Small Acid Soluble Proteins	14
SP Formation <i>in vivo</i> and <i>in vitro</i>	16
Mechanism of SP Repair by Spore Photoproduct Lyase	18
Binding Interactions between SP and SPL	23
Structural Insights into SPL Mechanism	24
[FeFe]-Hydrogenase	29
H-Cluster Maturation in [FeFe]-Hydrogenase	30
Maturation Enzyme HydE	34
Research Objectives.....	37
2. SOLUTION PHASE DYNAMICS OF THE DNA REPAIR ENZYME SPORE PHOTOPRODUCT LYASE AS PROBED BY H/D EXCHANGE.....	54
Contribution of Authors	54
Manuscript Information	55
Introduction	56
Materials and Methods.....	61
Protein Expression and Purification.....	61
Preparation of Enzyme/Ligand Mixtures.....	62
H/D Exchange Reactions	63
LC-ESI/MS with MicroTOF Mass Spectrometer	63
Analysis of H/D Exchange Data	65
Results.....	66
H/D Exchange into SPL Alone	66
Effect of Substrate on H/D Exchange	67
Discussion	69
Summary and Conclusions	78
3. IDENTIFICATION AND QUANTITATION OF A PUTATIVE SUBSTRATE FOR [FeFe]-HYDROGENASE MATURASE ENZYME HydE.....	85
Contribution of Authors	85
Manuscript Information	86

TABLE OF CONTENTS - CONTINUED

Introduction	87
Experimental Procedures	90
Protein Expression, Purification, and Reconstitution	90
EPR Sample Preparation and Spectroscopic Analysis.....	92
HydE Screening Assays.....	94
LCMS HydE Activity Assays.....	95
LC-ESI/MS with Q-TOF Mass Spectrometer.....	96
Results.....	98
Spectroscopic Characterization of HydE.....	98
Effect of Possible Substrates on Rates of HydE-Catalyzed SAM Cleavage	101
LCMS Analysis of HydE Catalyzed Cysteine Consumption	101
EPR and LCMS Analysis of SAM Bound to Purified HydE.....	104
Discussion.....	106
 4. MECHANISTIC INSIGHTS INTO HydE CATALYSIS	 113
Contribution of Authors	113
Manuscript Information	114
Introduction.....	115
Materials and Methods.....	117
Protein Expression, Purification, and Reconstitution	117
High Performance Liquid Chromatography and Mass Spectrometry Conditions	122
Results.....	128
Analysis of HydE-mediated Deuterium Transfer from Cysteine to dAdo.....	122
Effects of HydFΔEG on 5'-dAdo Production and Cysteine Consumption.....	124
Discussion.....	127
 5. MECHANISTIC INVESTIGATION OF [FeFe]-HYDROGENASE MATURASE HydG.....	 131
Contribution of Authors	131
Manuscript Information	132
Introduction.....	133
Materials and Methods.....	136
Growth and Assay Conditions	136
High Performance Liquid Chromatography and Mass Spectrometry Conditions	136
Results and Discussion	138

TABLE OF CONTENTS - CONTINUED

Conclusions.....	147
6. GENERAL CONCLUSIONS AND FUTURE DIRECTIONS.....	149
REFERENCE CITED	157
APPENDIX A: Supplemental Information for Chapter 3	174

LIST OF TABLES

Table	Page
2.1: Mass changes in SPL as a result of H/D exchange upon diluting in D2O	70
4.1: Comparison of the ratios of 5'-dAdo isotopic distribution on assays performed in the presence of HydE only	124
4.2: Comparison of the ratios of 5'-dAdo isotopic distribution on assays performed in the presence of HydE and HydF Δ EG	126
5.1: dAdo Deuterium Distribution with Intact HydG	142
5.2: dAdo Deuterium Distribution with C-terminal Truncated HydG in tris-D2O	143

LIST OF FIGURES

Figure	Page
1.1. The most common iron sulfur clusters in nature	2
1.2. General mechanism of catalysis of radical SAM enzymes	5
1.3. The Radical SAM enzyme superfamily	7
1.4. Partial TIM barrel structure of radical SAM enzyme	9
1.5. SPL catalyzed repair of SP	11
1.6. DNA lesions upon UV-Irradiation.....	17
1.7. Mechanism for the formation of SP.....	26
1.8 Proposed mechanism for SP repair by SP lyase with SAM.....	19
1.9 (5R and 5S) synthetic spore photoproduct analogues.....	22
1.10 The reliance of nucleotide directionality	23
1.11 A superimposition of the purported base flipping out mechanism.....	27
1.12 The active site of Fe-Fe Hydrogenase	32
1.13 The proposed maturation scheme of Fe-Fe Hydrogenase active site.....	36
2.1 SPL catalyzed repair of SP	57
2.2 Change in mass of SPL upon dilution into D2O buffer	66
2.3 The influence of the effector molecules on SPL.....	68

LIST OF FIGURES CONTINUED

Figure	Page
2.4 Deuterium uptake of SPL.....	72
2.5 Crystal structure of SPL.....	73
3.1. The H-cluster of [FeFe]-hydrogenase	88
3.2. Low temperature (12 K) EPR spectra.....	99
3.3 Temperature dependence and power saturation behavior.....	100
3.4 Time-dependent concentration of cysteine	102
3.5 Correlation of the rate of 5'-dAdo production with cysteine consumption	104
3.6 Small Molecule Co-purification with Enzymes.....	105
4.1. Isotopic distribution of 5-dAdo.....	123
4.2 Cysteine concentration and 5'-deoxyadenosine concentration in	125
4.3 Isotopic ratios between the primary and secondary peaks of dAdo	126
5.1 Reaction Catalyzed by HydG.....	136
5.2 5'-deoxyadenosine mass spectra in H ₂ O	139
5.3. 5'-deoxyadenosine mass spectra in D ₂ O buffer	141
5.4.5'-deoxyadenosine product from C-terminal truncated HydG.....	143

ABSTRACT

The resistance of Bacterial spores to UV radiation makes them a causative agent in many diseases and poses a threat to humans and animals alike. This unique resistance stems from the repair of a thymine dimer, 5-thymine-5,6-dihydrothymine (spore photoproduct, or SP) on exposure to UV irradiation. During the early stages of germination, this SP is repaired by an enzyme, spore photoproduct lyase (SPL) into two thymines. SPL is a member of the radical SAM superfamily of enzymes and requires S-adenosylmethionine (SAM) and a [4Fe-4S]^{1+/2+} cluster to perform its catalysis. The first part of this dissertation is dedicated towards understanding the solution phase dynamics of this protein on binding with its substrate and co-factor via hydrogen deuterium exchange. Analyses of the effects of SAM binding to SPL indicate that the protein does go through a conformational change localized around its active site. We have also demonstrated that the concomitant binding of SAM and dinucleotide SP contributes more significantly to the active site stabilization than what is observed with just SAM binding. Moreover we have provided initial evidence that the SPL might be utilizing the deformation of the phosphodiester back bone of SP to recognize, bind and initiate catalysis. We have unequivocally demonstrated that the catalytic [4Fe-4S] cluster plays a significant role in substrate/cofactor binding most likely due to the stabilization of the 8 residue loop region it resides on. The second part of this dissertation is focused towards understanding the role of maturase proteins in the assembly of the active site of [FeFe]-hydrogenase. The assembly and biosynthesis of the H-cluster requires three accessory enzymes HydE, HydG and HydF. Herein show that HydE utilizes cysteine as a substrate. We have also shown through LCMS and specifically deuterium labeled substrate, that catalysis is initiated via a H atom abstraction from the β carbon of cysteine. Our investigations into the mechanism of HydG mediated turnover of tyrosine reveal that catalysis is initiated via a single H atom abstraction from the phenolic position of the substrate. Taken together we believe that our investigations have provided some critical insights into specific roles of these enzymes.

CHAPTER 1

INTRODUCTION

Iron- Sulfur Clusters in Proteins

Metal-binding proteins constitute nearly half of all proteins in nature and have been implicated in a diverse array of biological processes, such as respiration, molecular oxygen reduction, photosynthesis and nitrogen fixation (1-3). Metal cofactors comprised of iron and sulfide are thought to be some of the earliest prosthetic groups in nature(4, 5). These iron sulfur (Fe-S) clusters ensconced in the protein active sites were first identified via electron paramagnetic resonance studies (EPR) of mitochondrial membranes (6) and soluble ferredoxin proteins (7, 8). Subsequent studies using a multitude of techniques as diverse as UV-visible spectroscopy, X-ray crystallography and chemical synthesis of cluster analogs resulted in the discovery of proteins containing a single iron to more complex systems consisting up to eight iron ions (9-11). The most commonly observed Fe-S clusters include [2Fe-2S], [3Fe-4S] and [4Fe-4S] clusters and cysteinyl sulfur is by far the most commonly observed protein derived ligand (12). However, it is not unusual to find histidine, serine, or arginine coordination to Fe-S clusters (13) (Figure 1). (14). Proteins containing Fe-S clusters can range from 6 kDa up to 500 kDa in primary sequence (15) and have been found in all kinds of cells accomplishing some of the most important physiological functions (16, 17). The characterization these unique clusters have engendered the rapidly expanding field of biomimetic Fe-S chemistry, thereby providing us with profound insights into the

indispensability of the protein environment surrounding the clusters (12). Another fascinating aspect of Fe-S chemistry is their predicted involvement in the synthesis of pre-biotic organic molecules (18). Taking into consideration the geo-chemical and atmospheric conditions of early earth (19), it is entirely plausible that simple self-assembling Fe-S clusters could have been the workhorses which produced primitive macromolecules and peptides .

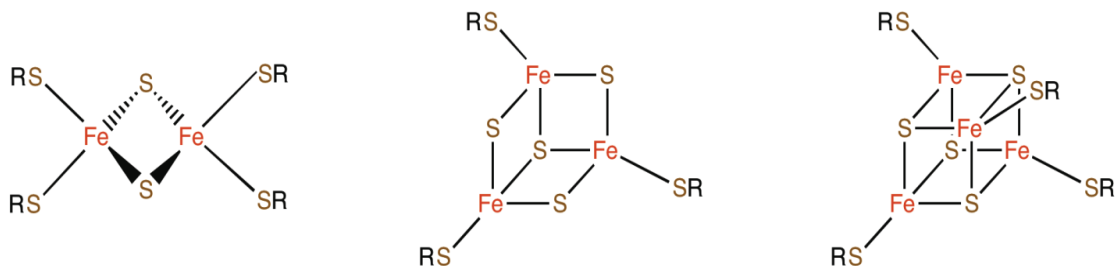


Fig1.1: The most common iron sulfur clusters found in nature are the [2Fe-2S],[3Fe-4S] and the [4Fe-4S].

Early on in the study of Fe-S cluster containing proteins, it was hypothesized that the singular role of these prosthetic groups was electron transfer. The exceptional intrinsic capability to delocalize electron density over both Fe and S ions allow Fe-S clusters to be the perfect candidate to mediate electron transfer reactions in biology (20, 21). The coordination environment of the Fe-S cluster dictates its range of redox potential and consequently the physiological role of the protein it's ensconced in. Indeed, depending on the coordination environment, Fe-S clusters can adopt redox potentials ranging from -500 mV to +400 mV. Such flexibility in redox potentials allows Fe-S containing proteins to serve a wide array of physiological functions (5). With the virtual explosion in the field

of metalloprotein biochemistry, we have started to broaden our horizons with respect to the diverse roles of Fe-S clusters beyond just electron transfer and structural stabilization. Interestingly, it has been shown that the 8Fe ferredoxins in *Clostridia* (22) serve as a repository of Fe as is the case in methanogenic archaea which contain 12 [4Fe-4S] clusters, all purportedly used for Fe storage. (23). Remarkably, DNA repair enzymes such as Endonuclease III possess redox inactive clusters which play an essential role in structuring a protein loop utilized for the recognition and repair of damaged DNA (24, 25). Moreover, metalloproteins containing Fe-S clusters have also been implicated in translation and transcriptional gene regulation (26). A singular example is the cytosolic iron responsive protein 1 (IRP1). In its iron replete form, IRP1 with its complement of [4Fe-4S] cluster functions as an aconitase, however under iron deprivation conditions it has been shown to bind to iron responsive elements in mRNA and control downstream iron homeostasis (27). Fe-S clusters have also been shown to be involved in controlling enzyme activity, typically acting in response to external stimuli. Two of the characteristic examples of such roles of Fe-S clusters are glutamine 5-phosphoribosyl-1-pyrophosphate (PRPP) amidotransferase in *Bacillus subtilis* (28) and mammalian ferrochelatases (29). The (PRPP amidotransferase enzyme is stabilized structurally in the presence of an intact [4Fe-4S] cluster, but the cluster is degraded in the presence of oxygen which subsequently results in the enzyme being proteolyzed (28). The ferrochelatase classes of enzymes contain [2Fe-2S] clusters essential for activity but are rapidly degraded in the presence NO. Interestingly the cluster is shown to be absent in the majority of the equivalent enzymes in bacteria thereby implying that the cluster might act as form of

defense mechanism that thwarts the infecting organism from using host synthesized heme. The role of Fe-S cluster containing proteins in catalyzing radical mediated reactions have been the focus of intense study for some time. A particular group iron and sulfur containing enzymes that utilize a site differentiated [4Fe-4S] cluster to catalyze radical based reactions are referred to as radical S-adenosylmethionine (SAM) superfamily of proteins.

Radical SAM Superfamily of Enzymes

The radical SAM protein superfamily of proteins are characterized by the use of a site-differentiated [4Fe-4S]^{2+/+} cluster and SAM to initiate diverse radical reactions in biology (30-33). The [4Fe-4S] cluster in these enzymes is bound by a conserved CX₃CX₂C cysteine motif, leaving one iron of the cluster not coordinated by the motif. SAM to promote cleavage of the S-C5' bond to generate a 5'-deoxyadenosyl radical intermediate (Figure 2). This 5'-dAdo radical intermediate, believed to be central to nearly all radical SAM reactions, then abstracts a hydrogen atom from a substrate molecule to initiate varied radical based reactions (Figure 3). The unique iron of the [4Fe-4S] cluster is coordinated by SAM via its carboxyl and amino moieties, and in the reduced state the cluster can transfer an electron to In most cases, SAM is utilized as a co-substrate with 5'-deoxyadenosine generated as a byproduct, however the enzymes lysine 2,3-aminomutase (LAM) and spore photoproduct lyase have been shown to use SAM as a cofactor (34-36). Radical SAM enzymes have been implicated in numerous biochemical reactions including the formation of protein based glycy radicals, sulfur

insertion, biosynthesis of complex cofactors, and repair of DNA to name just a few

(Figure 3)(30, 33)

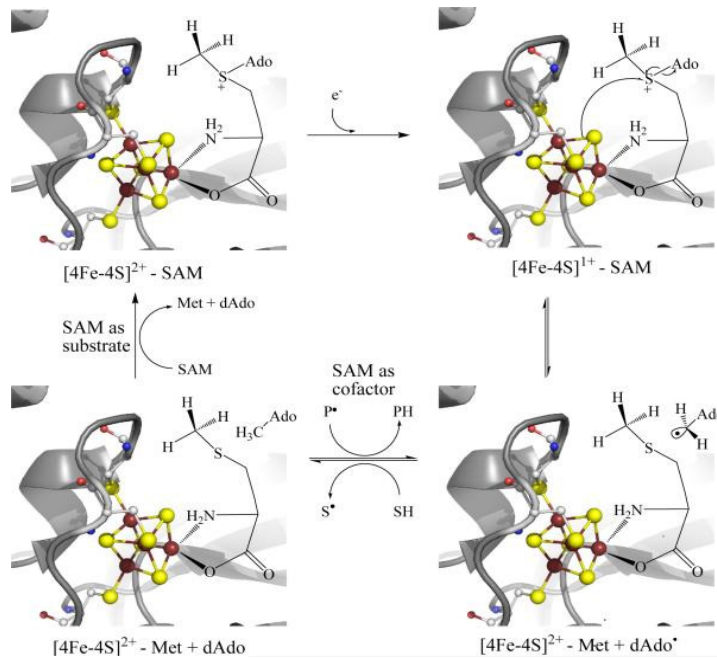


Figure 2: General mechanism of catalysis of radical SAM enzymes. Reaction commences with a single electron transfer to the sulfonium of SAM resulting in the cleavage of the S-C bond and formation of the d-Ado radical. The radical then abstracts an H atom from the substrate forming dAdo and a substrate radical. (this figure is obtained from reference 33)

Mechanistic Insights into Radical SAM Enzymes

The central feature of all members of the radical SAM superfamily is the presence of a redox active [4Fe-4S] cluster (30). The function of this cluster is two-fold with its preliminary role as a binding site for SAM via its unique iron site(37, 38) followed more critically by its function as an electron donor to the sulfonium center of SAM via an inner sphere electron transfer mechanism (39). Initial insights into the interactions of SAM

with the [4Fe-4S] cluster were obtained via X-ray absorption spectroscopic (XAS) studies of LAM. Utilizing cofactors seleno-SAM (*Se*-SAM) and analogous selenomethionine (*Se*-Met), it was shown that SAM directly interacts with the catalytic cluster with a distance of 2.7 Å between the Se and Fe ion (40). Additional studies utilizing electron nuclear double resonance (ENDOR) spectroscopy of pyruvate formate activating enzyme (PFL-AE), as well as LAM, demonstrated a bidentate coordination environment of the unique iron by the amino and carboxyl moieties of the methionine component of SAM (37). This distinctive coordination has been further confirmed via several high resolution crystal structures from this superfamily that reveal that SAM is held in position through various interactions between active site amino acids and the SAM molecule itself (see below) (38-41). Following the reduction of the cluster to the catalytically active [4Fe-4S]⁺ state, it is proposed that a single electron is transferred via inner sphere electron transfer to SAM resulting in the homolytic cleavage of the S-C5' bond. This the most commonly observed cleavage mechanism for members of this superfamily and leads to the formation of the highly reactive 5' deoxyadenosyl radical (d-Ado•) and methionine (42). Successively, the d-Ado• radical abstracts a H atom from the substrate forming d-Ado and a substrate radical which is then subsequently involved in a wide array of reactions. Thereafter, the mechanism employed by these enzymes diverges, dividing this family into two classes(43). In one class the product radical formed in an earlier step re-abstracts a H atom from d-Ado, thus reforming the d-Ado• species which can then recombine with methionine reforming SAM and donates an electron back to the [4Fe-4S]²⁺ cluster priming the enzyme for another turnover event (Figure 2). The most

well studied examples of this subclass include LAM and SPL, both of whom use SAM as a cofactor (35, 44).

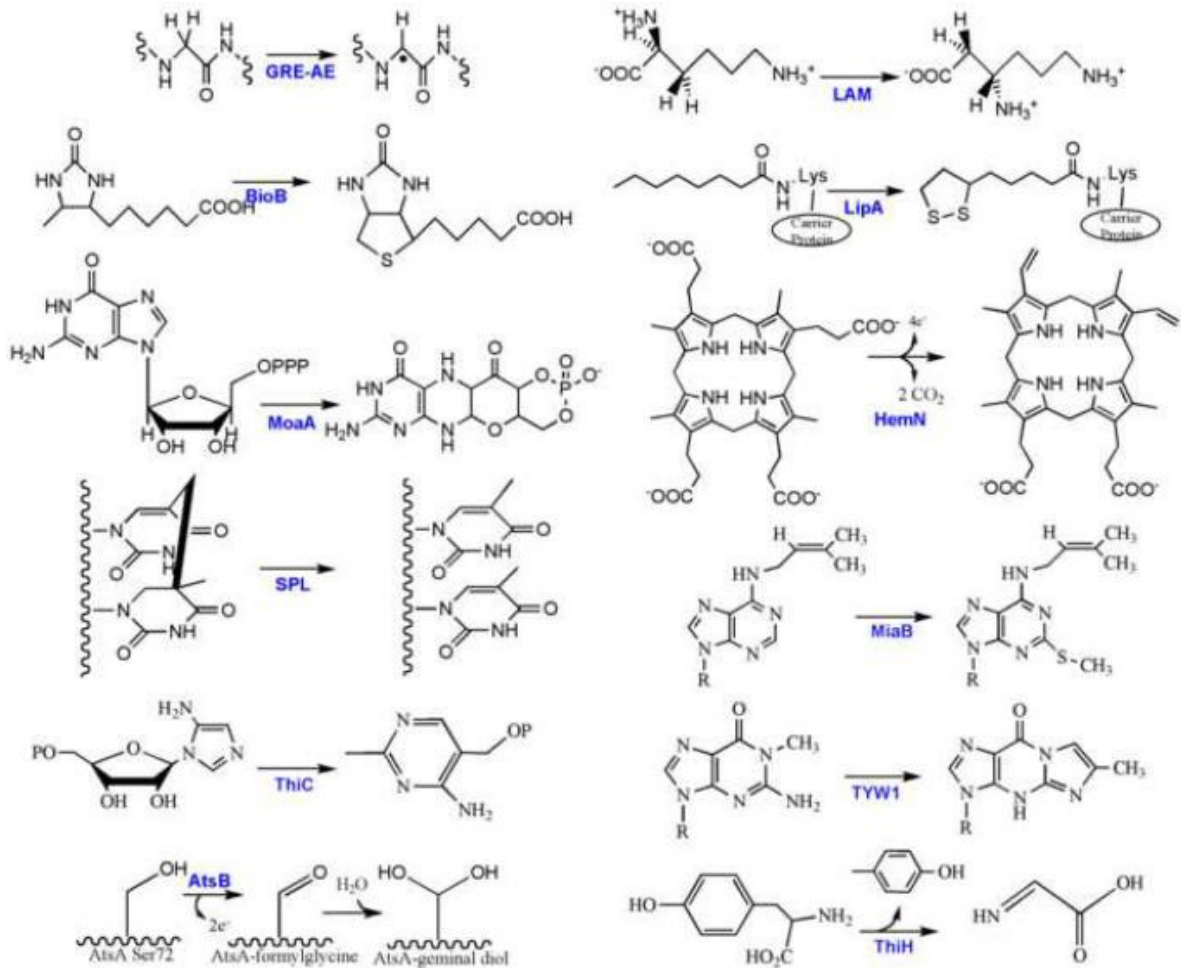


Figure3: The Radical SAM enzyme superfamily consists of over 2500 enzymes that catalyze a wide array of reactions. They range from glycyl radical activation, co-factor biosynthesis, rearrangement reactions to DNA repair. (Taken from reference 33)

In the second class of SAM enzymes, the H atom abstraction by d-Ado• is irreversible with a single molecule of SAM being consumed per turnover event with the subsequent release of d-Ado and methionine as products. Evidence for the role of SAM as either a cofactor or cosubstrate has also been supported by ENDOR studies measuring the

distances between SAM and the catalytic cluster. In the case of the enzymes using SAM as a co-factor (LAM), it has been shown that the methyl group of SAM is in closer proximity to the unique iron. This in turn implies a shorter sulfonium ion to iron ion distance relative to PFL-AE, an enzyme which uses SAM as a co-substrate (45). A probable rationalization of such a phenomenon is that when SAM is utilized catalytically, the unique iron becomes hexa coordinated (with methionine) upon SAM cleavage vs penta coordinated. Consequently the hexa coordinated methionine is proposed to be bound more tightly to the unique Fe site and thus is locked in for reformation of SAM when SAM is employed stoichiometrically, a counter strategy is utilized where the increased distances and coordination environment from the cluster allow the methionine to diffuse out, or is replaced by a fresh SAM molecule which subsequently primes the active site for the next catalytic cycle (46). Remarkably it has been recently observed that an alternative SAM cleavage pathway exists , such as in the diphthamide biosynthetic enzyme Dph2, wherein the reductive cleavage of SAM results in the formation of an amino carboxy propyl radical and methylthioadenosine as products(47, 48)

Structural Insights into Radical SAM Enzymes

Currently, there are about 2600 enzymes that have been classified as belonging to the radical SAM superfamily, although to-date only ten X-ray crystal structures have been solved (38). A comparison of the structures reveal a remarkable degree of similarity between enzymes demonstrating a remarkable variation on a single structural theme. Members of this family have been shown adopt a complete or partial triose-phosphate isomerase mutase (TIM) barrel like motif (Figure 4). Most of these enzymes consist of a

partial TIM barrel (6 α helices and 6 β sheets) with BioB and HydE containing complete TIM barrels with 8 α helices and 8 β sheets(49).

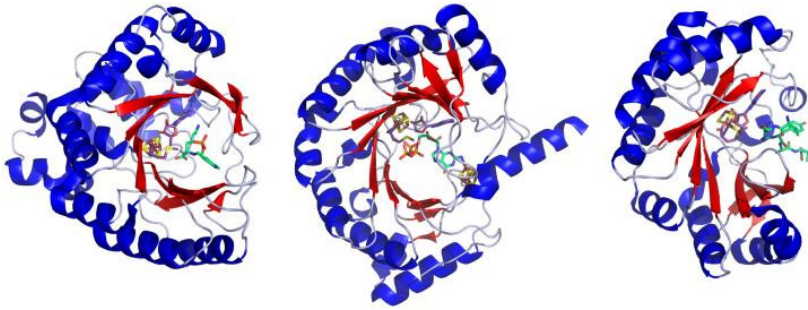


Figure 4: Partial TIM barrel structure of radical SAM enzymes lysine 2,3-aminomutase (LAM, left, minus its C-terminus), MoaA (center), and pyruvate formate-lyase activating enzyme (PFL-AE, right). Each structure has a single SAM molecule bound to the active site (this figure is obtained from ref 33)

In all cases, the choice of structural motif is dictated by two primary considerations, the size of the substrate and controlling the radical chemistry initiated by SAM cleavage. In almost all cases the catalytic cluster is coordinated by a loop region in the core with the canonical CX_3CX_2C motif(38). The unique iron is always coordinated by SAM (as mentioned earlier) and the latter acts to a certain extent to protect the cluster from solvent exposure. It is not yet known what the ligand for this unique iron is in the absence of SAM. Typically the active site that accommodates SAM is located within the lateral opening of the barrel with the SAM held in place via various H bonding and hydrophobic interactions with surrounding protein moieties(49). The most commonly identified SAM binding motifs in these enzymes is the classic GGE motif consisting of 2 conserved glycines followed by a glutamine or aspartate. It has been shown that the amino group of SAM interacts with the GGE motif ensuring the correct orientation of the

methionyl moiety with the unique iron in the cluster (38, 41). It is interesting to note that beyond the conservations in the cluster and SAM binding sites there are very little sequence similarities between radical SAM enzymes in general. This lack of conservation can be rationalized by the large variability in the substrates in this super family, ranging from small molecules, to oligonucleotides, to proteins. Among the multitude of radical SAM enzymes, this dissertation is focused on understanding the functions two of them. Spore photoproduct lyase a DNA repair enzyme in bacterial spores and HydE, an enzyme involved in the maturation of the active site of Fe-Fe Hydrogenase. The remainder of this section is dedicated to providing a brief description of the roles of these enzymes in nature.

Spore Photoproduct Lyase

It was first shown in the late 1960s and early 1970s that UV irradiation of bacterial spore DNA produced an unusual type of thymine dimer that was removed not by photoreactivation, but by a novel dark repair mechanism involving the enzyme spore photoproduct lyase (SPL) (50). SPL is encoded by the *splB* gene, part of the two-gene *spl* operon. The second gene, *splA*, is thought to encode a regulatory protein (51). The *spl* operon was shown to be expressed only in the forespore and only during sporulation, and remained unaffected by DNA damage in growing cells (52). Initial characterization of the SPL protein was reported in 1998 by Nicholson and co-workers, who purified the enzyme from dormant *B.subtilis* spores and from an *E.coli* overexpression system (53). They showed that SPL was a 41-kDa iron sulfur containing protein with sequence homology to anaerobic ribonucleotide reductase and pyruvate-formate lyase activating

enzyme. In addition, the SPL mediated repair of SP was shown to be dependent upon reducing conditions and the addition of SAM (Figure 5) (53).

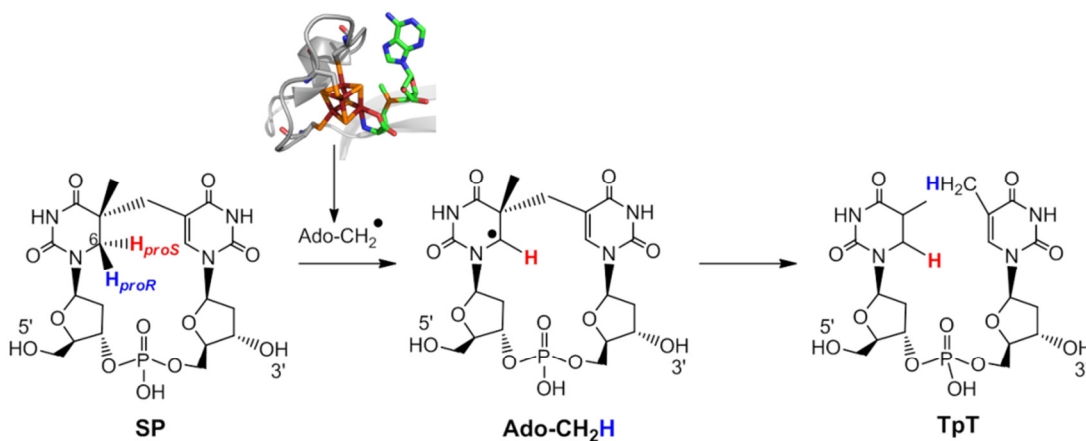


Figure 5: A general scheme of SPL catalyzed repair of SP. The d-Ado (Ado-CH₂•) abstracts an H atom from the pro-R position of SP to generate a substrate radical. The repaired thymine pair (TPT) is formed after a series of complex radical based chemistry including the cleavage of the methylene bridge.

Spore photoproduct lyase is now known to be a member of the radical

SAM protein superfamily, whose key characteristics are the use of a site-differentiated [4Fe-4S]^{2+/+} cluster and SAM to initiate diverse radical reactions in biology (30-32).

Spore photoproduct lyase exhibits biochemical and spectroscopic features typical for radical SAM enzymes, including the canonical CX₃CX₂C cluster binding motif that

coordinates the site-differentiated [4Fe-4S] cluster (53, 54). The unique iron of this

cluster is thought to bind SAM, as it does for other characterized members of the

superfamily (55). The UV-visible spectra of recombinant SPL from both *Clostridium*

acetobutylicum (*C.a.*) and *Bacillus subtilis* (*B.s.*) exhibit features characteristic of

enzymes containing an iron-sulfur cluster, including a broad absorbance with prominent

features at 410 nm and 450 nm that reduce in intensity upon reduction (55, 56). Electron paramagnetic resonance (EPR) spectra of the as-isolated enzyme typically shows an isotropic signal ($g = 1.99$) indicative of the presence of a $[3\text{Fe-4S}]^+$ cluster (55, 56); such a cluster is a common observation among radical SAM enzymes, where the cluster is oxygen-sensitive and labile, with the unique iron being prone to loss upon oxidation. Reduced SPL in contrast shows a nearly axial signal ($g = 2.03, 1.93$ and 1.92) indicative of a $[4\text{Fe-4S}]^+$ cluster (55-58). The EPR spectral properties of reduced SPL undergo interesting transformations on the addition of SAM; unlike many other radical SAM enzymes, the g -values are only moderately perturbed by the presence of SAM ($g = 2.03, 1.92, 1.82$), however the signal intensity is considerably decreased (56). Spectroscopic characterization of SPL from other organisms such as *Geobacillus stearothermophilus* have demonstrated the presence of a redox active $[4\text{Fe-4S}]$ cluster with similar UV-vis and EPR properties (59, 60). In order to probe the interaction between the $[4\text{Fe-4S}]$ cluster of SPL and SAM, Fontecave and coworkers used HYSCORE, a two-dimensional pulsed EPR technique. The coupling constant of 9.1 MHz was indicative of an interaction between the amino group of SAM with the unique iron in the $[4\text{Fe-4S}]$ cluster of SPL (57, 61).

DNA Damage and Repair

Deoxyribonucleic acid (DNA) is a macromolecule that contains the instructions for the development and functioning for almost all life on Earth. Due to its quintessential role in life, it was once thought to be extraordinarily stable and immune to environmental stressors (62). More recently however the durability and fidelity of DNA have come

under intense scrutiny. DNA damage can be caused by various factors native to the cell machinery itself such as the incorporation of mismatched base pairs during replication and recombination (63, 64). In addition to such innate errors, DNA subjected to environmental stressors such as reactive oxygen species and harmful chemicals can form lesions, which in turn affect the fidelity of transcription (65-68). Therefore in order to maintain the integrity of the encoded genetic information it is absolutely essential for the damaged DNA to be repaired quickly and in the most energy efficient manner (69-71). Among the many environmental stressors to which nucleic acids are subjected, damage by ultraviolet (UV) radiation has been shown to be particularly problematic (72, 73). On exposure of DNA to UV radiation, lesions can form between neighboring pyrimidine bases such as thymine (T) and cytosine(C). These photo-lesions can take multiple forms in vegetative cells, including cyclobutane pyrimidine dimers (CPD), (6-4) photoproducts, and dewar isomers (74, 75) (Figure 6). Some of the well characterized means of pyrimidine dimer reversal are nuclear excision repair (NER) and the photo reactions catalyzed by DNA photolyases (76-82), with photolyases unusual in catalyzing the direct reversal of the damaged nucleobases (83, 84). Photolyases use UV or blue light ($\lambda = 320 - 500 \text{ nm}$), a flavin, and either folate (methenyltetrahydrofolate (MTHF)) or deazaflavin (8-hydroxy-5-deazariboflavin (8-HDF)) (85-87) to repair CPD or (6-4) photoproducts. The predominant UV induced lesion in bacterial spores is a unique photoproduct, 5-thyminy-5,6-dihydrothymine, and is referred to as the spore photoproduct SP (Figure 5) (71, 83, 85-89). The radical SAM enzyme spore photoproduct lyase catalyzes the direct reversal of SP and is the focus of this present section.

Bacterial Spores and the Role
of Small Acid Soluble Proteins

The unusual DNA photochemistry in bacterial spores has been attributed to the unique conditions present inside the spore (90), which include low hydration levels, high levels of certain small molecules, such as dipicolinic acid, and an abundance of low molecular weight DNA binding proteins called small acid soluble proteins (SASP) (51, 91-93). The binding of these SASPs to DNA is proposed to change its conformation to a form that favors formation of SP at the cost of other photoproducts (94-96). These remarkable proteins are synthesized early during the sporulation process and eventually comprise up to 20% of the total spore weight. There are three types of these SASP proteins (α , β , γ), however, only the α/β types have been shown to bind the bacterial spore DNA (97). The α/β type SASPs range from 5-7 kDa in size and show no sequence homology to any other protein family, but display significant homology across and within *Bacillus* species (98). These proteins have been shown to bind DNA nonspecifically with a single protein molecule covering approximately a 5bp region of the DNA, and in this fashion they envelop the entire spore chromosome (99). Further insights into the interaction between SASP and DNA were provided by the X-ray crystal structure of SASP complexed with a 10bp DNA duplex (94). SASPs were shown to bind the minor groove of the target DNA via a helix turn helix motif in which the first helix lies along the minor groove of the DNA and the second helix is inserted inside the minor groove. Such binding is rare in nature as most DNA binding proteins utilize the major groove to bind target DNA (100).

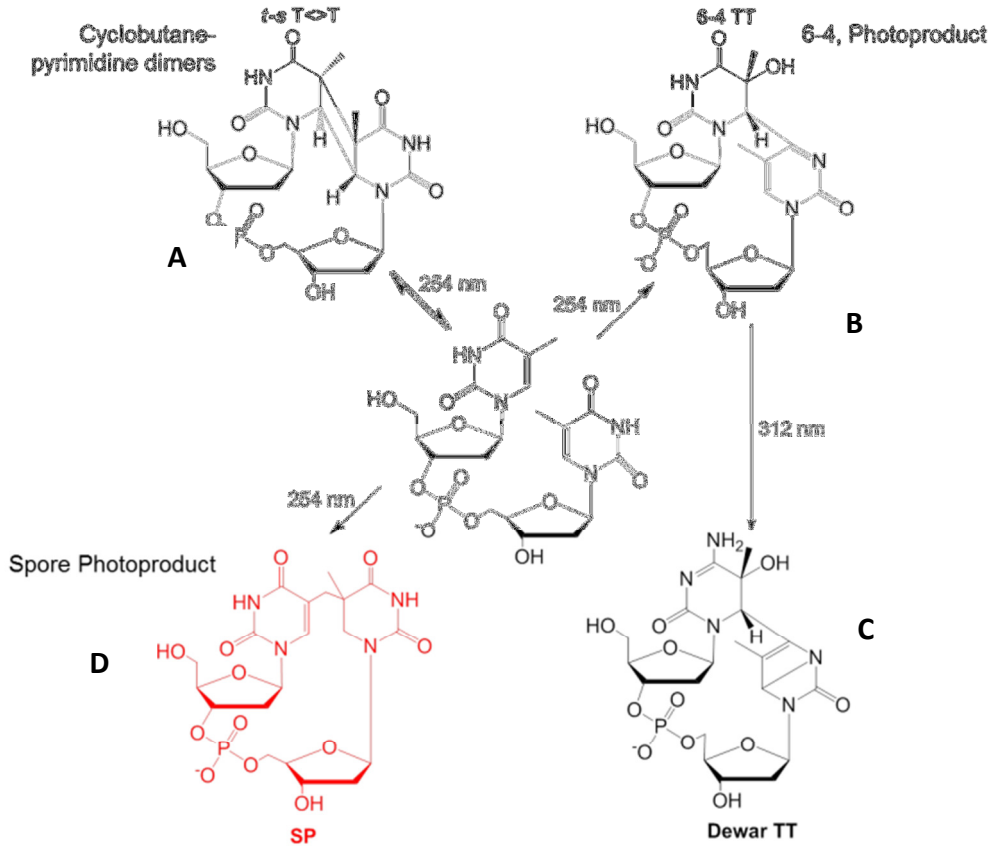


Figure 6. DNA lesions upon UV-Irradiation A) Cyclobutane pyrimidine dimer, B) pyrimidine-pyrimidine (6-4) photoproduct, C) Dewar Isomers D) spore photoproduct, (5-thyminy-5,6-dihydrothymine).

As initially proposed in 1991 and later confirmed through structural studies, binding of SASP to DNA changes its conformation from B type to an intermediate A-B type (94, 95). The reduced photosensitivity of A-DNA is well documented and is believed to result from the limited formation of CPD and 6,4-photoproducts due to the lower base pair twists and restricted conformation in A-DNA (101). In addition, structural studies of SASP bound DNA showed that the DNA in this complex is rigid due to the multitude of interactions between these proteins with their target (102). As mentioned earlier, SASP binding to DNA changes the latter's conformation from B type to an intermediate A-B

form (95), this resulting rigid complex is then unable to access the conformation necessary for the formation of CPD and 6,4-photoproduct (94). Taken together, this data indicates that this change in the DNA conformation is directly responsible for the preferential formation of SP lesions over CPD and photoproducts in bacterial spores. By altering spore DNA photochemistry to produce a lesion that is specifically reversed by SP lyase, SASPs contribute to the UV resistance and thus the viability of spores (89, 103). Further, SASPs have been shown to protect spore DNA from damage by harmful chemicals and heat, thereby providing additional protection and increasing survivability of the spore (104, 105).

SP Formation *in vivo* and *in vitro*

The first evidence hinting at the presence of a different type of thymine dimer in bacterial spores was reported by Donnellan and co-workers in 1965 (88). They found that the DNA in *Bacillus megaterium* spores exposed to UV radiation contained T-T dimers unlike those from vegetative cells, and they referred to this new lesion as spore photoproduct (SP) (88). In 1970 Varghese further characterized this unique dimer to be 5-thyminy-5,6-dihydrothymine, and proposed a mechanism for the formation of this lesion involving π bond cleavage to form a radical pair, followed by hydrogen atom abstraction from the adjacent thymine methyl to give the 5- α -thyminy and 5,6-dihydrothymine-5-yl radicals, which then recombine to form the spore photoproduct (106). Experimental support for this mechanism was recently provided by the Li group using deuterium labeled (TpT) (107) (Figure 7).

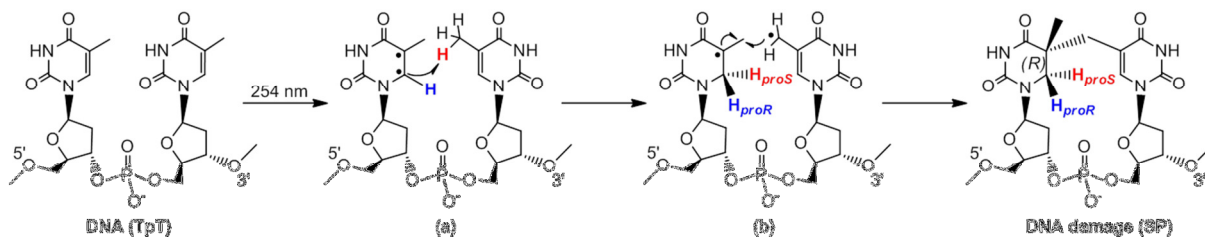


Figure 7: Proposed mechanism for the formation of SP. UV radiation results in the C₅-C₆ double bond on the thymine. The resulting radical pair abstracts an H atom from the neighboring thymine resulting in a methylene bridge

SP can be generated *in vitro* by UV irradiation of DNA under appropriate conditions, which generally include low hydration levels and the presence of SASPs and in some cases dipicolinic acid. These conditions are thought to mimic those inside the spore, and have been shown to lead to the preferential formation of SP over other photoproducts, with optimized SP yields of approximately 4%- 8% of total thymine (99, 108). The total yields of SP are relatively low, and the irradiated DNA invariably contains other types of DNA damage; for these reasons, the appropriate application of DNA hydrolysis and quantitative analysis of the hydrolytic products were required to assay for SP formation and repair (35, 55, 99, 108-110). Despite its inherent inhomogeneity, UV-irradiated DNA has served as the substrate for most studies focused on the enzymatic repair of SP. SP has also been synthesized in the laboratory, initially by Begley and coworkers who synthesized the SP dinucleotide from protected thymidine and dihydrothymidine (111, 112). Carell and coworkers followed up on this synthesis, providing the first stereochemically-defined synthetic dinucleoside spore photoproducts (113), which were subjected to enzymatic repair assays as described in a later section. Further syntheses of the dinucleoside and dinucleotide spore photoproduct have also been reported (56, 114),

and synthetic SP analogs have been incorporated into oligonucleotides (115, 116). In all cases, these synthetic efforts have proven to be invaluable in mechanistic studies of the enzymatic repair of SP, as is described further in the following sections.

Mechanism of SP Repair by Spore Photoproduct Lyase

Early insights into the mechanism of SP repair were provided by the work of Mehl and Begley, who suggested that the putative adenosyl radical intermediate served to abstract a hydrogen atom from the C-6 position of SP to initiate a radical-mediated β -scission (117). Observation of tritium transfer from C6(^3H)-SP, but not from methyl(^3H)-SP, to SAM during SP repair ultimately provided experimental support for this mechanism (Figure 8 step II) (35). Li and coworkers subsequently showed that the H-atom abstraction from C6 was stereospecific for the pro-R position (118). The observation of tritium in SAM, rather than 5'-dAdo, after SP repair also suggested that SAM was acting as a catalytic cofactor to reversibly generate the 5'-dAdo radical intermediate with reformation of SAM after turnover (Figure 8) (35). Subsequent work demonstrated that only catalytic amounts of SAM were required for SP repair, and that dAdo was not a stoichiometric product of repair, thereby further supporting a catalytic role for SAM (55). Support for step IVb in the mechanism was provided by the observation of tritium transfer from 5'(^3H)-SAM to the thymine products of SP repair (55). SP lyase in *Bacillus* species has been shown to contain four conserved cysteine residues, with three of these belonging to the canonical radical SAM cluster-binding motif of C_{xxx}C_{xx}C (54). The fourth cysteine (Cys141) has been shown to play no role in cluster formation, however a C141A variant was reported to abolish SPL activity,

suggesting an essential role for Cys141 in the repair mechanism (54). This was, however, a perplexing observation given that the essential Cys141 in *Bacillus* is always an Ala in SPL from *Clostridium*. It was subsequently shown that C141A SPL converted SP to a unique dinucleotide mono-phosphate with a sulfinate group attached to the methyl carbon of the 3'-thymine (119).

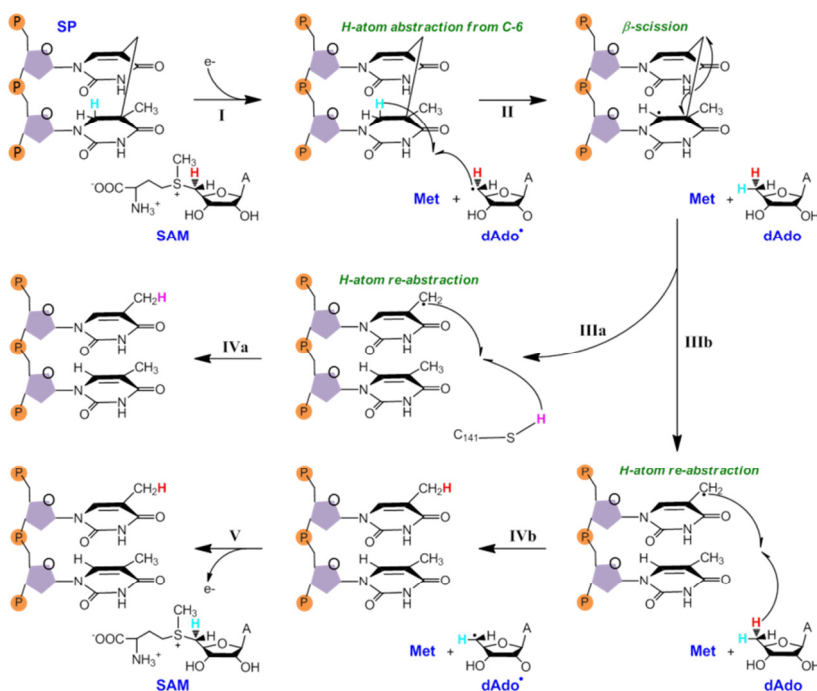


Figure 8: Proposed mechanism for SP repair by SP lyase with SAM.

These results suggested that the Cys-141 may be instrumental in controlling the radical reaction by acting as an H-atom donor to the allylic product radical. Li and coworkers carried out a series of label transfer experiments in which they did not observe the transfer of deuterium from 5'-D₂-SAM to the repaired product of SP repair (TpT) (118), in contrast to the tritium transfer from SAM to repaired product described above (55).

Further, Li and coworkers report the incorporation of deuterium from D₂O into the product TpT. Based on these results, as well as on earlier reports that a fourth cysteine was required in catalysis, Li and coworkers proposed an alternate mechanism in which the second half of the reaction, involving the return radical transfer from the TpT product radical to 5'-dAdo, occurs through this Cys141 residue. In other words, the TpT product radical abstracts an H atom from Cys to generate an intermediate thiyl radical (Figure 8, step IIIa), which subsequently abstracts a hydrogen atom from 5'-dAdo to regenerate the 5'-dAdo radical. Since the cysteine thiol hydrogen would be solvent exchangeable, such a mechanism could account for incorporation of deuterium from D₂O into the product TpT. The cysteine proposed to be involved in this manner is conserved, however, only in *Bacillus* species, and not in SPL from other organisms, thus calling into question the cysteine mechanism, or raising the issue that SPL from different sources may operate through a different mechanism. Final resolution of the discrepancies in experimental results, as well as formulation of a unified mechanism (if this is indeed the case), will require further experimental efforts.

A density functional theory (DFT) study by Himo and coworkers supports the feasibility of the mechanism shown in Figure 8. Their calculations provided estimates for the energetics of each step of the mechanism, and predicted that the final H-atom abstraction step, in which the product thyminy radical abstracts a hydrogen from 5'-dAdo, would be rate limiting. This is consistent with the expectation that forming a primary carbon-centered radical by H-atom abstraction with a secondary carbon radical would be an uphill process. While providing general support for the proposed

mechanism, Himo and coworkers also suggested an additional inter-thymine H atom transfer step, followed by abstraction of hydrogen from 5'dAdo. Such a scenario would involve the occurrence of the initial and final H-atom abstraction steps without significant movement of the 5'-dAdo intermediate.

The precise nature of the SP that was recognized by and repaired by SPL remained in question for many years. Specifically, the formation of SP results in creation of a new stereo center at the C5 position (120), meaning that two possible diastereoisomers could be produced (121). Begley and coworkers suggested that only the 5*R* configuration was possible *in vivo* due to constraints imposed by adjacent thymines in double stranded DNA (111). However such details could not be adequately addressed until the combination of synthetic methods to make SP, NMR methods to accurately define the SP stereochemistry, and biochemical methods to isolate active SPL, were all achieved. Synthetic SP dinucleoside was shown to be converted to two thymidines by the action of SPL (113, 114, 122), however the repair rates are significantly slower than when irradiated DNA was used as substrate. The dinucleotide SP substrate containing a phosphodiester bridge between the ribose moieties was shown to be a significantly better substrate as reflected by its increased rate of repair (56). Incorporation of the SP dinucleoside into a 12-mer piece of DNA produced a more physiologically relevant synthetic substrate that was shown to be repaired by the SPL from *Geobacillus stearothermophilus* (115). A synthetic SP containing a formacetal (-CH₂-) linker in place of the phosphodiester bridge was also a viable substrate; however the rate of repair was slower than what was observed using a 5*R*-SP dinucleotide substrate (116, 118).

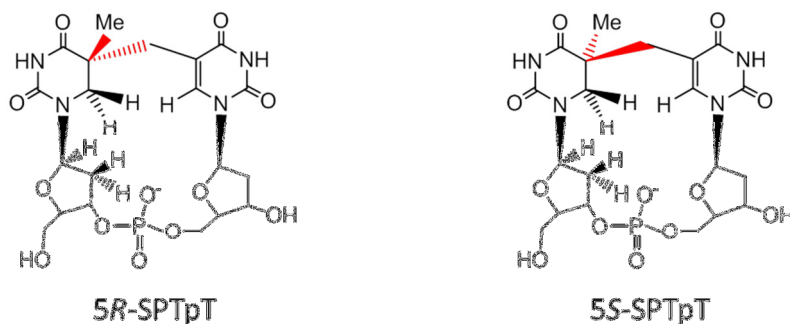


Figure 9: 5R (left) and 5S (right) synthetic spore photoproduct analogues including the phosphodiester linkage.

The availability of synthetic methods for making SP ultimately led to the preparation and assay of the pure 5R and 5S diastereomers (Figure 9). Contrary to the prediction of Begley that only the 5R diastereomer would be able to be formed in double-stranded DNA, initial reports indicated that with the synthetic substrates, SPL repaired only the 5S diastereomer (59, 113, 123). Subsequent work from the Broderick laboratory our laboratory reached the opposite conclusion: that SPL repairs only the 5R isomer of SP (56, 114). This latter conclusion was more consistent not only with the steric constraints of DNA, but also with a concurrent NMR characterization of the structure of SP generated by UV irradiation (124). The apparent discrepancy between the experimental results with stereochemically defined SP substrates was ultimately clarified by Carell and coworkers, who pointed out the importance of determining not only the stereochemistry at C5, but also whether the synthetic lesion is a 5' → 3' lesion or a 3' → 5' lesion (Figure 10) (115). In this paper, Carell and coworkers reported the synthesis of 5' → 3' 5R and 5S phosphoramidite dinucleoside SP lesions and their incorporation into a 12-mer double stranded DNA strand; these oligo-SPs were then co-crystallized with DNA polymerase from *Geobacillus stearothermophilus* (115). Using the DNA polymerase as matrix for

crystallization, Carell and co-workers attempted to model a phosphodiester linkage between the 3' and 5' OH groups present on ribose in the 5S and 5R isomers. They were able to show that while the linkage could be modeled easily on the 5R isomer and its presence produced only a slight change in the overall structure, it was impossible to model the phosphodiester linkage in the 5S isomer thereby showing that the 5S isomer is only a hypothetical compound (115). Subsequently, it was proposed by Carell and co-workers that if the SP formation reaction occurred in the 5' → 3' direction then it would give rise to the 5R-configured lesion, however, a reaction catalyzed in the 3' → 5' direction would provide the 5S-configured product.

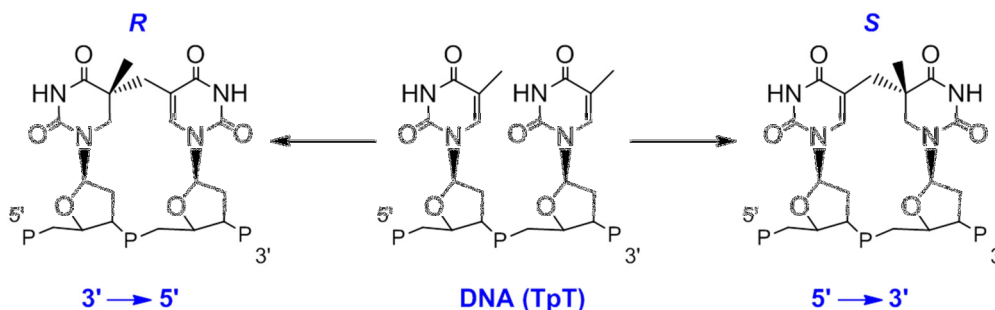


Figure 10: The reliance of nucleotide directionality on the physiologically relevant spore photoproduct

Binding Interactions between SP and SPL

Other than SPL, the other only well characterized means of pyrimidine dimer direct reversal is by the photolyase family of enzymes (77, 78). DNA photolyases have been shown to be structure specific, rather than sequence-specific, DNA binding proteins; with SPL binding shown to be independent of the DNA sequence, it has been suggested that the binding mechanism of both these enzymes might be similar (125). SPL binds

specifically to SP and not to CPD or other forms of the DNA damage, and induces a substantial distortion of the DNA backbone, similar to observations with DNA photolyase (110, 126). Initial work on SPL demonstrated that the enzyme specifically recognizes and binds SP but not CPD or 6, 4 photoproduct in a 35-bp double stranded oligonucleotide (110). Further, DNase I protection assays showed that SPL was able to protect at least a 9-bp region surrounding the damaged region (110). Moreover it was also noted that the binding of SPL to SP led to significant distortion of the DNA helix in the vicinity of the lesion (110). To better understand the binding events that lead to substrate recognition Carell and coworkers in a recent study showed that the SP lesion induced minimal distortions in the duplex structure in an overlay of the 5R lesion-containing DNA with undamaged DNA. This was especially remarkable when such SP induced DNA backbone perturbations were compared to other UV induced lesions such as 6,4-photoproduct and dewar isomers (115). Most DNA repair enzymes including those in the photolyase family are known to use discontinuity at the lesion site due to nucleotide extrusion to recognize and bind their substrate (125, 127). This brings up fresh questions as to the recognition pathway used by SPL to target its substrate as the distortion in the helical structure is minor; it seems likely therefore that SPL must be using some novel mechanism to target and bind the SP lesion.

Structural Insights into SPL Mechanism

A recent X-ray crystal structure of SPL has provided invaluable insights into the mechanism of lesion binding and catalysis by this enzyme (128). The structure depicts an enzyme with an α_6/β_6 partial triose phosphate isomerase (TIM) barrel, the fold

common to all structurally characterized radical SAM enzymes. The catalytic [4Fe-4S] cluster is located on an eight residue loop region at the top of the TIM barrel containing the cluster ligating Cys90, Cys94 and Cys97 residues. The fourth unique Fe is shown to be coordinated by SAM through its amino and carboxylate groups. The proposed mechanism of SP catalysis by SPL suggests an inner sphere electron transfer from the unique iron in the cluster to the sulfonium center in SAM followed by homolytic cleavage (55, 117). The crystal structure of SPL corroborates such a view, as the distances between the unique Fe ion and the sulfonium ion of SAM (3.6 Å) are optimum for such an electron transfer event to take place. In addition, the SAM molecule is held in position by various hydrogen bonding and hydrophobic interactions between amino acids in the protein core and the adenine, ribose, and methionine portions of SAM. The crystal structure also provides some profound insights into the possible recognition and binding mechanism of SP with SP lyase. The active site depicts a laterally opened barrel which is analogous to other radical SAM enzymes (such as PFL-AE) that act on macromolecules, ensuring easy active site access (41). Interestingly, the SPL structure features two anti-parallel β strands forming a long β hairpin region protruding out of the core domain. The authors hypothesize that this hairpin region containing Tyr305 and Arg304 may act in substrate binding, with the Tyr initially entering the DNA helix leading to the unwinding of the latter. It is also suggested that the Arg then plays an integral role in flipping out the damaged nucleotides into the active site by temporarily replacing those nucleotides and stabilizing the DNA strand (Figure 11). Such a base flipping mechanism has precedence in nature with DNA repair enzymes such as DNA

photolyase (126), uracil-DNA glycosylases (UDG) (129) and the T4 endonuclease V (130). It is suggested that concomitant to substrate binding the core of the enzyme undergoes significant conformational changes, particularly in the active site pocket and the β hairpin region. This is accomplished by Tyr98 in the catalytic core which is proposed to undergo an exquisite rotation of about 45° in order to make room for the SP along with residues Thr101 and Lys106 which undergo a conformational change to prime the active site for catalysis. In addition, the β hairpin then changes position by $\sim 2 \text{ \AA}$ in order to seal off the active site from solvent and permit the delicate radical mediated catalysis to proceed. Insightful as these results are, a lot still remains to be elucidated regarding intricacies of SPL mediated repair of SP. One of the draw backs in the crystal structure study is the use of a synthesized SP dinucleoside substrate, without the presence of the accompanying double stranded DNA. The lack of the quintessential phosphate backbone along with the exclusion of the oligonucleotide strand generates grave concerns as to the physiological relevance of the observed results. It has been previously shown that the catalytic activity of SPL is lowered significantly when a dinucleoside substrate is utilized instead of the SP generated by UV irradiation of plasmid DNA, as the latter acts as a much more physiologically relevant substrate (114). Therefore, the crystal structure of SPL bound to a double stranded oligonucleotide in the presence of SAM would go a long way in addressing some of these outstanding issues.

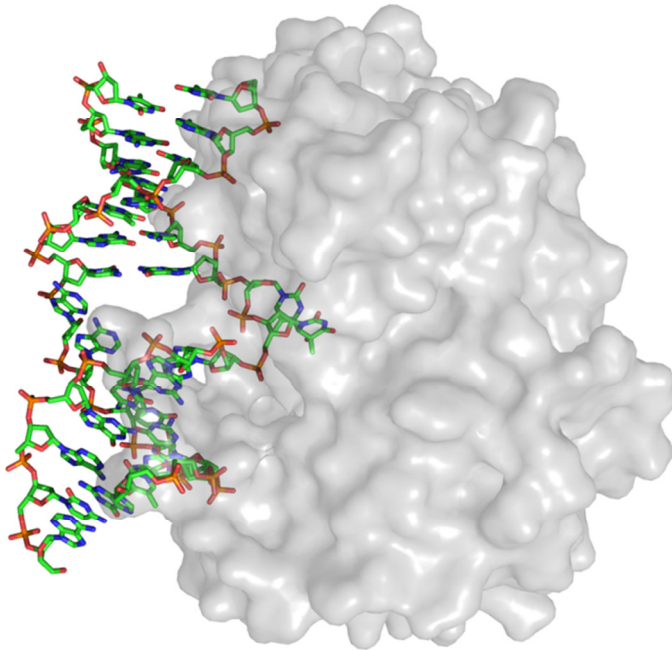


Figure 11: A superimposition of the purported base flipping out mechanism preceding repair in the active site of SPL . It is proposed that SPL binds to the major groove region and unwinds the DNA strand followed by the damaged TT pair being flipped out. This damaged region is then enveloped and stabilized into the active site pocket in a manner that facilitates catalysis.

The structure of SPL also provides some interesting perspectives into the mechanism of SPL mediated repair of SP. As mentioned previously, the generation of the 5'-dAdo radical leads to a H atom abstraction from the C6 position of the 5'-dihydrothymine leading to the β scission of the methylene bridge. The resulting substrate radical intermediate then re-abstracts an H atom from the 5'-dAdo (formed earlier in the reaction) to produce the repair product of 2 thymidines (55).

The authors suggest that a conserved cysteine, Cys140 (analogous to Cys141 in *B.subtilis*), on *Geobacillus thermodenitrificans* contributes towards catalysis by being the alternate source of the re-abstracted H atom. To further lead credence to this viewpoint,

they monitor the repair reactions catalyzed by two mutants, C140A and C140S, as well as analyze the structural ramifications of these mutations in the overall protein fold. Their results suggest that there are no structural differences between the mutants and the wild type SPL. Further, it is also observed that both in the wild type as well as the mutant proteins all the active site amino acid interactions between the substrate and SPL were rigidly maintained. This further suggests that Cys140 in *G. thermodenitrificans* (and by extension to Cys141 in *B. subtilis*) do not play any part in substrate recognition or binding. However, interpreting the influence of the aforementioned mutations on the repair reaction on an SP dinucleoside containing 12-mer oligonucleotide has been more challenging. In addition to observing a 2.5 fold decrease in activity for the mutant proteins, the authors reported the formation of product molecules purportedly containing SO₂ adducts. It was also noticed however that both the mutants produced fully repaired product oligonucleotides in significantly higher concentrations (as observed through peak intensity in the MS spectra) than their SO₂ containing analogs. This poses the question that if indeed the Cys140 is the only source of the H atom during repair, then why would its replacement not completely abolish enzyme activity? In addition, based on spectral intensities, it seems that comparable amounts of repaired oligonucleotides were produced in both the wild type as well as the mutant proteins, thereby suggesting an alternative explanation for the appearance of the SO₂ containing product analogs. Also, it is unclear as to the exact protocol followed in the reconstitution step of SPL used in these assays. Our experience with this technique typically involves the stepwise addition of FeCl₃ and Na₂S in the presence of a reducing agent such as dithiothreitol (DTT). The authors do not

mention the presence of any reducing agent in their reconstitution protocol, nor do they verify the cluster content via spectroscopic techniques. This could then partially be responsible for the ambiguity in the results observed for both sets of mutant proteins as the catalytic cluster could perhaps be improperly formed or reconstituted to low occupancy. In order to synergize their observations with the hypothesis of SAM acting as cofactor during catalysis, the authors suggest a mechanism analogous to those observed in class II ribonucleotide reductases with adenosylcobalamin (131). The authors propose that the substrate radical abstracts a H atom from Cys140 forming a thiyl radical as well as two repaired thymidines. The thiyl radical then abstracts a H atom from the 5'-dAdo in a reaction coupled to a different thermodynamically favorable reaction. They further suggest that the role of a highly conserved Tyr98 present in the enzyme active site may be to act in a proton coupled electron transfer conduit to reduce the earlier generated thiyl radical.

The Broderick group and others has thus far been at the forefront of investigating the mechanistic details of SPL derived catalysis of SPL. Therefore, the specific thrust of this dissertation is to understand the structural and conformational changes in SPL brought about by substrate and/or cofactor binding. This work also endeavors to amalgamate mass spectrometry techniques with anaerobic biochemistry approaches so as to open an diverse window into the workings of this enzyme from unique viewpoint.

[FeFe]-Hydrogenase

The Hydrogenase family of enzymes are proposed to catalyze the reversible reduction of protons to hydrogen gas ($2\text{H}^+ + 2\text{e}^- \rightleftharpoons \text{H}_2$) and are a key feature in the H_2 metabolism of

many microorganisms. There are two primary classes of hydrogenases [NiFe]- and [FeFe]-hydrogenases, with their nomenclature being reflective of the identity of the metal ions in their active site (132). The [FeFe]-hydrogenases have been shown to contain a unique active site metal cluster, known as the H-cluster, responsible for hydrogen catalysis (Figure 12). The [FeFe]-hydrogenases have a catalytic bias towards proton reduction, and are the most efficient producers of H₂ among the hydrogenases (132, 133). The active site H-cluster of this enzyme contains a [4Fe-4S] cubane bridged to a 2Fe binuclear center via a single cysteinyl thiolate. The Fe ions of the 2 Fe subcluster have been shown to be in octahedral coordination environments with the unique and biologically toxic CO and CN⁻ diatomic ligands and a five membered non protein bridging dithiolate ligand (134) (135, 136). The identity of the bridgehead atom in the bridging dithiolate ligand has yet to be experimentally identified but available evidence indicates it is either dithiomethylamine or dithiomethylether, with recent spectroscopic studies suggesting it is dithiomethylamine (137-139). Structural studies have shown that the bridging cysteine thiolate serves as the only linkage between the structural hydrogenase protein and the 2Fe subcluster, although the latter is shown to be ensconced in a defined cavity in the protein (140).

H-Cluster Maturation in [FeFe]-Hydrogenases

The synthesis of the non-protein ligands on the 2Fe subcluster of H-cluster is dependent on maturase enzymes that have been proposed to introduce modifications on a simple [2Fe-2S] cluster. The CO and CN⁻ ligands are synthesized and assembled by the combined actions of HydE, HydG, and HydF (141, 142). The first insights into the role

of these maturases were first obtained through bio-informatics on mutant strains of *C. reinhardtii* that were incapable of producing H₂ (143). Such an inability was traced to mutations on 2 genes *hydEF* and *hydG*, with proteins encoded by these genes being strictly conserved in all organisms with active hydrogenases (144). Sequence alignment studies of these enzymes showed that the HydE and HydG contain the canonical CX₃CX₂C sequence motif, thereby designating them to the radical SAM superfamily of enzymes. HydF was proposed to be a scaffold with an N-terminal GTPase domain and C-terminal Fe-S cluster binding domain (145). These initial observations were critical to shaping the early hypotheses of H-cluster maturation whereby it was proposed that either HydE or HydG were responsible for the synthesis of the bridging dithiolate ligand from an unknown substrate (but presumed to be a common metabolite) on a [2Fe-2S] cluster framework; This reactivity was proposed to occur first as it would effectively shift the reactivity away from the sulfides towards the iron ions for subsequent diatomic CO and CN⁻ ligand addition.

Diatomic ligand synthesis was proposed to occur through generation of a small amino acid radical (potentially a glycyl radical) by the actions of either HydE or HydG. This early hypothesis also invoked HydF as acting as a scaffolding protein during this process, with the mature cluster being translocated from HydF to the apo HydA (146). This hypothesis thereafter formed the basis of a series of experiments which further highlighted the individual roles of each of the maturases in the biosynthesis of the H-cluster.

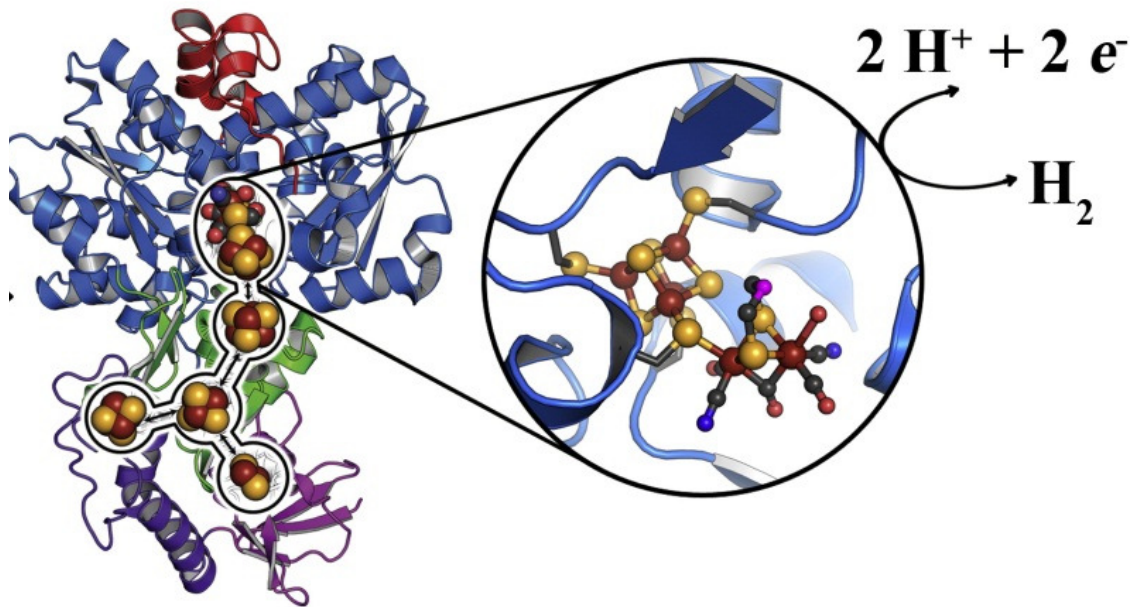


Figure 12: The active site of Fe-Fe Hydrogenase. The H cluster domain contain the complex metal bridged center is complemented by accessory F clusters (This has been obtained from reference 138)

To investigate the action of (*141*) maturation proteins on [FeFe]-hydrogenase, an *in vitro* *E. coli* based system was developed in which the [FeFe]-hydrogenase structural protein, also known as HydA, was expressed in the absence of the accessory proteins (HydA^{ΔEFG}). It was observed that HydA^{ΔEFG} existed as a stable protein but did not exhibit any hydrogenase activity. Remarkably, this inactive HydA^{ΔEFG} was then reactivated by addition of the cellular extracts in which the three accessory proteins (HydE, HydF and HydG from *Clostridium acetobutylicum*) were co-expressed (*141*). Furthermore, it was shown that when HydE, HydG, and HydF were expressed together, it produced a protein based activating element which could then be used to activate HydA^{ΔEFG}. Interestingly, it was shown that HydA^{ΔEFG} could be activated by purified HydF grown in the genetic

background of HydE and HydG (HydF^{EG}), and without the addition of any exogenously added small molecules (147). This led more credence to the idea that the precursor to the H-cluster was built by HydG and HydE, with HydF acting as a protein scaffold and eventually transferring the H-cluster precursor to HydA^{ΔEFG}. Low temperature EPR characterization of HydF expressed singly (HydF^{ΔEG}) showed signals that were consistent with both [4Fe-4S]⁺ and [2Fe-2S]⁺ clusters under reducing conditions. However, when grown in the presence of both enzymes (HydF^{EG}), only a signal corresponding to a [4Fe-4S]⁺ cluster was observed under reducing conditions. It was also observed that the addition of GTP enhanced the signal intensity of the cluster, thereby providing evidence for a role (although undefined) of GTP in cluster maturation(148) (134). Moreover, it was shown via fourier transform infrared spectroscopy (FTIR) that HydF^{EG} had features consistent with the presence of CO and CN⁻ ligands which are conspicuously absent in the FTIR spectra of HydF^{ΔEG}. Remarkably, analogous FTIR features are observed in the H-cluster of holo FeFe-hydrogenase which indicates a similarity in the cluster composition between HydF^{EG} and holo HydA(149).It was clearly evident by this point that HydF was acting as either a scaffold or carrier protein and that the two radical SAM enzymes were involved in the biosynthesis of the CO, CN⁻ and bridging dithiolate ligands. Thereafter, it was shown that HydG, which shares 27% sequence similarity with a previously characterized radical SAM enzyme ThiH (which cleaves tyrosine into *p*-cresol and dehydroglycine (150) cleaved tyrosine into *p*-cresol and presumably a glycine like derivative (150). Unlike ThiH, HydG was shown to contain an additional 90 amino acid C-terminal domain that contained conserved cysteine residues (CX₂CX₂₂C) and was

likely responsible for binding an additional FeS cluster. Further biochemical characterization demonstrated that HydG catalyzed tyrosine cleavage resulted in formation of not only *p*-cresol but both CO and CN⁻ diatomic moieties (Figure 13) (151, 152). Mutational studies on the C-terminal cluster of HydG indicated that this FeS cluster was directly responsible for synthesis of CO, with CN⁻ formation apparently occurring at a site distinct from the FeS cluster (145, 153). Collectively, the results suggested that the role of HydE was in the biosynthesis of the bridging dithiolate ligand of the H-cluster. Based on all the available evidence it is hypothesized that a 2Fe-2S cluster on HydF is acted upon by HydE to produce the bridging dithiolate ligand, thereby shifting the reactivity to the Fe. Thereafter, it is proposed that HydG biosynthesizes all five CO and CN⁻ ligands from tyrosine decomposition and forms the mature 2Fe subunit (154). At this time it is suggested that HydF translocates the mature cluster via a cationic channel from the surface of apo HydA to a cavity in the interior of the protein. Once this transfer is completed it is believed that the cationic channel collapses brought about by a series of conformational changes in two conserved loop regions (32, 140, 155).

Maturation Enzyme HydE

As mentioned above, the maturase enzyme HydE was classified as a member of the radical SAM superfamily of enzymes (156, 157). Initial EPR spectroscopic and biochemical characterization of reconstituted HydE indicated that it contained 2 distinct 4Fe-4S clusters and was able to reductively cleave SAM to produce 5'-d-Ado (157). Subsequent structural characterization of HydE from *Thermotoga maritima* showed a unique complete TIM barrel motif (α/β)₈ and contained a site differentiated [4Fe-4S]

cluster. Moreover, it was shown that HydE had about 27% sequence similarity with another radical SAM enzyme BioB, responsible for biotin synthesis. In addition, HydE contains 3 additional Cys residues that were discovered to coordinate an accessory FeS cluster (either [2Fe-2S] or [4Fe-4S] in nature) with variable occupancy depending on reconstitution conditions. While it was initially proposed that this second cluster may serve in a similar manner as the second cluster in BioB (which is acted on during turnover and is the source of the sulfides incorporated into dethiobiotin)(158), site-directed mutagenesis studies of the three accessory cysteine residues in HydE showed no significant deleterious effects on the ability to produce active [FeFe]-hydrogenase. Experiments of over 20,000 molecules resulted in the identification that the active site was capable of binding a small metabolite or amino acid with carboxylate and amino moieties, while soaking experiments identified that thiocyanate could bind within the interior cavity with high affinity (156). Moreover, HydE was shown to have a large interior cavity and *in silico* screening. The substrate and mechanism utilized by HydE to presumably synthesizes the dithiolate ligand is still under investigation. Very limited information is also available as to the identity of the putative product of HydE, that most likely leads to the synthesis of the dithiolate ligand. Moreover the composition of the bridge head atom in the dithiolate ligand remains under debate. The role of HydE in H-cluster maturation is only inferred from the available biochemical evidence that exists for HydF and HydG.

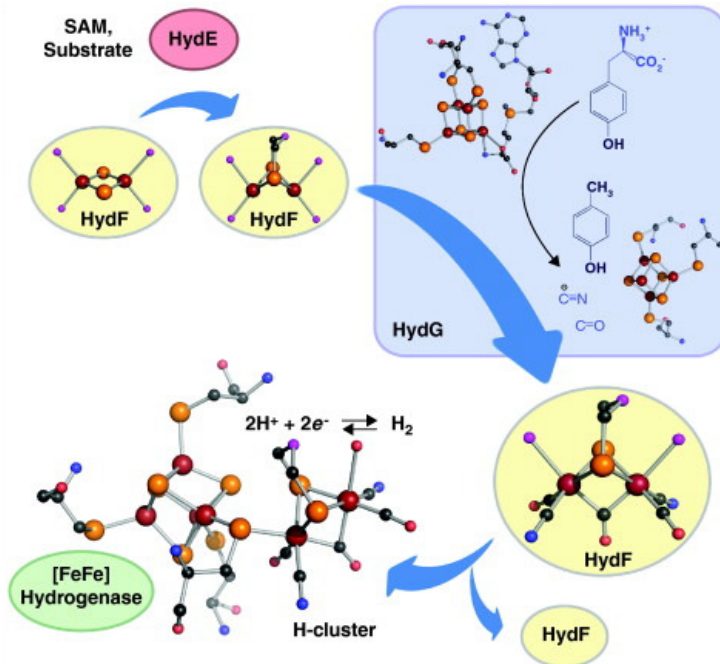


Figure 13: The proposed maturation scheme of Fe-Fe Hydrogenase active site. The radical SAM enzymes biosynthesize the diatomic ligands on the 2Fe-2S scaffold HydF. The resulting 2Fe center is translocated on to apo HydA (This has been obtained from reference 136)

In fact, in a recent publication, it was hypothesized that HydE simply acts as a chaperone protein for HydF during the 2Fe subcluster translocation process to HydA^{AEFG} (159). We do not favor this hypothesis and believe that HydE is playing a central role in the synthesis of the bridging dithiolate ligand. Insights into the putative substrate for HydE may be provided by studies involving cell lysates of the maturase enzymes which showed that the addition of cysteine and tyrosine stimulated [FeFe] hydrogenase activity, potentially indicating that cysteine acts as a substrate for HydE (160). Clarification on this issue is clearly needed and currently only a very preliminary characterization of HydE is available in the literature (157). This thesis describes advances made in both the

spectroscopic and biochemical characterization of HydE, as well as outlining efforts made towards identifying a substrate for this enzyme

Research Objectives

The primary topics of the research behind this dissertation are threefold. The first topic of interest was to understand the solution phase dynamics of SPL in the presence of damaged DNA substrate and SAM. We were also interested in investigating the effects of the [4Fe-4S] catalytic cluster on dynamics of substrate and cofactor binding of this enzyme. Initial work in our lab had focused primarily on understanding the stereospecificity of the substrate of SP lyase, particularly investigating and characterizing the stereochemistry of the 5*R*-SP and 5*S*-SP. Additionally, spectroscopic characterization of the [4Fe-4S] cluster in SP lyase and its interaction with SAM was investigated using UV-Vis, low temperature electron paramagnetic resonance (EPR), and X-ray absorption spectroscopy (XAS). Initial insights into the nature of binding of SP with SPL and SAM was initially approached in our lab through electrophoretic mobility shift assays and EMSA and fluorescence studies which specifically probed the K_d as well as changes in the protein secondary structure. The work described in this dissertation was initiated before the crystal structure of SPL was published and response to questions regarding the secondary structural changes brought about by substrate binding under anaerobic conditions. In order to answer these seminal queries we decided to utilize a technique seldom utilized in bio-inorganic chemistry to probe structural changes in enzymes containing oxygen sensitive metal clusters. We approached this problem via hydrogen deuterium exchange reactions as monitored through high performance liquid

chromatography and mass spectrometry. We were able to monitor changes in protein conformation on ligand binding in real time and were able to probe the effects of the [4Fe-4S] catalytic cluster on the binding interactions.

The second topic of research related to the biochemical characterization of HydE with the ultimate goal being identification of its substrate and elucidation of its role in H-cluster maturation. We were specifically interested in identifying not only the substrate, but the mechanism of action and product of HydE catalysis. The crystal structure of HydE guided us to the initial line of investigation when it predicted the putative nature and binding parameters of potential substrate molecules. Furthermore, studies involving cell lysates of the maturase enzymes showed that the addition of cysteine and tyrosine stimulated [FeFe] Hydrogenase activity(160) Work in our lab involving the screening of all twenty amino acids and some common metabolite compounds indicated that under conditions involving reconstituted HydE, SAM, and cysteine that an increase in 5'-dAdo production was achieved (161). This was strong evidence of cysteine being a putative substrate of HydE due to the enhanced rate of SAM cleavage in the presence of the former. However without the bio-analytical detection and quantitation of cysteine degradation we were unable confirm the hypothesis that cysteine was the substrate for HydE. To answer these pivotal questions we employed enzyme assays under anaerobic conditions followed by detection and quantitation via LC-MS. We were able to detect the disappearance of cysteine over time and correlate that with the formation of 5'-dAdo. Additionally we were able to investigate the effects of the scaffold protein HydF on HydE kinetics. Our research shows that the presence of HydF decreases levels of

nonproductive 5'-dAdo formation significantly, reducing it to background levels.

Moreover, the data shows that the presence of HydF in HydE assays causes an increased disappearance in cysteine over time. Assays performed with different labeled versions of cysteine subsequently identified that HydE abstracts the deuterium label from the β carbon position, which we were able to detect via incorporation into 5'-dAdo. This in turn indicates that during catalysis, 5'-dAdo• is able to abstract an H atom from the β carbon of cysteine; these results provide a significant first step towards identifying the mechanism of cysteine degradation and product formation by HydE.

The final line of investigation was to probe the mechanism of tyrosine cleavage by HydG. Work in our laboratory and that of others demonstrated that HydG catalyzes the degradation of tyrosine into *p*-cresol, CO and CN⁻ (151, 152). However, the mechanism of action, specifically which H atom from tyrosine is abstracted during catalysis was unknown. By employing tyrosine molecules differentially labeled with deuterium in HydG activity assays, we were able to identify the phenolic H atom as the site of abstraction by 5'-dAdo• through LC-MS techniques. This was demonstrated by detection of the D label in 5'-dAdo as reflected in a change in *m/z*.

References

1. Lu, Y., Berry, S. M., and Pfister, T. D. (2001) Engineering novel metalloproteins: design of metal-binding sites into native protein scaffolds, *Chemical Reviews* 101, 3047-3080.
2. Barker, P. D. (2003) Designing redox metalloproteins from bottom-up and top-down perspectives, *Current Opinion in Structural Biology* 13, 490-499.
3. Lill, R. (2009) Function and biogenesis of iron-sulphur proteins, *Nature* 460, 831-838.
4. Beinert, H. (2000) Iron-sulfur proteins: ancient structures, still full of surprises, *Journal of Biological Inorganic Chemistry* 5, 2-15.
5. Meyer, J. (2008) Iron-sulfur protein folds, iron-sulfur chemistry, and evolution, *Journal of Biological Inorganic Chemistry* 13, 157-170.
6. Sands, R. H., and Beinert, H. (1960) Studies on mitochondria and submitochondrial particles by paramagnetic resonance (EPR) spectroscopy, *Biochemical and Biophysical Research Communications* 3, 47-52.
7. Tagawa, K., and Arnon, D. I. (1962) Ferredoxins as electron carriers in photosynthesis and in the biological production and consumption of hydrogen gas. *Nature* 195, 537 - 543
8. Mortenson, L., Valentine, R., and Carnahan, J. (1962) An electron transport factor from *Clostridium pasteurianum*, *Biochemical and Biophysical Research Communications* 7, 448.
9. Beinert, H. (1997) Iron-Sulfur Clusters: Nature's Modular, Multipurpose Structures, *Science* 277, 653-659.
10. Beinert, H., Meyer, J., and Lill, R. (2004) Iron-sulfur proteins, *Encyclopedia of Biological Chemistry* 2, 482-489.
11. Rees, D. C. (2002), Great metalloclusters in enzymology, *Annual Review of Biochemistry* 71, 221-246.
12. Rao, P. V., and Holm, R. (2004) Synthetic analogues of the active sites of iron-sulfur proteins, *Chemical Reviews* 104, 527-560.
13. Moulis, J. M., Davasse, V., Golinelli, M. P., Meyer, J., and Quinkal, I. (1996) The coordination sphere of iron-sulfur clusters: lessons from site-directed mutagenesis experiments, *Journal of Biological Inorganic Chemistry* 1, 2-14.

14. Sellers, V. M., Johnson, M. K., and Dailey, H. A. (1996) Function of the [2Fe-2S] cluster in mammalian ferrochelatase: a possible role as a nitric oxide sensor, *Biochemistry* 35, 2699-2704.
15. Sazanov, L. A., and Hinchliffe, P. (2006) Structure of the Hydrophilic Domain of Respiratory Complex I from *Thermus thermophilus*, *Science* 311, 1430-1436.
16. Johnson, D. C., Dean, D. R., Smith, A. D., and Johnson, M. K. (2005) Structure, function, and formation of biological iron-sulfur clusters, *Annual Reviews of Biochemistry*. 74, 247-281.
17. Johnson, M. K. (1998) Iron-sulfur proteins: new roles for old clusters, *Current Opinion in Chemical Biology* 2, 173-181.
18. Wächtershäuser, G. (2006) From volcanic origins of chemoautotrophic life to bacteria, archaea and eukarya, *philosophical transactions of the Royal Society: Biological Sciences* 361, 1787-1808.
19. Kopp, R. E., Kirschvink, J. L., Hilburn, I. A., and Nash, C. Z. (2005) The paleoproterozoic snowball Earth: A climate disaster triggered by the evolution of oxygenic photosynthesis, *Proceedings of the National Academy of Sciences* 102, 11131-11136.
20. Glaser, T., Hedman, B., Hodgson, K. O., and Solomon, E. I. (2000) Ligand K-edge X-ray absorption spectroscopy: a direct probe of ligand-metal covalency, *Accounts of Chemical Research* 33, 859-868.
21. Brzóška, K., Meczynska, S., and Kruszewski, M. (2006) Iron-sulfur cluster proteins: electron transfer and beyond, *Acta Biochim Pol.* 53, 685.
22. Thauer, R. K., and Schönheit, P. (1982) Iron-Sulfur complexes of ferredoxin as a storage form of iron in *Clostridium pasteurianum*, iron-sulfur proteins, *Archives of Microbiology* 3, 285-288
23. Golinelli, M. P., Chatelet, C., Duin, E. C., Johnson, M. K., and Meyer, J. (1998) Extensive ligand rearrangements around the [2Fe-2S] cluster of *Clostridium pasteurianum* ferredoxin, *Biochemistry* 37, 10429-10437.
24. Cunningham, R. P., Asahara, H., Bank, J. F., Scholes, C. P., Salerno, J. C., Surerus, K., Munck, E., McCracken, J., Peisach, J., and Emptage, M. H. (1989) Endonuclease III is an iron-sulfur protein, *Biochemistry* 28, 4450-4455.

25. Kuo, C. F., McRee, D. E., Fisher, C. L., O'Handley, S. F., Cunningham, R. P., and Tainer, J. A. (1992) Atomic structure of the DNA repair [4Fe-4S] enzyme endonuclease III, *Science* 258, 434.
26. Fleischhacker, A. S., and Kiley, P. J. (2011) Iron-containing transcription factors and their roles as sensors, *Current Opinion in Chemical Biology* 15, 335-341.
27. Beinert, H. (2010) Catalysis and Gene Regulation, *Metals in Biology* 29, 45-51.
28. Smith, J. L., Zaluzec, E. J., Wery, J. P., Niu, L., Switzer, R. L., Zalkin, H., and Satow, Y. (1994) Structure of the allosteric regulatory enzyme of purine biosynthesis, *Science* 264, 1427.
29. Wu, C. K., Dailey, H. A., Rose, J. P., Burden, A., Sellers, V. M., and Wang, B. C. (2001) The 2.0 Å structure of human ferrochelatase, the terminal enzyme of heme biosynthesis, *Nature Structural & Molecular Biology* 8, 156-160.
30. Frey, P. A., Hegeman, A. D., and Ruzicka, F. J. (2008) The radical SAM superfamily, *Critical Reviews in Biochemistry and Molecular Biology* 43, 63-88.
31. Sofia, H. J., Chen, G., Hetzler, B. G., Reyes-Spindola, J. F., and Miller, N. E. (2001) Radical SAM, a novel protein superfamily linking unresolved steps in familiar biosynthetic pathways with radical mechanisms: functional characterization using new analysis and information visualization methods, *Nucleic Acids Research* 29, 1097-1106.
32. Shepard, E. M., and Broderick, J. B. (2010) *S*-Adenosylmethionine and iron-sulfur clusters in biological radical reactions: The radical SAM superfamily, *Comprehensive Natural Products II*, 625-661.
33. Duschene, K. S., Veneziano, S. E., Silver, S. C., and Broderick, J. B. (2009) Control of radical chemistry in the AdoMet radical enzymes, *Current Opinion in Chemical Biology* 13, 74-83.
34. Chirpich, T. P., Zappia, V., Costilow, R. N., and Barker, H. A. (1970) Lysine 2,3-aminomutase, *Journal of Biological Chemistry* 245, 1778-1789.
35. Cheek, J., and Broderick, J. B. (2002) Direct H atom abstraction from spore photoproduct C-6 initiates DNA repair in the reaction catalyzed by spore photoproduct lyase: Evidence for a reversibly generated adenosyl radical intermediate, *Journal of the American Chemical Society* 124, 2860-2861.
36. Peter L, R. (2011) Radicals from *S*-adenosylmethionine and their application to biosynthesis, *Current Opinion in Chemical Biology* 15, 267-275.

37. Walsby, C. J., Ortillo, D., Broderick, W. E., Broderick, J. B., and Hoffman, B. M. (2002) An anchoring role for FeS clusters: Chelation of the amino acid moiety of *S*-adenosylmethionine to the unique iron site of the [4Fe-4S] cluster of pyruvate formate-lyase activating enzyme, *Journal of the American Chemical Society* 124, 11270-11271.
38. Vey, J. L., and Drennan, C. L. (2011) Structural insights into radical generation by the radical SAM superfamily, *Chemical Reviews* 111, 2487-2506.
39. Berkovitch, F., Nicolet, Y., Wan, J. T., Jarrett, J. T., and Drennan, C. L. (2004) Crystal structure of biotin synthase, an *S*-Adenosylmethionine-dependent radical enzyme, *Science* 303, 76-79.
40. Chen, D., Walsby, C., Hoffman, B. M., and Frey, P. A. (2003) Coordination and mechanism of reversible cleavage of *S*-adenosylmethionine by the [4Fe-4S] center in lysine 2, 3-aminomutase, *Journal of the American Chemical Society* 125, 11788-11789.
41. Vey, J. L., Yang, J., Li, M., Broderick, W. E., Broderick, J. B., and Drennan, C. L. (2008) Structural basis for glycy radical formation by pyruvate formate-lyase activating enzyme, *Proceedings of the National Academy of Sciences* 105, 16137-16141.
42. Magnusson, O. T., Reed, G. H., and Frey, P. A. (2001) Characterization of an allylic analogue of the 5'-deoxyadenosyl radical: An intermediate in the reaction of lysine 2, 3-aminomutase, *Biochemistry* 40, 7773-7782.
43. Booker, S. J. (2009) Anaerobic functionalization of unactivated C-H bonds, *Current Opinion in Chemical Biology* 13, 58-73.
44. Moss, M., and Frey, P. (1990) Activation of lysine 2, 3-aminomutase by *S*-adenosylmethionine, *Journal of Biological Chemistry* 265, 18112-18115.
45. Nicolet, Y., Amara, P., Mouesca, J.-M., and Fontecilla-Camps, J. C. (2009) Unexpected electron transfer mechanism upon AdoMet cleavage in radical SAM proteins, *Proceedings of the National Academy of Sciences* 106, 14867-14871.
46. Hiscox, M. J., Driesener, R. C., and Roach, P. L. (2012) Enzyme catalyzed formation of radicals from *S*-adenosylmethionine and inhibition of enzyme activity by the cleavage products, *Biochimica et Biophysica Acta (BBA) - Proteins and Proteomics* 1824, 1165-1177.
47. Zhang, Y., Zhu, X., Torelli, A. T., Lee, M., Dzikovski, B., Koralewski, R. M., Wang, E., Freed, J., Krebs, C., and Ealick, S. E. (2010) Diphthamide biosynthesis requires an organic radical generated by an iron-sulphur enzyme, *Nature* 465, 891-896.

48. Zhu, X., Dzikovski, B., Su, X., Torelli, A. T., Zhang, Y., Ealick, S. E., Freed, J. H., and Lin, H. (2011) Mechanistic understanding of *Pyrococcus horikoshii* Dph2, a [4Fe-4S] enzyme required for diphthamide biosynthesis, *Molecular BioSystems* 7, 74-81.
49. Dowling, D. P., Vey, J. L., Croft, A. K., and Drennan, C. L. (2012) Structural diversity in the AdoMet radical enzyme superfamily, *Biochimica et Biophysica Acta (BBA)-Proteins & Proteomics* 11, 1178-1195
50. Donnellan Jr, J. E., and Stafford, R. S. (1968) The ultraviolet photochemistry and photobiology of vegetative cells and spores of *Bacillus megaterium*, *Biophysical Journal* 8, 17-28.
51. Nicholson, W. L., Munakata, N., Horneck, G., Melosh, H. J., and Setlow, P. (2000) Resistance of *Bacillus* endospores to extreme terrestrial and extraterrestrial environments, *Microbiology and Molecular Biology Reviews* 64, 548-572.
52. Pedraza-Reyes, M., Gutiérrez-Corona, F., and Nicholson, W. L. (1994) Temporal regulation and forespore-specific expression of the spore photoproduct lyase gene by sigma-G RNA polymerase during *Bacillus subtilis* sporulation, *Journal of Bacteriology* 176, 3983-3991.
53. Rebeil, R., Sun, Y., Chooback, L., Pedraza-Reyes, M., Kinsland, C., Begley, T. P., and Nicholson, W. L. (1998) Spore photoproduct lyase from *Bacillus subtilis* spores is a novel iron-sulfur DNA repair enzyme which shares features with proteins such as class III anaerobic ribonucleotide reductases and pyruvate-formate lyases, *Journal of Bacteriology* 180, 4879-4885.
54. Fajardo-Cavazos, P., Rebeil, R., and Nicholson, W. L. (2005) Essential cysteine residues in *Bacillus subtilis* spore photoproduct lyase identified by alanine scanning mutagenesis, *Current Microbiology* 51, 331-335.
55. Buis, J. M., Cheek, J., Kalliri, E., and Broderick, J. B. (2006) Characterization of an active spore photoproduct lyase, a DNA repair enzyme in the radical S-adenosylmethionine superfamily, *Journal of Biological Chemistry* 281, 25994-26003.
56. Silver, S. C., Chandra, T., Zilinskas, E., Ghose, S., Broderick, W. E., and Broderick, J. B. (2010) Complete stereospecific repair of a synthetic dinucleotide spore photoproduct by spore photoproduct lyase, *Journal of Biological Inorganic Chemistry* 15, 943-955.
57. Chandor, A., Douki, T., Gasparutto, D., Gambarelli, S., Sanakis, Y., Nicolet, Y., Ollagnier-de-Choudens, S., Atta, M., and Fontecave, M. (2007) Characterization of the DNA repair spore photoproduct lyase enzyme from *Clostridium acetobutylicum*: A radical-SAM enzyme, *Comptes Rendus Chimie* 10, 756-765.

58. Rebeil, R., and Nicholson, W. L. (2001) The subunit structure and catalytic mechanism of the *Bacillus subtilis* DNA repair enzyme spore photoproduct lyase, *Proceedings of the National Academy of Sciences* 98, 9038-9043.
59. Pieck, J. C., Hennecke, U., Pierik, A. J., Friedel, M. G., and Carell, T. (2006) Characterization of a new thermophilic spore photoproduct lyase from *Geobacillus stearothermophilus* (SpIG) with defined lesion containing DNA substrates, *Journal of Biological Chemistry* 281, 36317-36326.
60. Chandor, A., Berteau, O., Douki, T., Gasparutto, D., Sanakis, Y., Ollagnier-de-Choudens, S., Atta, M., and Fontecave, M. (2006) Dinucleotide spore photoproduct, a minimal substrate of the DNA repair spore photoproduct lyase enzyme from *Bacillus subtilis*, *Journal of Biological Chemistry* 281, 26922-26931.
61. Gambarelli, S., Luttringer, F., Padovani, D., Mulliez, E., and Fontecave, M. (2005) Activation of the anaerobic ribonucleotide reductase by *S*-Adenosylmethionine, *Chemistry BioChemistry* 6, 1960-1962.
62. Friedberg, E. C., and Hanawalt, P. C. (1988) DNA repair pp532-548.
63. Branzei, D., and Foiani, M. (2005) The DNA damage response during DNA replication, *Current Opinion in Cell Biology* 17, 568-575.
64. Cox, M. M., Goodman, M. F., Kreuzer, K. N., Sherratt, D. J., Sandler, S. J., and Marians, K. J. (2000) The importance of repairing stalled replication forks, *Nature* 404, 37-41.
65. Bjedov, I., Tenaillon, O., Gérard, B., Souza, V., Denamur, E., Radman, M., Taddei, F., Matic, I. (2003) Stress-induced mutagenesis in bacteria, *Science* 300, 1404-1409.
66. De Mott, M. S., and Dedon, P. C. (2010) Chemistry of inflammation and DNA damage: Biological impact of reactive nitrogen species, *The Chemical Biology of DNA Damage*, 423, 21-51.
67. Nohmi, T. (2006) Environmental stress and lesion-bypass DNA polymerases, *Annual Review of Microbiology* 60, 231-253.
68. Rogerio, M. (1997) Iron homeostasis, oxidative stress, and DNA damage, *Free Radical Biology and Medicine* 23, 783-792.
69. Lindahl, T., and Wood, R. D. (1999) Quality control by DNA repair, *Science* 286, 1897-1905.

70. Budzowska, M., and Kanaar, R. (2009) Mechanisms of dealing with DNA damage-induced replication problems, *Cell Biochemistry and Biophysics* 53, 17-31.
71. Eker, A., Quayle, C., Chaves, I., and van der Horst, G. (2009) DNA repair in mammalian cells, *Cellular and Molecular Life Sciences* 66, 968-980.
72. Ravanat, K. (2001) Direct and indirect effects of UV radiation, *Journal of Photochemistry and Photobiology*, 74, 231-245
73. Cadet, J., Sage, E., and Douki, T. (2005) Ultraviolet radiation-mediated damage to cellular DNA, *Mutation Research, Fundamental and Molecular Mechanisms of Mutagenesis* 571, 3-17.
74. Iwai, S. (2008) Pyrimidine Dimers: UV-Induced DNA Damage, *Modified Nucleosides*, pp 97-131.
75. Douki, T., and Cadet, J. (2001) Individual determination of the yield of the main UV-induced dimeric pyrimidine photoproducts in DNA suggests a high mutagenicity of CC photolesions, *Biochemistry* 40, 2495-2501.
76. Sancar, A. (1996) DNA excision repair, *Annual Review of Biochemistry* 65, 43-81.
77. Sancar, A. (2003) Structure and function of DNA photolyase and cryptochrome blue-light photoreceptors, *Chemical Reviews* 34, 143-169.
78. Sancar, A. (1994) Structure and function of DNA photolyase, *Biochemistry* 33, 2-9.
79. Tremblay, M., Toussaint, M., D'Amours, A., and Conconi, A. (2009) Nucleotide excision repair and photolyase repair of UV photoproducts in nucleosomes: assessing the existence of nucleosome and non-nucleosome rDNA chromatin in vivo, *Biochemistry and Cell Biology* 87, 337-346.
80. Wang, T. C., and Rupert, C. S. (1977) Transitory germinative excision repair in *Bacillus subtilis*, *Journal of Bacteriology* 129, 1313-1319.
81. Li, J., Bhat, A., and Xiao, W. (2011) Regulation of nucleotide excision repair through ubiquitination, *Acta Biochimica et Biophysica Sinica* 43, 919-929
82. Menoni, H., Shukla, M. S., Gerson, V., Dimitrov, S., and Angelov, D. (2011) Base excision repair in dinucleosomes, *Nucleic Acids Research*. 4, 203-209
83. Brettel, K., and Byrdin, M. (2010) Reaction mechanisms of DNA photolyase, *Current Opinion in Structural Biology* 20, 693-701.

- 84.Sancar, A. (2008) Structure and function of photolyase and in-vivo enzymology, *Journal of Biological Chemistry* 283, 32153-32157.
- 85.Eker, A. P. M., Dekker, R. H., and Berends, W. (1981) Photoreactivating enzyme from *Streptomyces grieseus*. On the nature of the chromomophore cofactor in streptomyces grieseus photoreactivating enzymes, *Photochemistry and Photobiology* 33, 65-72.
- 86.Eker, A. P. M., Hessels, J. K. C., and van de Velde, J. (1988) Photoreactivating enzyme from the green alga *Scenedesmus acutus*. Evidence for the presence of two different flavin chromophores, *Biochemistry* 27, 1758-1765.
- 87.Jorns, M. S., Sancar, G. B., and Sancar, A. (1984) Identification of a neutral flavin radical and characterization of a second chromophore in *Escherichia coli* DNA photolyase, *Biochemistry* 23, 2673-2679.
- 88.Donnellan, J. E., and Setlow, R. B. (1965) Thymine photoproducts but not thymine dimers found in ultraviolet-irradiated bacterial spores, *Science* 149, 308-310.
- 89.Setlow, P. (2001) Resistance of spores of *Bacillus* species to ultraviolet light, *Environmental and Molecular Mutagenesis* 38, 97-104.
- 90.Setlow, P. (2007) I will survive: DNA protection in bacterial spores, *Trends In Microbiol* 15, 172-180.
- 91.Magill, N. G., Loshon, C. A., and Setlow, P. (1990) Small, acid-soluble, spore proteins and their genes from two species of *Sporosarcina*, *FEMS Microbiology Letters* 72, 293-297.
- 92.Mason, J. M., and Setlow, P. (1986) Essential role of small, acid-soluble spore proteins in resistance of *Bacillus subtilis* spores to UV light, *Journal of Bacteriology* 167, 174-178.
- 93.Moeller, R., Setlow, P., Reitz, G., and Nicholson, W. L. (2009) Roles of small, acid-soluble spore proteins and core water content in survival of *Bacillus subtilis* spores exposed to environmental solar UV radiation, *Applied Environmental Microbiology* 75, 5202-5208.
- 94.Lee, K. S., Bumbaca, D., Kosman, J., Setlow, P., and Jedrzejewski, M. J. (2008) Structure of a protein-DNA complex essential for DNA protection in spores of *Bacillus* species, *Proceedings of the National Academy of Sciences* 105, 2806-2811.

95. Mohr, S. C., Sokolov, N. V., He, C. M., and Setlow, P. (1991) Binding of small acid-soluble spore proteins from *Bacillus subtilis* changes the conformation of DNA from B to A, *Proceedings of the National Academy of Sciences* 88, 77-81.
96. Fairhead, H., Setlow, B., and Setlow, P. (1993) Prevention of DNA damage in spores and in vitro by small, acid-soluble proteins from *Bacillus* species, *Journal of Bacteriology* 175, 1367-1374.
97. Setlow, P. (1988) Small, Acid-Soluble Spore Proteins of *Bacillus* Species: Structure, synthesis, genetics, function, and degradation, *Annual Review of Microbiology* 42, 319-338.
98. Tovar-Rojo, F., and Setlow, P. (1991) Effects of mutant small, acid-soluble spore proteins from *Bacillus subtilis* on DNA in vivo and in vitro, *Journal of Bacteriology* 173, 4827-4835.
99. Nicholson, W. L., Setlow, B., and Setlow, P. (1991) Ultraviolet irradiation of DNA complexed with alpha/beta-type small, acid-soluble proteins from spores of *Bacillus* or *Clostridium* species makes spore photoproduct but not thymine dimers, *Proceedings of the National Academy of Sciences* 88, 8288-8292.
100. Jones, S., van Heyningen, P., Berman, H. M., and Thornton, J. M. (1999) Protein-DNA interactions: A structural analysis, *Journal of Molecular Biology* 287, 877-896.
101. Kundu, L. M., Linne, U., Marahiel, M., and Carell, T. (2004) RNA is more UV resistant than DNA: The formation of UV-induced DNA lesions is strongly sequence and conformation dependent, *Chemistry – A European Journal* 10, 5697-5705.
102. Griffith, J., Makhov, A., Santiago-Lara, L., and Setlow, P. (1994) Electron microscopic studies of the interaction between a *Bacillus subtilis* alpha/beta-type small, acid-soluble spore protein with DNA: Protein binding is cooperative, stiffens the DNA, and induces negative supercoiling, *Proceedings of the National Academy of Sciences* 91, 8224-8228.
103. Setlow, B., and Setlow, P. (1987) Thymine-containing dimers as well as spore photoproducts are found in ultraviolet-irradiated *Bacillus subtilis* spores that lack small acid-soluble proteins, *Proceedings of the National Academy of Sciences* 84, 421-423.
104. Fairhead, H., Setlow, B., Waites, W. M., and Setlow, P. (1994) Small, acid-soluble proteins bound to DNA protect *Bacillus subtilis* spores from being killed by freeze-drying, *Applied Environmental Microbiology* 60, 2647-2649.

105. Setlow, B., and Setlow, P. (1993) Binding of small, acid-soluble spore proteins to DNA plays a significant role in the resistance of *Bacillus subtilis* spores to hydrogen peroxide, *Applied Environmental Microbiology* 59, 3418-3423.
106. Varghese, A. J. (1970) 5-Thyminy-5,6-dihydrothymine from DNA irradiated with ultraviolet light, *Biochemical and Biophysical Research Communications* 38, 484-490.
107. Lin, G., and Li, L. (2010) Elucidation of spore-photoproduct formation by isotope labeling, *Angew Chemical International Edition English* 49, 9926-9929.
108. Fairhead, H., and Setlow, P. (1992) Binding of DNA to alpha/beta-type small, acid-soluble proteins from spores of *Bacillus* or *Clostridium* species prevents formation of cytosine dimers, cytosine-thymine dimers, and bipyrimidine photoadducts after UV irradiation, *Journal of Bacteriology* 174, 2874-2880.
109. Fajardo-Cavazos, P., Salazar, C., and Nicholson, W. L. (1993) Molecular cloning and characterization of the *Bacillus subtilis* spore photoproduct lyase (spl) gene, which is involved in repair of UV radiation-induced DNA damage during spore germination, *Journal of Bacteriology* 175, 1735-1744.
110. Slieman, T. A., Rebeil, R., and Nicholson, W. L. Spore photoproduct (SP) lyase from *Bacillus subtilis* specifically binds to and cleaves SP (5-Thyminy-5,6-Dihydrothymine) but not cyclobutane pyrimidine dimers in UV-irradiated DNA, *American Society for Microbiology*. 571, 249-246.
111. Kim, S. J., Lester, C., and Begley, T. P. (1995) Synthesis of the dinucleotide spore photoproduct, *The Journal of Organic Chemistry* 60, 6256-6257.
112. Nicewonger, R., and Begley, T. P. (1997) Synthesis of the spore photoproduct, *Tetrahedron Letters* 38, 935-936.
113. Friedel, M. G., Berteau, O., Pieck, J. C., Atta, M., Ollagnier-de-Choudens, S., Fontecave, M., and Carell, T. (2006) The spore photoproduct lyase repairs the 5*S*- and not the 5*R*-configured spore photoproduct DNA lesion, *Chemical Communications* 4, 445-447.
114. Chandra, T., Silver, S. C., Zilinskas, E., Shepard, E. M., Broderick, W. E., and Broderick, J. B. (2009) Spore photoproduct lyase catalyzes specific repair of the 5*R* but not the 5*S* spore photoproduct, *Journal of the American Chemical Society* 131, 2420-2421.
115. Heil, K., Kneutinger, A. C., Schneider, S., Lischke, U., and Carell, T. (2011) crystal structures and repair studies reveal the identity and the base-pairing properties of the UV-

- induced spore photoproduct DNA lesion, *Chemistry – A European Journal* 17, 9651-9657.
116. Lin, G., Chen, C.-H., Pink, M., Pu, J., and Li, L. (2011) Chemical synthesis, crystal structure and enzymatic evaluation of a dinucleotide spore photoproduct analogue containing a formacetal linker, *Chemistry – A European Journal* 17, 9658-9668.
117. Mehl, R. A., and Begley, T. P. (1999) Mechanistic studies on the repair of a novel DNA photolesion: The spore photoproduct, *Organic Letters* 1, 1065-1066.
118. Yang, L., Lin, G., Liu, D., Dria, K. J., Telser, J., and Li, L. (2011) Probing the reaction mechanism of spore photoproduct lyase (SPL) via diastereoselectively labeled dinucleotide SP TpT substrates, *Journal of the American Chemical Society* 133, 10434-10447.
119. Chandor-Proust, A., Berteau, O., Douki, T., Gasparutto, D., Ollagnier-de-Choudens, S., Fontecave, M., and Atta, M. (2008) DNA repair and free radicals, new insights into the mechanism of spore photoproduct lyase revealed by single amino acid substitution, *Journal of Biological Chemistry* 283, 36361-36368.
120. Cadet, J., Anselmino, C., Douki, T., and Voituriez, L. (1992) New trends in photobiology: Photochemistry of nucleic acids in cells, *Journal of Photochemistry and Photobiology* 15, 277-298.
121. Douki, T., and Cadet, J. (2003) Formation of the spore photoproduct and other dimeric lesions between adjacent pyrimidines in UVC-irradiated dry DNA, *Photochemical & Photobiological Sciences* 2, 433-436.
122. Butenandt, J., Burgdorf, L. T., and Carell, T. (1999) Synthesis of DNA lesions and DNA-lesion-containing oligonucleotides for DNA-repair studies, *Synthesis* 5, 1085-1105.
123. Burckstummer, E., and Carell, T. (2008) Synthesis and properties of DNA containing a spore photoproduct analog, *Chemical Communications*.12, 4037-4039.
124. Mantel, C., Chandor, A., Gasparutto, D., Douki, T., Atta, M., Fontecave, M., Bayle, P.-A., Mouesca, J.-M., and Bardet, M. (2008) Combined NMR and DFT studies for the absolute configuration elucidation of the spore photoproduct, a UV-induced DNA lesion, *Journal of the American Chemical Society* 130, 16978-16984.
125. Husain, I., Sancar, G. B., Holbrook, S. R., and Sancar, A. (1987) Mechanism of damage recognition by *Escherichia coli* DNA photolyase, *Journal of Biological Chemistry* 262, 13188-13197.

126. Mees, A., Klar, T., Gnau, P., Hennecke, U., Eker, A. P. M., Carell, T., and Essen, L.-O. (2004) Crystal structure of a photolyase bound to a CPD-like DNA lesion after in situ repair, *Science* 306, 1789-1793.
127. Wei, Y. (2006) Poor base stacking at DNA lesions may initiate recognition by many repair proteins, *DNA Repair* 5, 654-666.
128. Benjdia, A., Heil, K., Barends, T. R. M., Carell, T., and Schlichting, I. (2012) Structural insights into recognition and repair of UV-DNA damage by Spore Photoproduct Lyase, a radical SAM enzyme, *Nucleic Acids Research* 18, 9308-9318
129. Slupphaug, G., Mol, C. D., Kavli, B., Arvai, A. S., Krokan, H. E., and Tainer, J. A. (1996) A nucleotide-flipping mechanism from the structure of human uracil-DNA glycosylase bound to DNA, *Nature* 384, 87-92.
130. McCullough, A. K., Dodson, M. L., Schärer, O. D., and Lloyd, R. S. (1997) The role of base flipping in damage recognition and catalysis by T4 endonuclease V, *Journal of Biological Chemistry* 272, 27210-27217.
131. Lawrence, C. C., and Stubbe, J. (1998) The function of adenosylcobalamin in the mechanism of ribonucleoside triphosphate reductase from *Lactobacillus leichmannii*, *Current Opinion in Chemical Biology* 2, 650-655.
132. Vignais, P. M., Billoud, B., and Meyer, J. (2001) Classification and phylogeny of hydrogenases, *FEMS Microbiology Reviews* 25, 455-501.
133. Peters, J. W., Lanzilotta, W. N., Lemon, B. J., and Seefeldt, L. C. (1998) X-ray crystal structure of the Fe-only hydrogenase (CpI) from *Clostridium pasteurianum* to 1.8 angstrom resolution, *Science* 282, 1853-1858.
134. Shepard, E. M., Boyd, E. S., Broderick, J. B., and Peters, J. W. (2011) Biosynthesis of complex iron-sulfur enzymes, *Current Opinion in Chemical Biology* 15, 319-327.
135. Nicolet, Y., Lemon, B. J., Fontecilla-Camps, J. C., and Peters, J. W. (2000) A novel FeS cluster in Fe-only hydrogenases, *Trends in Biochemical Sciences* 25, 138-143.
136. Mulder, David W., Shepard, Eric M., Meuser, Jonathan E., Joshi, N., King, Paul W., Posewitz, Matthew C., Broderick, Joan B., and Peters, John W. (2011) Insights into [FeFe] hydrogenase structure, mechanism, and maturation, *Structure* 19, 1038-1052.
137. Silakov, A., Wenk, B., Reijerse, E., and Lubitz, W. (2009) 14N HYSORE investigation of the H-cluster of [FeFe] hydrogenase: Evidence for a nitrogen in the dithiol bridge, *Physical Chemistry Chemical Physics* 11, 6592-6599.

138. Pandey, A. S., Harris, T. V., Giles, L. J., Peters, J. W., and Szilagyi, R. K. (2008) Dithiomethylether as a ligand in the hydrogenase H-cluster, *Journal of the American Chemical Society* 130, 4533-4540.
139. Ryde, U., Greco, C., and De Gioia, L. (2010) Quantum refinement of [FeFe] hydrogenase indicates a dithiomethylamine ligand, *Journal of the American Chemical Society* 132, 4512-4513.
140. Mulder, D. W., Boyd, E. S., Sarma, R., Lange, R. K., Endrizzi, J. A., Broderick, J. B., and Peters, J. W. (2010) Stepwise [FeFe] hydrogenase H-cluster assembly revealed in the structure of HydA^{ΔEFG}, *Nature* 465, 248-251.
141. McGlynn, S., Ruebush, S., Naumov, A., Nagy, L., Dubini, A., King, P., Broderick, J., Posewitz, M., and Peters, J. (2007) In vitro activation of [FeFe] hydrogenase: New insights into hydrogenase maturation, *Journal of Biological Inorganic Chemistry* 12, 443-447.
142. McGlynn, S. E., Mulder, D. W., Shepard, E. M., Broderick, J. B., and Peters, J. W. (2009). Hydrogenase cluster biosynthesis: Organometallic chemistry nature's way, *Dalton Transactions* 22, 4274-4285.
143. Posewitz, M. C., King, P. W., Smolinski, S. L., Zhang, L., Seibert, M., and Ghirardi, M. L. (2004) Discovery of two novel radical *S*-Adenosylmethionine proteins required for the assembly of an active [Fe] hydrogenase, *Journal of Biological Chemistry* 279, 25711-25720.
144. Meyer, J. (2007) [FeFe] hydrogenases and their evolution: A genomic perspective, *Cellular and Molecular Life Sciences* 64, 1063-1084.
145. King, P. W., Posewitz, M. C., Ghirardi, M. L., and Seibert, M. (2006) Functional studies of [FeFe] hydrogenase maturation in an *Escherichia coli* biosynthetic system, *Journal of Bacteriology* 188, 2163-2172.
146. Peters, J. W., Szilagyi, R. K., Naumov, A., and Douglas, T. (2006) A radical solution for the biosynthesis of the H-cluster of hydrogenase, *FEBS Letters* 580, 363-367.
147. McGlynn, S. E., Shepard, E. M., Winslow, M. A., Naumov, A. V., Duschene, K. S., Posewitz, M. C., Broderick, W. E., Broderick, J. B., and Peters, J. W. (2008) HydF as a scaffold protein in [FeFe] hydrogenase H-cluster biosynthesis, *FEBS Letters* 582, 2183-2187.
148. Shepard, E. M., McGlynn, S. E., Bueling, A. L., Grady-Smith, C., George, S. J., Winslow, M. A., Cramer, S. P., Peters, J. W., and Broderick, J. B. (2010) Synthesis of the

2Fe-subcluster of the [FeFe]-hydrogenase H-cluster on the HydF scaffold, Proceedings of the National Academy of Sciences 107, 10448-10453.

149.Czech, I., Silakov, A., Lubitz, W., and Happe, T. (2010) The [FeFe]-hydrogenase maturase HydF from *Clostridium acetobutylicum* contains a CO and CN⁻ ligated iron cofactor, FEBS Letters 584, 638-642.

150.Pilet, E., Nicolet, Y., Mathevon, C., Douki, T., Fontecilla-Camps, J. C., and Fontecave, M. (2009) The role of the maturase HydG in [FeFe]-hydrogenase active site synthesis and assembly, FEBS Letters. 583, 506-511.

151.Driesener, R. C., Challand, M. R., McGlynn, S. E., Shepard, E. M., Boyd, E. S., Broderick, J. B., Peters, J. W., and Roach, P. L. (2010) [FeFe] hydrogenase cyanide ligands derived from *S*-adenosylmethionine-dependent cleavage of tyrosine, *Angewandte Chemie International Edition* 49, 1687-1690.

152.Shepard, E. M., Duffus, B. R., George, S. J., McGlynn, S. E., Challand, M. R., Swanson, K. D., Roach, P. L., Cramer, S. P., Peters, J. W., and Broderick, J. B. (2010) [FeFe] hydrogenase maturation: HydG-catalyzed synthesis of carbon monoxide, *Journal of the American Chemical Society* 132, 9247-9249.

153.Tron, C., Cherrier, M. V., Amara, P., Martin, L., Fauth, F., Fraga, E., Correard, M., Fontecave, M., Nicolet, Y., and Fontecilla-Camps, J. C. (2011) Further characterization of the [FeFe] hydrogenase maturase HydG, *European Journal of Inorganic Chemistry* 2011, 1121-1127.

154.Kuchenreuther, J. M., George, S. J., Grady-Smith, C. S., Cramer, S. P., and Swartz, J. R. (2011) Cell-free H-cluster synthesis and [FeFe] hydrogenase activation: All Five CO and CN⁻ ligands derive from tyrosine, *PLoS ONE* 6, e20346.

155.Joshi, N., Shepard, E. M., Byer, A. S., Swanson, K. D., Broderick, J. B., and Peters, J. W. (2012) Iron-sulfur cluster coordination in the [FeFe]-hydrogenase H cluster biosynthetic factor HydF, FEBS Letters 22, 3939-3943

156.Nicolet, Y., Rubach, J. K., Posewitz, M. C., Amara, P., Mathevon, C., Atta, M., Fontecave, M., and Fontecilla-Camps, J. C. (2008) X-ray structure of the [FeFe] hydrogenase maturase HydE from *Thermotoga maritima*, *Journal of Biological Chemistry* 283, 18861-18872.

157.Rubach, J. K., Brazzolotto, X., Gaillard, J., and Fontecave, M. (2005) Biochemical characterization of the HydE and HydG iron-only hydrogenase maturation enzymes from *Thermotoga maritima*, FEBS Letters 579, 5055-5060.

158. Jameson, G. N., Coper, M. M., Hernández, H. L., Johnson, M. K., and Huynh, B. H. (2004) Role of the [2Fe-2S] cluster in recombinant *Escherichia coli* biotin synthase, *Biochemistry* 43, 2022-2031.
159. Kuchenreuther, J. M., Britt, R. D., and Swartz, J. R. (2012) New insights into [FeFe] hydrogenase activation and maturase function, *PLoS ONE* 7, e45850.
160. Kuchenreuther, J. M., Stapleton, J. A., and Swartz, J. R. (2009) tyrosine, cysteine, and *S*-adenosyl methionine stimulate in vitro [FeFe] hydrogenase activation, *PLoS ONE* 4, e7565.
161. Boswell, N.W.B. (2011) Montana State University Bozeman.

CHAPTER TWO

SOLUTION PHASE DYNAMICS OF THE DNA REPAIR ENZYME SPORE
PHOTOPRODUCT LYASE AS PROBED BY
H/D EXCHANGE

Contribution of Authors and Co-Authors

Manuscript in Chapter 2

Author: Shourjo Ghose

Contributions: Protein purifications. Research design, assay set up, method development, LCMS analysis. Manuscript preparation

Co-author: Jonathan Hilmer

Contributions: Research design, method development, LCMS analysis, theoretical calculations, provided some text and edits of manuscript

Co-author: Kaitlin Duschene

Contributions: Generated scheme 1 and figure 5

Co-author: Brian Bothner

Contributions: Provided valuable insight into the techniques involved with H/D exchange, interpretation of results and manuscript editing.

Co-author: Joan B. Broderick

Contributions: Overall conception and financial support of project, assistance in research design and interpretation of results, extensive detailed editing of manuscript.

Manuscript Information Page

Shourjo Ghose, Jonathan K. Hilmer, Kaitlin Duschene, Brian Bothner, and Joan B. Broderick*

Journal: FEBS Letters

Status of the manuscript:

Prepared for submission to a peer-reviewed journal

Officially submitted to a peer-reviewed journal

Accepted by a peer-reviewed journal

Published in a peer-reviewed journal

CHAPTER 2

SOLUTION PHASE DYNAMICS OF THE DNA REPAIR ENZYME SPORE
PHOTOPRODUCT LYASE AS PROBED BY H/D EXCHANGE

Shourjo Ghose, Jonathan K. Hilmer, Kaitlin Duschene, Brian Bothner, and Joan B. Broderick*

Department of Chemistry and Biochemistry, Montana State University, Bozeman, MT
59717

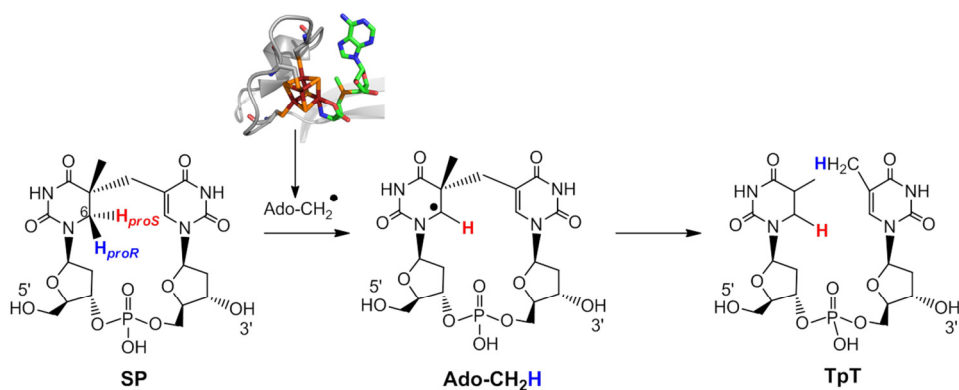
Abstract

Spore photoproduct lyase (SPL) catalyzes the direct reversal of spore photoproduct (SP), the major UV-induced DNA lesion in spore-forming organisms, in a reaction that utilizes S-adenosylmethionine (SAM) as a cofactor. We have utilized H/D exchange under anaerobic conditions to explore the conformational changes in SPL brought about upon binding of SAM, undamaged oligonucleotide, and the minimal substrate 5R -SPTpT dinucleotide. The results show that in the presence of SAM, binding of the 5R -SPTpT dinucleotide results in a significant reduction in H/D exchange, indicating a shift of 20 amide protons from a rapidly-exchangable state to a fully-protected conformation. Although the oligonucleotide is larger than the 5R -SPTpT, its binding induced fewer shifts in the H/D exchange population, with 10 protons protected relative to enzyme alone. In the absence of SAM, neither the oligonucleotide nor the dinucleotide ligand produced a significant perturbation in H/D exchange, indicating SAM is a requisite binding partner. Performing the same experiments in aerobic conditions reduced the magnitude of ligand-induced structural changes, confirming the importance of the oxygen-sensitive iron-sulfur cluster for SAM and substrate binding.

Introduction

Bacterial spores exhibit remarkable resistance to various environmental stressors, including wet and dry heat, variations in temperature, and UV radiation [1]. The UV resistance of bacterial spores can be attributed to the unusual photochemistry of spore DNA, coupled with the efficient repair of accumulated damage. On exposure of spores

to UV radiation, a unique methylene bridged thymine dimer, 5-thyminy-5,6-dihydrothymine (spore photoproduct or SP) accumulates as the main photoproduct [2-4]. However, this accumulated photo-damage is rapidly repaired upon spore germination, thereby giving rise to the unusual UV resistance of the bacterial spore [1, 5]. The repair of SP is catalyzed by a specialized enzyme, spore photoproduct lyase (SPL), and involves the direct reversal of SP into two thymines in a light-independent reaction (Scheme 1).



Scheme 1: Repair of SP by SP lyase using a radical mediated mechanism. SP lyase is a radical SAM enzyme that repairs the spore specific DNA damage SP. The enzyme utilizes a site differentiated [4Fe-4S] cluster bound to a SAM molecule, which it cleaves to initiate repair.

SPL is a member of the radical S-adenosylmethionine (AdoMet) protein superfamily: this large superfamily includes enzymes that play critical roles in metabolism, and they are found in all kingdoms of life. Radical AdoMet enzymes are involved in cofactor biosynthesis, including biotin [6, 7] [8], the lipoyl cofactor [9-11], the molybdopterin cofactor [12, 13], and the complex metal clusters at the active sites of nitrogenase [14] and hydrogenase [15-17]. Members of this superfamily also generate protein radicals

required for anaerobic glycolysis and anaerobic ribonucleotide reduction [18] and catalyze important modifications of the translational machinery [19, 20].

Radical AdoMet enzymes have in common the utilization of a site-differentiated [4Fe-4S]⁺ cluster (most commonly coordinated by a CX₃CX₂C motif) to reductively cleave AdoMet to generate a 5'-deoxyadenosyl radical intermediate, which subsequently abstracts a hydrogen atom from substrate to initiate catalysis [18, 21-23]. A radical mechanism for repair of SP by SPL first suggested by Mehl and Begley in 1999 [24] has received considerable experimental and computational support in recent years [25-27]. It is generally accepted from these studies that SPL, like lysine 2,3-aminomutase (LAM) but unlike most characterized radical AdoMet enzymes, utilizes AdoMet as a cofactor rather than a substrate and AdoMet is not consumed during SP repair[26].

Compared to the kinetics and cofactor involvement, the structural details of SPL/DNA binding and damage recognition is less well understood.. DNaseI footprinting has been used to demonstrate that SPL can bind to DNA containing an SP lesion and protect it from digestion [28]. It has been suggested that SPL recognizes the SP lesion in a sequence-independent manner, as a result of helical distortion of the phosphodiester backbone, and that additional distortion induced by SPL binding helps to initiate repair [28]. Such a model is consistent with the binding mechanisms of a multitude of DNA binding proteins such as Uvr(A)BC exonuclease [29], DNA photolyase [30, 31], and phage T4 endonuclease V[32]. Studies using stereochemically-defined synthetic SP substrates have demonstrated that SPL repairs only the 5R(5'→3')SP, with the presence of a phosphodiester linkage in SP enhancing the rate of repair [33-35]. These results

suggest that SPL has an active site that is capable of productive binding of only a single, well-defined diastereomer of SP. A recently published crystal structure of SPL bound to the 5*R*-SP di-nucleoside and SAM [36] reveals a characteristic $\alpha_6\beta_6$ partial triose-phosphate isomerase (TIM) barrel consisting of a laterally open active site that could accommodate a large substrate. It was proposed that SPL has a mechanism of binding similar to other DNA-binding enzymes such DNA endonuclease and probably employed a base-flipping mechanism to bind and initiate repair of SP [36, 37] Despite the insights provided by this crystal structure, many outstanding questions remain unanswered: among these are the role of the catalytic 4Fe-4S cluster in substrate recognition and binding, the possible role of SAM in ordering the enzyme active site prior to SP binding, and the local and global structural changes brought about by cofactor and substrate binding in a non-restricted aqueous environment.

In order to obtain more insight into the role of protein dynamics in the binding and recognition of DNA damage by SPL in solution, we have carried out hydrogen-deuterium (H/D) exchange) reactions with mass spectrometry detection. The basic mechanism of HDX involves an abstraction of an amide proton by OH/D⁻ followed by its replacement by an deuterium from the abstracting solvent, as described in the general Linderstrom-Lang scheme [40]. In this scheme, it is a prerequisite for exchange that the amide proton be available for exchange: exchange can be inhibited due to proton participation in hydrogen bonds, especially in the case of bonds within secondary structural elements[38, 39] These inhibitory bonds can be found in the core of a protein, but they are not specifically restricted to that region: model studies have found amide protons with slow

exchange rate despite close proximity to solvent. In these cases, strong hydrogen bonding was shown to be sufficient to inhibit HDX[38-40]

The net sum of hydrogen bonding and similar effects is to reduce the observed H/D exchange rate, compared to the rate observed for hypothetical unstructured or random coil conformations. In this way, HDX can be a sensitive, specific, and relevant probe for structural conformations of proteins in solution: if an experimental treatment reduces the exchange rate for a number of protons relative to the control, it can be inferred that the experimental conditions may have resulted in an increase in hydrogen bonding. When coupled with mass spectrometry (HDX-MS), this approach does not require large quantities or high concentrations of protein, and experiments can be conducted very rapidly[41, 42]. The additional challenges of working with oxygen-sensitive proteins such as SPL can also be addressed with mass spectrometry: the rapid rate of analysis minimizes potential for oxidation, and the small sample sizes and automated HPLC equipment both aid in the practical concerns of maintaining an anaerobic environment. Our primary objective in this endeavor is to investigate the total changes brought about by ligand and/or cofactor binding to SPL, with constraints of biologically relevant conditions in solution. In addition to collecting novel data on the SP/ligand system, our experiments also demonstrate the validity and utility of the HDX-MS approach for difficult real-world protein studies, where traditional approaches (X-ray crystallography, nuclear magnetic resonance) are unavailable and/or unviable. Moreover, we propose here that our system does indeed possess the sensitivity to differentiate between isomers of

small molecule substrates and therefore can be employed as a general screening mechanism for potential ligands in other protein systems.

In order to achieve a thorough characterization of potential conformational changes brought about by cofactor/ substrate binding, we decided to utilize the physiologically relevant pure synthetic 5*R*-SPTpT dinucleotide. This stereochemically defined substrate analog has been shown to act as an excellent mimic for SP in previous studies done by the Broderick group and is shown to be repaired by SPL with a specific activity of $7.1 \pm 0.6 \text{ nmol min}^{-1} \text{ mg}^{-1}$ [42]. In all cases, our experiments were also repeated with dinucleoside analog (5*R*-SP) of the aforementioned small molecule, to obtain a qualitative measure of global conformational change induced by ligand binding.

Our results provide evidence for a conformational change of SPL upon binding AdoMet, and this conformational change is enhanced upon binding substrate. Further, we demonstrate that AdoMet binding is a requisite precursor to substrate binding, indicating that an AdoMet-induced conformational change enhances the binding affinity for substrate.

Materials and Methods

Protein Expression and Purification

The *N*-terminal hexa-histidine tagged SP lyase from *Clostridium acetobutylicum* (*C.a*) was expressed using *Escherichia coli* Tuner(DE3)pLysS cells transformed with a pET14b expression vector containing the *splB* gene. The resulting protein was grown in minimal media and purified anaerobically by Ni-HisTrap chromatography and FPLC as previously described [43, 44]. The protein was anaerobically dialyzed in 20 mM sodium phosphate,

350 mM NaCl, 5% glycerol, pH 7.5. The protein was then concentrated using an Amicon concentrator fitted with an YM-10 membrane to a final concentration of ~650 μ M. All protein samples used in assays were prepared in the MBRAUN box ($O_2 \leq 1$ ppm) unless mentioned otherwise. The protein and iron concentration were determined by methods previously described [45, 46]. SAM was synthesized as previously described [47].

Preparation of Enzyme/Ligand Mixtures

A 6-mer oligoneucleotide (5'-GCAAGT-3' and complement 5'-ACTTGC-3') were obtained from Integrated DNA Technologies (Coralville, IA). Equimolar amounts of each strand were mixed in water and then annealed by heating to boiling, followed by removal of the heat source and slow cooling of the water temperature to 25°C. Proteins were prepared in advance in a buffer consisting of 40mM sodium phosphate, 350mM NaCl, 5% glycerol, pH 7.5 under appropriate anaerobic conditions. Protein solutions were diluted to an identical concentration for all assays, and identical aliquots (10 μ L) were split for each pair of control/reaction experiments. A ligand solution or control buffer was added to each of the half of the matched control/experimental protein samples. The ligand solutions consisted of the following: 6mer oligo, synthetic 5R-SPTpT, 5R-SP [43, 44], and SAM. All anaerobic assays were conducted the with buffer and/or D_2O preveosly degassed on the schlenk line. The degassed buffer and/or D_2O was brought into the MBRAUN glove box and the assays prepared as mentioned above. All aerobic samples were handled in an identical fashion as their anaerobic counterpart with the exception of the degassing step and were thereafter prepared on benchtop. The preparation of all enzyme/ligand mixtures was conducted identically, with matched

timing for solution preparation steps and for the delay (10min) between preparation and subsequent H/D exchange reactions.

H/D Exchange Reactions

The 10 μ L aliquots of protein/ligand solutions were transferred to autosampler vials and sealed: the capped tubes were then covered with teflon tape to minimize O₂ contamination. Two Hamilton gas tight syringes were filled with 40 μ L of anaerobic D₂O-containing buffer (20 mM sodium phosphate, 350 mM NaCl, 5% glycerol, pD 7.9) and their tips covered with Teflon tape. The D₂O and sample were then mixed by puncturing the septum of the MS vial and manually mixed with the Hamilton syringe. Following mixing, the vial was placed into the HPLC autosampler and the automated sampling series was begun immediately: the interval between samples was 2 min. The autosampler was not within an anaerobic environment, but the anaerobic reactions remained sealed in the autosampler vials for the duration of the reactions (30 min). Injection of the sample into the HPLC system provided the quenching step, as described below.

LC-ESI/MS with MicrOTOF Mass Spectrometer

The HPLC system was composed of an Agilent 1100 HPLC with binary pump, temperature-controlled autosampler and column compartment, and a C4 reverse phase column (8x1 mm, Microchrom Biosciences). Solvents consisted of H₂O with 0.1% (v/v) formic acid in channel "A" and acetonitrile with 0.1% formic acid in channel "B". The autosampler and reactions were held at 25°C, and the column compartment was maintained at 4°C to maximize reproducibility. Prior to sample injection, the C4 column

was equilibrated with 20% “B” at 0.6 mL/min: this flow rate was maintained throughout the run. Concurrent with sample injection ($t = 0.01$ min), the solvent composition was changed via the binary pump to 100% “B”: the residual water in the system and column were sufficient to slightly delay the elution of the protein from the flow-through. The protein elution peak was centered at approximately 0.4 minutes. Following protein elution, at 1.21 min the solvent composition was changed back to 20% B for column re-equilibration. The mass spectra were obtained on a Bruker micrOTOF Mass Spectrometer equipped with an ESI source. The capillary exit voltage was 120V and gas temperature was 200°C. All data were recorded in positive mode between 300 and 3000 m/z in profile mode. The hardware summation time was 1 second with no rolling averaging.

Quenching of the H/D exchange reaction was a consequence of sample injection into the HPLC system. A flow rate of 600 $\mu\text{L}/\text{min}$ carried the sample from the autosampler (maintained at 25 °C) to the column compartment and reverse-phase column (maintained at 4 °C) in less than 2 seconds. Although this temperature produces more back-exchange compared to 0 °C, it is more stable. The solvents also provide quenching due to the low pH and reduced water composition of the loading solvent: 80/20 H₂O/acetonitrile with 0.1% (v/v) formic acid. A control reaction was run immediately following each experimental reaction to account for hidden variation in the instrumentation, and replicates of control/experiment reaction pairs were conducted on separate days to ensure unbiased results.

Analysis of H/D Exchange Data

With the described chromatographic system, the protein eluted at 0.4 min during the 2 min run. The resulting mass spectra were then averaged and processed using the Data Analysis 4.0 software suite supplied by Bruker Daltonics. The Maximum Entropy routine was used for charge-state deconvolution of the raw data, which were then exported into text files: these steps were automated via scripts to ensure reproducibility. The deconvoluted spectra were processed using Python and Scipy scripts, a reference spectrum of a 0% D₂O sample was used to calculate the cross-correlation with the experimental spectra for the true HDX reactions. The cross-correlation function produced a symmetric peak centered at the deuterium uptake of the experimental sample, describing the shift between reference and experimental peaks. These calculations were manually verified against the more common centroid peak assignment method, but the use of cross-correlation was less sensitive to bias, permitted the use of noisier spectra, and permitted a fully-automated processing workflow. The shape and symmetry of the cross-correlation shift plot also provided quality control for deviations in peak shapes between the reference and experimental spectra: none were observed. A minimum of three trials were conducted for each experiment. Although a control protein reaction was run with every experimental reaction, the H/D exchange rates of this control reaction were not used to apply any correction factors: all experimental replicates are unique and unmodified, and they were collected non-sequentially with delay intervals (up to days) to ensure they were independent measurements. The data thus obtained were plotted using

Origin 8.0 (MicroCal, MA). The standard deviation was reported as the variation in deuterium uptake between the independent trials at each time point.

Results

H/D Exchange into SPL Alone

The enzyme in non-deuterated buffer (Fig 2) has a mass of 41118.0 Da. On dilution with D₂O, a rapid initial uptake of deuterons is observed as indicated by a mass increase of 186 Da within the first five minutes. The rate of deuterium uptake slows in subsequent injections, reaching a plateau at approximately 30 min with an average mass increase of 228.8 (\pm 2.2 Da), indicating significant exposure of solvent-exchangeable protons in SPL alone.

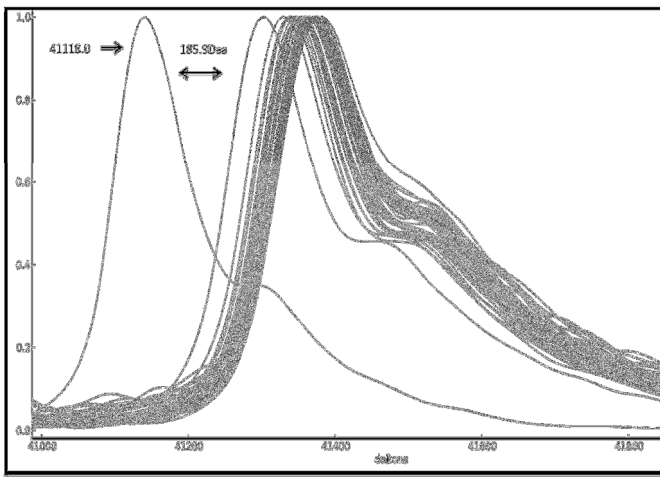


Figure 2: Change in mass of SPL upon dilution into D₂O buffer. Data was collected over 30 minutes at 5 minute intervals. The mass of the non deuterated SPL is 41118.0 kDa. The shift of the mass peak is indicative of the mass increase of the enzyme on deuteration. The initial deuterium uptake is significant as indicated by the discernible shift in the spectra. The uptake slows down significantly over time. The spectral feature at 41300 m/z is most likely a species of the intact protein with an oxidized methionine, most likely the thiol group with a sulfone adduct.

The mass change due to deuterium uptake for SPL, in absence of cofactor/ligands, was the same regardless of whether the exchange was carried out under aerobic or anaerobic conditions (data not shown). Experiments were terminated after 30 minutes for three primary reasons: the short length of time ensures that the anaerobic experiments have experienced minimal O₂ contamination, SPL degradation such as oxidation or [4Fe-4S] cluster loss is avoided, and the rate of H/D exchange is slowed to insignificant levels by that time. Collection of additional data of experimental relevance would require hours or days, and it is not possible to maintain the enzyme system for that length of time.

Effect of SAM on H/D Exchange

In the presence of SAM, dilution of SPL into D₂O also resulted in effectively full exchange within 30 minutes: this pattern repeated in all experimental trials. However, the magnitude of the mass increase in the presence of SAM is smaller than that observed in its absence, indicating that some of the exchangeable protons on SPL transitioned to an effectively inexchangeable conformation upon SAM binding. The average difference in uptake at 30 min between the SPL alone and the aerobic SPL+SAM samples was 6.3 ± 0.6 , indicating that the binding of SAM protects approximately 6 protons from H/D exchange (Table 1, Fig 3A). SAM binding to radical SAM enzymes is known to involve the [4Fe-4S] cluster, which is generally oxygen sensitive, suggesting the possibility that anaerobic conditions would affect SAM binding and thus H/D exchange.

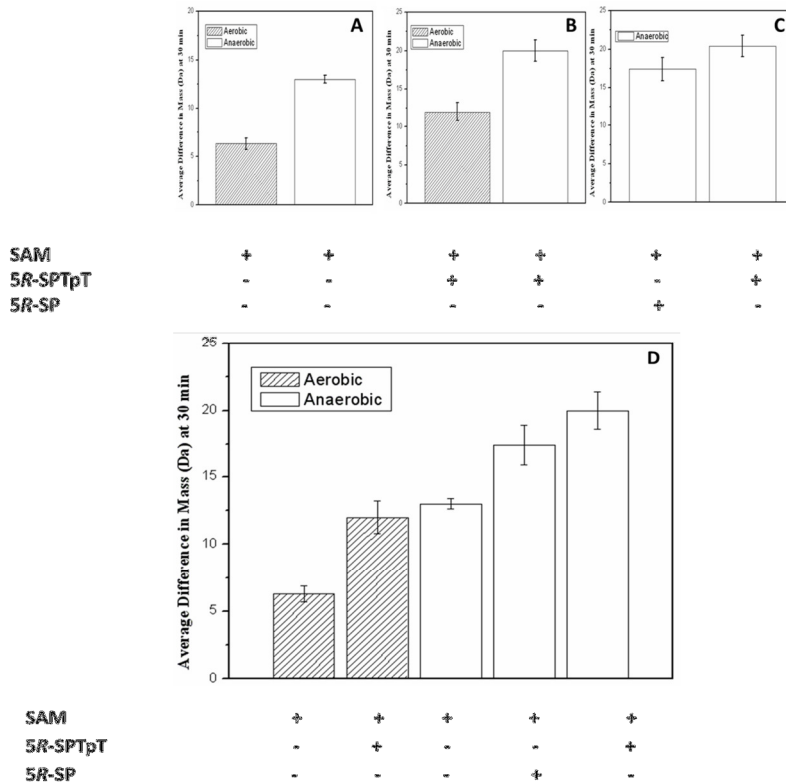


Figure 3: The influence of the effector molecules on SPL as depicted by the comparative difference in deuterium uptake over 30mins. Panel A, B depict the average difference in deuterium uptake with SAM and SAM+5RSPTpT respectively. In the both these cases the experiments were repeated under aerobic and anaerobic conditions. Panel C depicts the difference in deuterium uptake by SPL in the presence of SAM+5RSPTpT and SAM+5RSP, both under anaerobic conditions. Panel D is an overall comparison of the differential deuterium uptake as a function of different conditions and affecter molecules. In all cases the average difference in mass (ΔM (Da)) is calculated by subtracting the average mass of D labeled SPL with the effector molecule at 30min from the average mass of D labeled SPL only at 30min. The data is indicative of significant difference in deuterium uptake between the aerobic and anaerobic trials of the same effector molecule. The most significant difference in uptake is observed when the enzyme is bound to SAM and 5R-SPTpT concomitantly. The standard error was reported as the difference in deuterium uptake between the trials at each injection point.

H/D exchange was therefore also carried out on anaerobic SPL + SAM samples, resulting in a further decrease in deuterium uptake, with a difference in mass change of 13.0 ± 0.4 relative to SPL alone (Table 1, Fig 3A).

Effect of Substrate on H/D Exchange

In the absence of SAM, the presence of a minimal substrate, dinucleotide 5*R*-SPTpT, provided only minimal perturbation of the H/D exchange of SPL, decreasing the mass change by 1.1 ± 0.5 Da (Table 1). A short 6-mer oligonucleotide provided a similar slight perturbation, with a decrease in mass change of 2.6 ± 1.3 Da (Table 1). In the presence of both SAM and the 6-mer oligonucleotide (5'-GCAAGT-3'), the deuterium uptake was comparable to the samples containing only SPL and SAM, with a decrease in deuterium uptake of 6.9 ± 3.4 Da under aerobic conditions, and 10.4 ± 0.8 under anaerobic conditions (Table 1).

Interestingly, a significant decrease in exchangeable sites is observed in SPL samples containing both SAM and the synthetic SP dinucleotide 5*R*-SPTpT (Fig 4). Compared to the samples with SPL alone, those samples containing SPL + SAM + 5*R*-SPTpT showed a decrease in deuterium uptake of 12.0 ± 1.2 Da under aerobic conditions, and 20.4 ± 1.4 Da under anaerobic conditions; these numbers are nearly double those observed for SPL in the presence of SAM alone (Table 1, Fig 3B). Given the small size of SAM, and the small size of the 5*R*-SPTpT dinucleotide substrate, we can conclude that the change in deuterium uptake reflects a reordering of H-bonding arrangement brought about by a dynamic perturbation in the enzyme, rather than simply steric blocking of exchangeable sites by SAM and substrate binding. The crystal structure of SPL was solved recently, utilizing the 5*R*-SP dinucleoside and SAM as minimal substrates [36]. Therefore, we decided to conduct H/D exchange experiments using identical ligands and probe the effects of the phosphodiester linkage on deuterium uptake.

Sample	Difference in ΔM (Da) ($\Delta M_{\text{SPL}} - \Delta M_{\text{sample}}$)
SPL only (control)	N/A
SPL+5R-SPTpT	1.1 ± 0.5
SPL+6mer Oligo	2.6 ± 1.3
SPL+SAM (Aerobic)	6.3 ± 0.6
SPL+SAM (Anaerobic)	13.0 ± 0.4
SPL+SAM+6mer oligo (Aerobic)	6.9 ± 3.4
SPL+SAM+6mer oligo (Anaerobic)	10.4 ± 0.8
SPL+SAM+5R-SPTpT (Aerobic)	12.0 ± 1.2
SPL+SAM+5R-SP (Anaerobic)	17.0 ± 1.5
SPL+SAM+5R-SPTpT (Anaerobic)	20.4 ± 1.4

Table 1: Mass changes in SPL as a result of H/D exchange upon diluting in D₂O. H/D exchange was probed in SPL alone as a control, and then experiments were carried out in the presence of SAM, synthetic dinucleotide spore photoproduct (5R-SPTpT), synthetic dinucleoside spore photoproduct (5R-SP) a 6-mer oligo, or combinations of these as indicated. The difference in mass (ΔM (Da)) is calculated by subtracting the mass of D labeled SPL with the effector molecule at 30min from the mass of D labeled SPL only at 30min. The first column of data shows the mass change of the SPL in each sample as measured 30 min after dilution in D₂O. The second column of data shows the average difference in mass change at 30 min between SPL alone and SPL bound to SAM and/or SP and/or oligo.

Under anaerobic conditions, the samples containing the dinucleoside substrate and SAM showed a small increase in the number of exchangeable sites as compared to the dinucleotide counterpart. This is reflected in an uptake of 17.0 ± 1.5 Da in dinucleoside samples, which is about 3.4 Da less than the dinucleotide counterpart (Table 1 Fig 3 C). Experiments with 5*R*-dinucleoside was not conducted as the mass differences observed with its dinucleotide counterpart was negligible. SPL displays initial, rapid deuterium uptake in the first few minutes after mixing with D₂O, buffer followed by an approach to a limiting value. This behavior is consistent throughout all the experiments irrespective of ligand binding, and all experiments demonstrate completion exchange within the timescale of our experiments: calculations indicate that there should be remaining un-exchanged protons, but they are exchanging at a rate which is so dramatically slowed that they are effectively static and silent compared to our observed exchanging protons. and dynamic changes in SPL upon binding to undamaged DNA and a dinucleotide 5*R*-SPTpT and 5*R*-SP dinucleoside substrate

Experiments conducted over longer periods (60 min, data not shown), confirmed this behavior. This is a critical observation because it rules out one mechanism of H/D exchange for SPL: global protein exposure (“unfolding”).

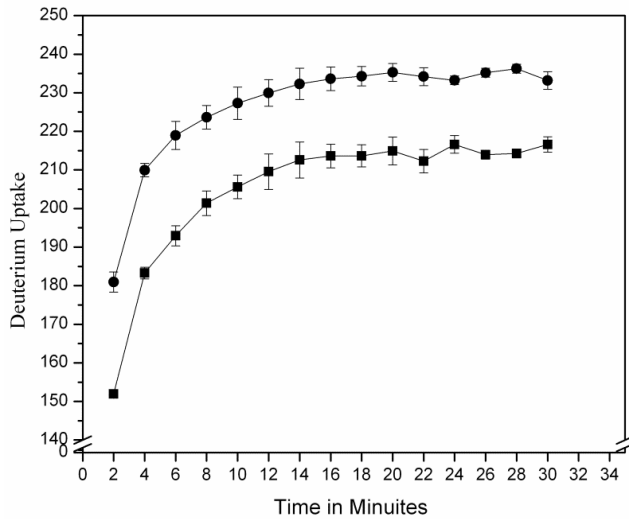


Fig 4: Deuterium uptake of SPL (250 μ M) with and without [SAM (27mM) + SPTpT (375mM)] in the absence of oxygen. The initial uptake of deuterons was around 151.9 \pm 1.0 Da for the bound (■) sample and 180.9 \pm 2.6 Da for the unbound (●). Uptake slowed down after the seventh injection with the maximum uptake being at 215.6 \pm 4.7 Da for the bound and 235.2 \pm 2.3 Da for the unbound

Discussion

Here we have used H/D exchange as a probe to explore the solution phase conformational Global protein exposure is a mechanism that must be examined carefully, since it has the potential to produce misleading results in H/D exchange experiments in the context of ligand binding[48]. If a protein exchanges primarily through a non ligand-bound state, despite the presence of high concentration of ligand, resulting HDX measurements will be a metric of protein/ligand affinity instead of protein structure[48]. Our results exclude this possibility due to the different magnitudes of “unexchangeable” protons: The populations of exchangeable protons would be the same (and small) in global unfolding, so their existence in SPL confirms the presence of limited allosterics upon ligand binding. It should be noted that these allosterics are specifically those

motions and bonds relevant to H/D exchange experiments: large-scale motions which preserve the network of hydrogen bonding may occur but fail to produce substantial differences in the H/D exchange results. The shift of a subset of protons from highly accessible to highly inaccessible states is also consistent with the crystal structure of SPL: SPL has been shown to have a remarkably open conformation, consistent with an enzyme evolved to accommodate a large substrate, DNA in this case (Figure 5 Panel A)[36]. Nor is this structural characteristic uncommon among radical SAM enzymes as evidenced by the structure of PFL-AE[23].

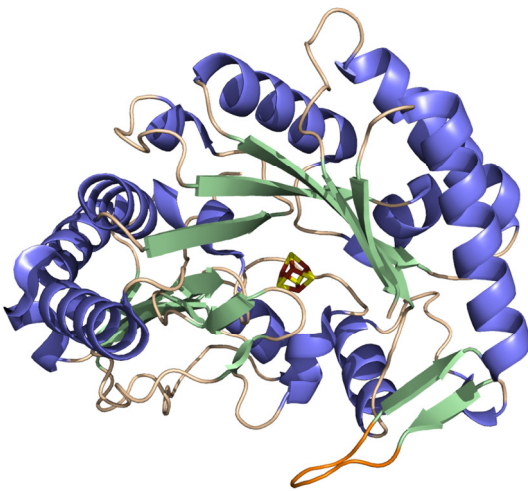


Figure 5: The figure represents the crystal structure of SPL only with the β hairpin highlighted in yellow. The Fe-S cluster resides on the 8 residue loop and is proposed to induce stabilization in that region. The structure depicts a wide lateral opening common in enzymes evolved to fit large substrates such as a double stranded DNA

Based on the structure of SPL, we propose that likely candidates for the rapid H/D exchange include the long β hairpin located between strand $\beta 5$ and $\alpha 6$ [36]. This hairpin motif has been shown to project out of the core domain and its conformation remains

unchanged when SPL is free of substrate (Fig 5) [36]. Other likely candidates for rapid deuterium uptake include the loop regions near the active site of the SPL, including the 8 residue loop region binding the [4Fe-4S] cluster (Fig 5). All these regions would be amenable to exchange reactions in the absence of SAM and substrate due to the wide lateral opening of the SPL TIM barrel. Our data show that in the absence of SAM, addition of DNA oligonucleotide or the synthetic substrate 5R-SPTpT results in little alteration in deuterium uptake (Table 1). These results suggest either that SPL has low affinity for substrate or DNA in the absence of SAM, or that only minimal conformational changes occur upon binding DNA or substrate in the absence of SAM. Upon addition of SAM alone, however, the protein undergoes a significant structural change, as reflected by the difference in maximal uptake of deuterium between the bound and unbound forms (Figure 3A). Although this change occurs under aerobic conditions (where the [4Fe-4S] cluster is not intact), it is more pronounced under anaerobic conditions (Figure 3A). We believe that this is most likely due to an alteration in the H-bonding partners of the specific amino acids that are involved in the stabilization of SAM in the active site[36]. Computational simulations of the H/D exchange model in the presence of ligand[48] support this conclusion, with minimal ΔG° between the exposed conformations in the presence or absence of ligand. This state implies that the transition to a H/D exchangeable conformation is tightly coupled with loss of ligand: the ligand-bound state is highly protected from deuterium exchange, but that protection is restricted to a small number of amino acids. This conclusion is consistent with kinetic

characterization of SPL with similar ratios of synthetic substrate, which have indicated the presence of predominant levels of ES steady-state complexes [36, 43, 44, 49].

We believe that the differential deuterium uptake pattern can be correlated to the ability of SAM, to cause significant structural perturbations regardless of the integrity of the iron-sulfur cluster. This is consistent with the observation that SAM binds SPL by a variety of interactions such as hydrogen bonding, hydrophobic interactions and salt bridges [36]. The amino group of the methionyl moiety of SAM interacts with Ser142 and Asp143 and the carboxylate moiety interacts with Lys174 and Ser195, while the adenine and ribose groups are held in place via hydrogen bonding interactions with Tyr96, Tyr98, Ala234 and Ala273 [36]. It is likely that these interactions and the associated conformational changes upon SAM binding contribute to the substantially decreased levels of deuterium exchange in the presence of SAM. The increase in H/D exchange protection under anaerobic conditions can be ascribed to the presence of a [4Fe-4S] cluster in the anaerobic enzyme that increases SPL stability and also coordinates the bound SAM. The Broderick lab has painstakingly developed exquisite techniques of anaerobic protein purification that allows for the survival of the intact [4Fe-4S] cluster through the purification process, precluding the need for chemical reconstitution [25, 44]. Our results from the as-purified enzyme with its native [4Fe-4S] cluster suggest that upon SAM binding, the active site undergoes a transition to a more ordered state, as reflected in the significant increase in H/D protection from the SPL only (ligand-free) to the anaerobic and aerobic trials of SPL bound to SAM. We ascribe this increase in protection to the binding pocket and not to an allosteric effect distant from the binding site, based

upon the ligand-bound crystal structure of SPL (see below) and the lack of signature H/D trends resulting from allosteric interactions or global exposure. On the addition of the 6mer oligonucleotide to SPL in the presence of SAM (aerobic), the deuterium uptake is very similar to that of SPL + SAM, indicating that the principal conformational change is induced by SAM binding, and the contribution of the 6mer is relatively minor. However, the effect of the dinucleotide substrate 5*R*-SPTpT plus SAM on SPL H/D exchange is significantly greater than that of SAM alone (Figure 3D). The results suggest that 5*R*-SPTpT binding induces significant conformational changes in the active site of SPL, as compared to SAM or 5*R*-SPTpT binding alone. In order to probe the effects of the phosphodiester linker of 5*R*-SPTpT on binding, we decided to conduct H/D exchange experiments with the 5*R*-SP dinucleoside substrate. The 5*R*-SP has been previously characterized through kinetic assays to be a relatively poor substrate for SPL. [43]. It is believed that SPL, like other DNA repair enzymes [50], utilize the damage-induced deformation on the DNA backbone to recognize and bind the spore photoproduct [51]. Moreover the lack of the backbone most likely leads to significant freedom around the methylene bridge of SP dinucleoside, thereby preventing the molecule from adopting the correct orientation for efficient catalysis. The role of the linker in binding has been well established in other DNA repair enzymes, bound to lesions containing either a phosphate bridge or a formacetal linker [52, 53]. In all cases a conserved arginine residue has been shown to interact directly with the linker to correctly orient the substrate in the active site.[52, 54]. Although the crystal structure of SPL was solved with a dinucleoside substrate, the presence Lys309 and Arg273 in regions associated with the linker is

suggestive of their interaction with the phosphodiester backbone[36, 55]. We believe that our difference in uptake of 3.4 Da between the 5*R*-SPTpT and 5*R*-SP substrates is largely due to the interactions of these two amino acids with the phosphodiester backbone of the dinucleotide SP. The structure of SPL bound to the dinucleoside SP lesion also implicates Tyr98, in close vicinity to the substrate, which undergoes a $\sim 45^\circ$ rotation to accommodate the lesion, as well as Thr101 and Lys106 which undergo conformational changes. In addition, it is also reported that the β hairpin, which experiences a conformational change of 2\AA on lesion binding, might also be involved in base flipping interactions commonly observed in DNA repair enzymes such as DNA photolyases [53, 56]. Our results suggest H/D exchange protection is highly localized and lacks large-scale allosteric or global characteristics. Combined with the existing structural data on SPL and other radical SAM enzymes, it is reasonable to conclude that these highly localized effects can be assigned to the active site, and are involved in substrate recognition and binding. Such localized structural changes have been commonly observed in other DNA repair enzymes such as (6-4) photolyase and CPD photolyases, where the damaged regions are stabilized in the active site through hydrogen bonding [52, 54]. We believe that a similar sequence of events follows on SPL binding to its substrate, where the binding event breaks the existing H-bonding interactions in the active site, leading to a new H-bonding network and stabilizing the lesion pair. Comparison between reactions conducted anaerobically vs aerobically shows an additional protection of protons (Fig 3D). This again points to the relevance of the [4Fe-4S] cluster in enhancing protein stability and maintaining the correct conformation for SAM and ligand binding.

Summary and Conclusions

The data presented herein demonstrates that the number of exchangeable protons on SPL decreases by 20 upon binding SAM and the minimal substrate 5*R*-SPTpT. The sum of existing structural data and our H/D exchange measurements supports assignment of these protected region (due to H bonding or lack of solvent exposure) to the active site, and not to allosteric effects. Our results suggest that binding of SAM and 5*R*-SPTpT effectively seals off the active site, thus protecting a large number of protons which can be rapidly exchanged in the ligand-free state. The presence of the [4Fe-4S] cluster is also important for this interaction, as performing the experiment under aerobic conditions (with associated loss of the cluster) results in decreased protection from H/D exchange. It is interesting to note that even binding of SAM alone results in protection of thirteen exchangeable sites under anaerobic conditions, while binding of substrate alone offers insignificant protection from H/D exchange. Conformational changes associated with cofactor and/or substrate binding have been implicated in other radical SAM enzymes [57-59], and may serve to provide a solvent inaccessible and protected active site to safely catalyze radical reactions.

References

1. Setlow, P. (2007) I will survive: DNA protection in bacterial spores. *Trends Microbiol* 15, 172-180.
2. Varghese, A. J. (1970) 5-Thyminy-5,6-dihydrothymine from DNA irradiated with ultraviolet light. *Biochemical and Biophysical Research Communications* 38, 484-490,
3. Donnellan, J.E. & Setlow, R.B. (1965) Thymine photoproducts but not thymine dimers found in ultraviolet-irradiated bacterial spores. *Science* 149, 308-310.
4. Donnellan, Jr J.E. & Stafford, R.S. (1968) The Ultraviolet photochemistry and photobiology of vegetative cells and spores of *Bacillus megaterium*. *Biophysical Journal* 8, 17-28.
5. Setlow, P. (1995) Mechanisms for the prevention of damage to DNA in spores of *Bacillus* species. *Annual Review of Microbiology* 49, 29-54.
6. Duin, E.C., Lafferty, M.E., Crouse, B.R., Allen, R.M., Sanyal, I., Flint, D.H. & Johnson, M.K (1997) [2Fe-2S] to [4Fe-4S] cluster conversion in *Escherichia coli* biotin synthase. *Biochemistry* 36, 11811-11820.
7. Sanyal, I., Cohen, G. Flint, D.H. (1994) Biotin synthase: Purification, characterization as a [2Fe-2S] cluster protein, and in vitro activity of the *Escherichia coli* bioB gene product. *Biochemistry* 33, 3625-3631.
8. Berkovitch, F., Nicolet, Y., Wan, J.T., Jarrett, J.T. & Drennan, C.L. (2004) Crystal structure of biotin synthase, an *S*-adenosylmethionine-dependent radical enzyme. *Science* 303, 76-79.
9. Reed, K.E., Cronan, J.E, Jr (1993) Lipoic acid metabolism in *Escherichia coli*: Sequencing and functional characterization of the lipA and lipB genes. *Journal of Bacteriology* 175, 1325-1336.
10. Miller, J.R., Busby, R.W., Jorda, S.W., Cheek, J., Henshaw, T.F., Ashley, G.W., Broderick, J.B., Cronan, J.E. & Marletta M.A. (2000) *Escherichia coli* LipA Is a Lipoyl Synthase: In Vitro biosynthesis of lipoylated pyruvate dehydrogenase complex from octanoyl-acyl carrier protein†. *Biochemistry* 39, 15166-15178.
11. Hayden, M.A., Huang, I.Y., Iliopoulos, G., Orozco, M. & Ashley, G.W. (1993) Biosynthesis of lipoic acid: Characterization of the lipoic acid auxotrophs *Escherichia coli* W1485-lip2 and JRG33-lip9. *Biochemistry* 32, 3778-3782.

12. Wuebbens, M.M., Rajagopalan, K.V. (1995) Investigation of the early steps of molybdopterin biosynthesis in *Escherichia coli* through the use of in vivo labeling studies. *Journal of Biological Chemistry* 270, 1082-1087.
13. Rieder, C., Eisenreich, W., O'Brien, J., Richter, G., Götze, E., Boyle, P., Blanchard, S., Bacher, A., Simon, H. (1998) Rearrangement reactions in the biosynthesis of molybdopterin. *European Journal of Biochemistry* 255, 24-36.
14. Curatti, L., Ludden, P.W., Rubio, L.M. (2006) NifB-dependent in vitro synthesis of the iron-molybdenum cofactor of nitrogenase. *Proceedings of the National Academy of Sciences* 103, 5297-5301.
15. Posewitz, M.C., King, P.W., Smolinski, S.L., Zhang, L., Seibert, M., Ghirardi, M.L. (2004) Discovery of two novel radical S-adenosylmethionine proteins required for the assembly of an active [Fe] hydrogenase. *Journal of Biological Chemistry* 279, 25711-25720.
16. King, P.W., Posewitz, M.C., Ghirardi, M.L., Seibert, M. (2006) Functional studies of [FeFe] hydrogenase maturation in an *Escherichia coli* Biosynthetic System. *Journal of Bacteriology* 188, 2163-2172.
17. McGlynn, S., Ruebush, S., Naumov, A., Nagy, L., Dubini, A., King, P., Broderick, J., Posewitz, M., Peters, J. (2007) In vitro activation of [FeFe] hydrogenase: New insights into hydrogenase maturation. *Journal of Biological Inorganic Chemistry* 12, 443-447.
18. Duschene, K.S., Veneziano, S.E., Silver, S.C., Broderick, J.B. (2009) Control of radical chemistry in the AdoMet radical enzymes. *Current Opinion in Chemical Biology* 13, 74-83.
19. Boal, A.K., Grove, T.L., McLaughlin, M.I., Yennawar, N.H., Booker, S.J., Rosenzweig, A.C. (2011) Structural basis for methyl transfer by a radical SAM enzyme. *Science* 332, 1089-1092.
20. Yan, F., LaMarre, J.M., Röhrich, R., Wiesner, J., Jomaa, H., Mankin, A.S., Fujimori, D.G. (2010) RlmN and Cfr are radical SAM enzymes involved in methylation of ribosomal RNA. *Journal of the American Chemical Society* 132, 3953-3964.
21. Shepard, E.M., Broderick, J.B. (2010) S-adenosylmethionine and iron-sulfur clusters in biological radical reactions: The radical SAM superfamily. *Comprehensive Natural Products II*. pp. 625-661.
22. Frey, P.A., Hegeman, A.D., Ruzicka, F.J. (2008) The radical SAM superfamily. *Critical Reviews in Biochemistry and Molecular Biology* 43, 63-88.

- 23.Vey, J.L., Drennan, C.L. (2011) Structural insights into radical generation by the radical SAM superfamily. *Chemical Reviews* 111, 2487-2506.
- 24.Mehl, R.A., Begley, T.P. (1999) Mechanistic studies on the repair of a novel DNA photolesion: The spore photoproduct. *Organic Letters* 1, 1065-1066.
- 25.Buis, J.M., Cheek, J., Kalliri, E., Broderick, J.B. (2006) Characterization of an active spore photoproduct lyase, a DNA repair enzyme in the radical S-adenosylmethionine superfamily. *Journal of Biological Chemistry* 281, 25994-26003.
- 26.Cheek, J., Broderick, J.B. (2002) Direct H atom abstraction from spore photoproduct C-6 initiates DNA repair in the reaction catalyzed by spore photoproduct lyase: Evidence for a reversibly generated adenosyl radical intermediate. *Journal of the American Chemical Society* 124, 2860-2861.
- 27.Himo, F. (2005) C-C bond formation and cleavage in radical enzymes, a theoretical perspective. *Biochimica et Biophysica Acta (BBA) - Bioenergetics* 1707, 24-33.
- 28.Slieman, T.A., Rebeil, R., Nicholson, W.L. (2000) Spore photoproduct (SP) lyase from *Bacillus subtilis* specifically binds to and cleaves SP (5-Thyminy-5,6-Dihydrothymine) but not cyclobutane pyrimidine dimers in UV-irradiated DNA. *Journal of Bacteriology* 182, 6412-6417
- 29.Shi, Q., Thresher, R., Sancar, A., Griffith, J. (1992) Electron microscopic study of (A)BC excinuclease : DNA is sharply bent in the UvrB-DNA complex. *Journal of Molecular Biology* 226, 425-432.
- 30.Sancar, A. (1994) Structure and function of DNA photolyase. *Biochemistry* 33, 2-9.
- 31.Sancar,A. (2003) Structure and function of DNA photolyase and cryptochrome blue-light photoreceptors. *Chemical Reviews* 103, 2203-2237.
- 32.Lee, B.J., Sakashita, H., Ohkubo, T., Ikehar, M., Doi, T., Morikawa, K., Kyogoku, Y., Osafune, T., Iwai, S., Ohtsuka. E., (1994) Nuclear magnetic resonance study of the interaction of T4 endonuclease V with DNA. *Biochemistry* 33, 57-64.
- 33.Chandra, T., Silver, S.C., Zilinskas, E., Shepard, E.M., Broderick, W.E., Broderick, J.B. (2009) Spore photoproduct lyase catalyzes specific repair of the 5R but not the 5S spore photoproduct. *Journal of the American Chemical Society* 131, 2420-2421.
- 34.Silver, S.C., Chandra, T., Zilinskas, E., Ghose, S., Broderick, W.E., Broderick, J.B. (2010) Complete stereospecific repair of a synthetic dinucleotide spore photoproduct by spore photoproduct lyase. *Journal of Biological Chemistry* 15, 943-955.

35. Heil K, Kneuttinger. A.C., Schneider, S., Lischke, U., Carell, T. (2011) Crystal structures and repair studies reveal the identity and the base-pairing properties of the UV-induced spore photoproduct DNA lesion. *Chemistry – A European Journal* 17, 9651-9657.
36. Benjdia, A., Heil, K., Barends, T.R.M., Carell, T., Schlichting, I. (2012) Structural insights into recognition and repair of UV-DNA damage by spore photoproduct lyase, a radical SAM enzyme. *Nucleic Acids Research*, 40, 9308-9318.
37. Paspaleva, K., Moolenaar, G.F., Goosen, N. (2009) Damage recognition by UV damage endonuclease from *Schizosaccharomyces pombe*. *DNA Repair* 8, 600-611.
38. Skinner, J.J., Lim, W.K., Bédard, S., Black, B.E., Englander, S.W. (2012) Protein hydrogen exchange: Testing current models. *Protein Science*, 21, 987-995
39. Englander, S., Mayne, L., Bai, Y., Sosnick, T. (2008) Hydrogen exchange: The modern legacy of Linderstrøm-Lang. *Protein Science* 6, 1101-1109.
40. Englander, S.W., Kallenbach, N.R. (1983) Hydrogen exchange and structural dynamics of proteins and nucleic acids. *Quarterly Reviews of Biophysics* 16, 521-655.
41. Engen, J.R. (2009) Analysis of protein conformation and dynamics by hydrogen/deuterium exchange MS. *Analytical Chemistry* 81, 7870-7875.
42. Zhang, Z., Smith, D.L. (1993) Determination of amide hydrogen exchange by mass spectrometry: A new tool for protein structure elucidation. *Protein Science* 2, 522-531.
43. Chandra, T., Silver, S.C., Zilinskas, E., Shepard, E.M., Broderick, W.E., Broderick, J.B. (2009) Spore photoproduct lyase catalyzes specific repair of the 5R but not the 5S spore photoproduct. *Journal of the American Chemical Society* 131, 2420-2421.
44. Silver, S.C., Chandra, T., Zilinskas, E., Ghose, S., Broderick, W.E., Broderick, J.B. (2010) Complete stereospecific repair of a synthetic dinucleotide spore photoproduct by spore photoproduct lyase. *Journal of Biological Inorganic Chemistry* 15, 943-955.
45. Bradford, M.M. (1976) A rapid and sensitive method for the quantitation of microgram quantities of protein utilizing the principle of protein-dye binding. *Analytical Biochemistry* 72, 248-254.
46. Beinert, H. (1978) Micro methods for the quantitative determination of iron and copper in biological material. *Methods in Enzymology* pp. 435-445.

47. Walsby, C.J., Ortillo, D., Yang, J., Nnyepi, M.R., Broderick, W.E., Hoffman, B.M., Broderick, J.B. (2005) Spectroscopic approaches to elucidating novel iron–sulfur chemistry in the “radical-SAM” protein superfamily. *Inorganic Chemistry* 44, 727-741.
48. Wildes, D., Marqusee, S. (2005) Hydrogen exchange and ligand binding: Ligand-dependent and ligand-independent protection in the Src SH3 domain. *Protein Science* 14, 81-88.
49. Heil, K., Kneuttinger, A.C., Schneider, S., Lischke, U., Carell, T. (2011) Crystal structures and repair studies reveal the identity and the base-pairing properties of the UV-induced spore photoproduct DNA lesion. *Chemistry – A European Journal* 17, 9651-9657.
50. Husain, I., Sancar, G.B., Holbrook, S.R., Sancar, A. (1987) Mechanism of damage recognition by *Escherichia coli* DNA photolyase. *Journal of Biological Chemistry* 262, 13188-13197.
51. Slieman, T.A., Rebeil, R., Nicholson, W.L. (2000) Spore photoproduct (SP) lyase from *Bacillus subtilis* specifically binds to and cleaves SP (5-thymine-5,6-dihydrothymine) but not cyclobutane pyrimidine dimers in UV-irradiated DNA. *Journal of Bacteriology* 182, 6412-6417.
52. Kiontke, S., Geisselbrecht, Y., Pokorny, R., Carell, T., Batschauer, A., Essen, L.O. (2011) Crystal structures of an archaeal class II DNA photolyase and its complex with UV-damaged duplex DNA. *The EMBO Journal* 30, 4437-4449.
53. Mees, A., Klar, T., Gnau, P., Hennecke, U., Eker, A.P.M., Carell, T., Essen, L.O. (2004) Crystal structure of a photolyase bound to a CPD-like DNA lesion after in situ repair. *Science* 306, 1789-1793.
54. Maul, M.J., Barends, T.R., Glas, A.F., Cryle, M.J., Domratcheva, T., Schneider, S., Schlichting, I., Carell, T. (2008) Crystal structure and mechanism of a DNA (6-4) photolyase. *Angewandte Chemie International Edition* 47, 10076-10080.
55. Benjdia, A. (2012) DNA photolyases and SP lyase: structure and mechanism of light-dependent and independent DNA lyases. *Current Opinion in Structural Biology* 22, 711-720.
56. Maul, M.J., Barends, T.R.M., Glas, A.F., Cryle, M.J., Domratcheva, T., Schneider, S., Schlichting, I., Carell, T. (2008) Crystal structure and mechanism of a DNA (6-4) photolyase. *Angewandte Chemie International Edition* 47, 10076-10080.

57.Vey, J.L., Yang, J., Li, M., Broderick, W.E., Broderick, J.B. Drennan, C.L. (2008) Structural basis for glycyl radical formation by pyruvate formate-lyase activating enzyme. *Proceedings of the National Academy of Sciences* 105, 16137-1614.

58.Goto-Ito, S., Ishii, R., Ito, T., Shibata, R., Fusatomi, E., Sekine, Si., Bessho, Y., Yokoyama, S. (2007) Structure of an archaeal TYW1, the enzyme catalyzing the second step of wye-base biosynthesis. *Acta Crystallographica Section D* 63, 1059-1068.

59.Kato, M., Araiso, Y., Noma, A., Nagao, A., Suzuki, T., Ishitani, R., Nureki, O. (2011) Crystal structure of a novel C-domain-containing protein, TYW5, involved in tRNA modification. *Nucleic Acids Research* 39, 1576-1585.

CHAPTER 3

IDENTIFICATION AND QUANTITATION OF A PUTATIVE SUBSTRATE FOR
[FE FE]-HYDROGENASE MATURASE ENZYME HYDEContribution of Authors and Co-Authors

Manuscript in Chapter 3

Author: Shourjo Ghose

Contributions: Protein purifications. research design, assay optimization, method development, LCMS analysis, manuscript writing and preparation.

Co-author: Nicholas Boswell

Contributions: Initial screening of small molecules to determine stimulation of SAM cleavage

Co-author: Eric Shepard

Contributions: Research design, electron paramagnetic resonance. manuscript writing and preparation

Co-author: John W. Peters

Contributions: Provided valuable insight discussions of the [FeFe]-hydrogenase and its maturation. Manuscript editing.

Co-author: Joan B. Broderick

Contributions: Overall conception, direction, and funding of the project. Provided insights into the experimental approach and design. Manuscript writing and preparation.

Manuscript Information Page

Shourjo Ghose, Nicholas Boswell, Eric M. Shepard, John W. Peters, and Joan B. Broderick*

Journal: Biochemistry

Status of the manuscript:

Prepared for submission to a peer-reviewed journal

Officially submitted to a peer-reviewed journal

Accepted by a peer-reviewed journal

Published in a peer-reviewed journal

CHAPTER 3

IDENTIFICATION AND QUANTITATION OF A PUTATIVE SUBSTRATE FOR
[FeFe]-HYDROGENASE MATURASE ENZYME HydE

Shourjo Ghose, Nicholas Boswell, Eric M. Shepard, John W. Peters, and Joan B.
Broderick

Department of Chemistry & Biochemistry and the Astrobiology Biogeocatalysis

Research Center, Montana State University, Bozeman, MT 59717

Abstract

The assembly and biosynthesis of the H-cluster in [FeFe]-hydrogenase requires the action of 3 accessory enzymes HydE, HydG and HydF. Herein we have identified the putative substrate for HydE, cysteine, via high performance liquid chromatography and mass spectrometry. We have also demonstrated that HydE could be potentially utilizing HydF as a co-substrate thereby reinforcing the role HydF in the H-cluster maturation as that of a scaffold. We have also shown preliminary evidence that the role of SAM in HydE catalysis could be that of a co-factor instead of a co-substrate.

Introduction

Hydrogenases utilize organometallic metal clusters at their active sites to catalyze the reversible reduction of protons to H₂. The cluster at the active site of the [FeFe]-hydrogenase is called the H-cluster, and is composed of a [4Fe-4S] cubane connected via a bridging cysteine thiolate to a 2Fe subcluster that is further coordinated by carbon monoxide and cyanide ligands, as well as a bridging dithiolate (Figure 1) (1, 2). It is at this 2Fe subcluster, stabilized in lower oxidation states by the π -acid ligands, that protons are thought to bind and be reduced. The H-cluster is unique to the [FeFe] hydrogenases, although the presence of CO and CN⁻ ligands is a feature common to other hydrogenases,

including the [NiFe] hydrogenase. Structural, spectroscopic, and computational studies have revealed important structural and electronic parameters in catalysis, and have both spurred and been informed by elegant chemical synthetic approaches directed towards functional mimics of the [FeFe]-hydrogenase (3).

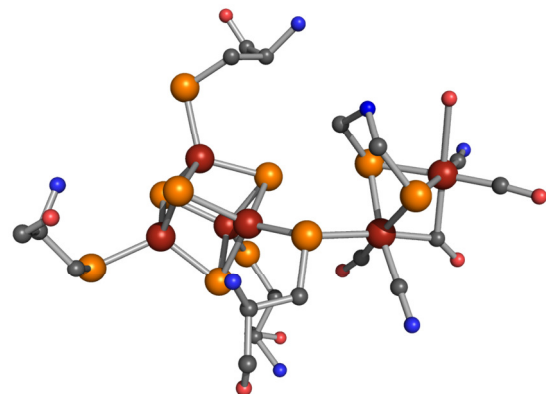


Figure 1. The H-cluster of [FeFe]-hydrogenase. The [4Fe-4S] cubane is connected via a single bridging cysteine to a 2 Fe subcluster. The 2Fe subcluster contains biologically rare ligands in the form of 3 CO and 2CN⁻ ligands. The site of H₂ catalysis is proposed to be the distal Fe on the 2Fe subcluster.

Details of the synthesis and assembly of this unusual organometallic H-cluster in the [FeFe] hydrogenases have begun to emerge in recent years. Assembly of the H-cluster requires three hydrogenase maturation proteins HydE, HydF, and HydG (4). HydE and HydG are radical S-adenosylmethionine (SAM) enzymes, while HydF is a GTPase (4, 5). Radical SAM enzymes are characterized by the presence of a site-differentiated [4Fe-4S] cluster coordinated by three cysteines in a conserved motif (generally CxxxCxxC), with SAM coordinating the unique fourth iron. These enzymes catalyze biological radical reactions initiated by reductive cleavage of SAM to generate a 5'-deoxyadenosyl (dAdo) radical intermediate (6-8). The dAdo radical abstracts a hydrogen atom from a substrate

to initiate one of the diverse chemical reactions characterized by this enzyme superfamily, such as sulfur insertion, generation of protein based glycy radical, heme biosynthesis, and DNA repair (8-10). Recent reports have provided insight into the possible roles of each of the maturation proteins and a theoretical pathway for cluster assembly. Spectroscopic and structural characterization of HydA expressed in the absence of the maturation proteins (HydA^{ΔEFG}) have demonstrated that the hydrogenase protein contains the [4Fe-4S] subcluster of the H-cluster, but not the unique 2Fe subcluster (11-13). The inference drawn from these results is that the [4Fe-4S] subcluster can be synthesized by standard iron sulfur cluster assembly machinery (Isc or Suf systems), while the 2Fe subcluster requires the dedicated maturation proteins (14). HydF has been demonstrated to act as a carrier or assembly scaffold for the 2Fe subcluster, and to transfer this subcluster to HydA^{ΔEFG} in the final step of hydrogenase maturation (15, 16). The EPR spectrum of HydF expressed in the absence of HydE and HydG (HydF^{ΔEG}) exhibits signals indicative of [4Fe-4S]⁺ and [2Fe-2S]⁺ clusters, while HydF expressed in a background of HydE and HydG (HydF^{EG}) exhibits only the [4Fe-4S]⁺ cluster signal (16). This observation coupled to the presence of CO and CN⁻ vibrational bands on HydF^{EG}, but lacking from HydF^{ΔEG}, suggested a model in which HydE and HydG modify a [2Fe-2S] cluster precursor on HydF to an EPR silent H-cluster precursor (16, 17). Interestingly, a recent study utilizing a cell-free approach to probe H-cluster biosynthesis concluded that the 2Fe subcluster, or a precursor thereof, is synthesized on HydG; HydF was proposed to stabilize the cluster intermediate species and act as a transferase in activating HydA^{ΔEFG}. The role of HydE in this study was

purported to be a facilitator in the cluster translocation process from HydF to HydA^{ΔEFG} (18). Despite the different proposals regarding the nature of HydF's role during H-cluster maturation, biochemical studies have clearly shown that targeted and sequential protein-protein binding interactions take place between HydE, HydG, and HydF (19, 20). The role of GTP binding and hydrolysis by HydF is not well resolved, however it appears to not be associated with the activation of HydA^{ΔEFG} by HydF^{EG} (16). Until recently the substrates required for the radical SAM enzymes involved in H-cluster biosynthesis were unknown, although both tyrosine and cysteine were found to stimulate hydrogenase activation in cell extracts (21). Tyrosine was additionally shown to stimulate the reductive cleavage of SAM by HydG, and *p*-cresol was identified as a product of tyrosine cleavage (22). The central role of tyrosine in H-cluster biosynthesis was ultimately revealed when CO and CN⁻ were shown to be products of HydG catalyzed tyrosine degradation (23-25). Here we report the first evidence for a putative substrate for HydE. We also show preliminary tantalizing evidence that HydE might be using SAM as a cofactor instead of a co-substrate.

Experimental Procedures

Protein Expression, Purification, and Reconstitution

HydE was expressed in *E. coli* BL21(DE3) as described previously (15). Single colonies from streaked plates were used to inoculate 50 mL of phosphate buffered Luria-Bertani (LB) medium, pH 7.5, containing ampicillin. These cultures were grown for 12-15 hours at 37°C and 225 rpm in a thermostatted shaker and were used to inoculate 9-L cultures of 50 mM phosphate buffered (pH 7.5) LB medium supplemented with 5 g/L

NaCl, 5 g/L glucose. The 9 L cultures were grown in a thermostatted shaker at 37°C and 225 rpm until an optical density (OD₆₀₀) of 0.5 – 0.6 was reached. The cells were then induced with 1 mM isopropyl thiogalactopyranoside (IPTG) and the medium was supplemented with ferrous ammonium sulfate (FAS, 0.06 g/L). The cultures were grown for an additional 2.5 – 3.0 hours prior to cooling to room temperature and addition additional FAS (0.06 g/L). The cell cultures were then placed under nitrogen at 4°C for an additional 15 hours. Cells were then harvested by centrifugation and immediately flash frozen in liquid N₂ before being stored at -80°C until further use. Cell lysis and purification of the proteins were accomplished anaerobically in a Coy anaerobic chamber (Coy Laboratories, Grass Lake, MI). Cell pellets were resuspended in a lysis solution containing 50 mM HEPES pH 7.4, 10 mM imidazole, 500 mM KCl, 5% glycerol, 20 mM MgCl₂, 1 mM phenylmethylsulfonyl fluoride (PMSF), 1% Triton X-100, 0.2 mg/mL lysozyme, 0.03 mg/mL DNase and 0.03 mg/mL RNase. Cells were incubated in the lysis mixture for 1 hr on ice with gentle stirring at which time the mixture was centrifuged for 30 min at 18000 rpm. The supernatant was loaded onto a 5 mL HisTrap Ni²⁺-affinity column or a gravity Ni²⁺ affinity column (GE Healthcare) that was pre-equilibrated with Buffer A (50 mM HEPES pH 7.4, 500 mM KCl, 5% glycerol, 10 mM imidazole), The column was then washed with 10 column volumes of buffer A followed by a step gradient of increasing imidazole in buffer B (50 mM HEPES pH 7.4, 500 mM KCl, 5% glycerol, 500 mM imidazole). The eluting protein fractions were collected and analyzed by sodium dodecyl sulfate polyacrylamide gel electrophoresis (SDS-PAGE) and those determined to be 95% or more pure were pooled. The pooled fractions were then

dialyzed against 50 mM HEPES pH 7.4, 500 mM KCl, and 5% glycerol. The dialyzed protein was then placed in O-ring sealed tubes, flash frozen, and stored at -80 °C until further use. Protein concentrations were determined by the method of Bradford using a kit sold by Bio-Rad and bovine serum albumin as a standard (26). Iron content was determined using the method developed by Fish (27).

Purified HydE was chemically reconstituted under anaerobic conditions in a Coy anaerobic chamber by addition of 5 mM DTT and a ~6-fold excess of FeCl₃ and Na₂S, as described previously (24). After incubation for 2-3 hours, the protein was centrifuged to remove excess Fe and S and subsequently desalted and buffer exchanged over a G-25 Sephadex column (GE Healthcare) pre-equilibrated in 50 mM HEPES pH 7.4, 500 mM KCl, and 5% glycerol. UV-Vis spectroscopy under anaerobic conditions was used to confirm the iron-sulfur cluster content of the purified, reconstituted protein. The room temperature spectra were taken with a dual beam Varian Cary 50 BIO UV-Vis or Cary 6000i UV-Vis-NIR spectrophotometer at a scan rate of 600 nm/minute. The reconstituted protein was concentrated using a Minicon-B-15 concentrator (Millipore) and then placed in O-ring sealed tubes, flash frozen in liquid N₂, and stored at -80 °C until further use

EPR Sample Preparation and Spectroscopic Analysis

Reconstituted HydE (3.4 ± 0.1 Fe/protein, 154 μ M final conc) was prepared for EPR analysis in an anaerobic MBraun Box (<1 ppm O₂). Oxidized samples were prepared by addition of 5 mM potassium ferricyanide and were incubated for 20 minutes prior to flash

freezing. Photoreduced samples were prepared by supplementing the as-reconstituted protein with 50 mM Tris pH 7.4, 100 μ M deazariboflavin, and 5 mM dithiothreitol (DTT). Samples were then placed in an ice water bath and illuminated with a 300 W Xe light for one hour. To directly compare the effects of SAM addition, two photoreduced samples were prepared simultaneously and following the 1 hour photo-illumination period, 1 mM SAM was added in the absence of light to one sample, and then both samples were immediately flash frozen in liquid nitrogen.

Low temperature EPR analysis was performed using a Bruker EMX X-band spectrometer equipped with a liquid helium cryostat and Oxford Instrument temperature controller. Typical EPR parameters were: 9.37 GHz microwave frequency, 1.84 mW microwave power, 12 K sample temperature, and 81.92 ms time constant. Accurate g -value assignment and data simulations were carried out using the EasySpin software program(28) and spin quantitation of samples was calculated by comparison to integrated peak areas for a series of copper(II)-triethanolamine standards (Origin 7.0, Microcal, MA). To study temperature dependence of the iron sulfur cluster content, the EPR spectrum of the photoreduced sample with added SAM was studied from 14 K up to 60 K in 10 K increments. The saturation of the EPR signal of the same sample with microwave power ranging from 18 μ W to 36 mW was studied at 12 K. The experimental data were then plotted by comparing the $\log(\text{signal}/\text{square root power})$ vs. power as described in reference (29).

HydE Screening Assays

Assays with and without potential substrates were carried out in parallel in an MBraun anaerobic chamber maintained at <1 ppm O_2 . Reaction mixtures consisted of 25 μ M reconstituted HydE, 1 mM SAM, 2 mM dithionite, 50 mM HEPES, pH 7.4, 500 mM KCl, and 5% glycerol. Potential substrates were present at 2 mM unless noted otherwise. The assay mixtures were held at 37 °C in an IsoTemp block (Fisher Scientific) throughout the course of the assay. Aliquots (50 μ L) were taken at various time points and the reaction was quenched with 1 M HCl and the protein was removed by boiling for 10 min followed by centrifugation at 13000 rpm. The components of the supernatant were then separated over a Phenomenex Curosil PFP (5 μ m, 4.6 x 150 mm) analytical column by high-performance liquid chromatography (HPLC). Prior to sample injection the column was pre-equilibrated in 98% solvent A (0.1% acetic acid in water) and 2% solvent B (0.1% acetic acid in acetonitrile) at a flow rate of 1 ml/min. Following sample injection the mobile phase composition was held at 98% A/ for 7 minutes followed by a linear gradient from 98% A to 40% A, from 7 minutes to 24 minutes. From 24 minutes to 27 minutes the composition was held at 40% A and was then changed back to 98% A for re-equilibration. All HPLC runs were 35 minutes long and the column was held at 25 °C throughout the course of the analysis. Eluting analytes were monitored via UV at 254 nm and the amount of 5'-deoxyadenosine ($R_T = 12$ min) was quantitated by comparison to peak integrations from standard samples (Origin 7.0, Microcal, MA). The rate of change of the dAdo peak was deemed to be an indicator for change in HydE activity. Assays

examining the potential for deoxyadenosine stimulation in the presence of cysteine by PFL-AE and HydG were performed as described above.

LCMS HydE Activity Assays

Assays were carried out in the MBraun box (≤ 1 ppm O₂) using buffers and reagents that were freshly degassed on a Schlenk Line. Assays comprised 25 μ M reconstituted HydE, 2 mM dithionite, 50 mM HEPES, 0.5 M KCl, 5% glycerol, at pH 7.5 and 200 μ M L-cysteine. Assays containing all components but SAM were pre-incubated for 5 minutes at 37 °C and the reaction was initiated by the addition of 1 mM SAM. Aliquots of 50 μ L were taken at different time points and quenched with 3 μ L of 1M HCl. The samples were then centrifuged at 13,000 rpm for 15 min at 4 °C to remove precipitated protein and the supernatant was then flash frozen in liquid N₂ and stored at -80 °C until analysis. To determine the level of cysteine consumed over the reaction period, control assays were performed which were identical to the experimental with the exception that they did not contain SAM. In order to obtain a basal rate of deoxyadenosine production by HydE in the absence of cysteine (uncoupled cleavage), additional control assays were performed in the above manner but lacked cysteine. In all cases the concentration of 5'-deoxyadenosine was calculated by subtracting the amount of 5'-deoxyadenosine produced in the control reaction, without the presence of cysteine (uncoupled cleavage) from that of the experimental. Samples selected for LC-MS were prepared by diluting them 100-fold in 10% methanol, 90% water. During a LCMS run, two consecutive analytical trials were performed for each injected sample, so as to exclude any ambiguity resulting from peak shifts or change in peak area. Aliquots from experimental replicates

were run on the LCMS system for a minimum of two times on different days to eliminate the effects of day to day instrumental drift. The samples used to obtain a standard curve were always prepared fresh and were treated in an identical manner as experimental samples; and a minimum of two consecutive analytical trials were conducted for each standard per run. All analytes were observed in the $[M+H]^+$ form, including cysteine and 5'-deoxyadenosine (Supplement), and quantitation was performed as described below. Due to its ubiquitous presence and high signal quality, the HEPES elution peak was used as a quality control check and as mass accuracy validation.

LC-ESI/MS with Q-TOF Mass Spectrometer

The chromatography system was composed of an Agilent 1290 series UHPLC with binary pump, temperature-controlled auto-sampler and column compartment. The auto-sampler module and reactions were held at 25 °C using the active temperature control option. The separation of the various analytes was performed using normal phase chromatography with a Cogent “Diamond Hydride” HPLC column (MicroSolv, 150 x 2.1 mm), held at 50 °C. Solvents consisted of H₂O with 0.1% formic acid in channel A and acetonitrile with 0.1% formic acid in channel B, with a constant flow rate of 0.8 mL/min at all times. Prior to sample injection, the column was equilibrated with 100% B. Sample injection was performed with the autosampler, and following injection the solvent composition was maintained at 100% B for 2 minutes. A linear gradient was then used from 100% B to 50% B, from 2 min to 6 min. From 6 min to 8.5 min the composition was held at 50% B for elution of strongly-retained compounds. At 8.51 minutes the composition was changed back to 100% B and held until 10.0 minutes for re-

equilibration. Due to delays from sample injection, the overall time between samples was approximately 11 minutes.

Mass spectra were obtained on an Agilent 6538 Q-TOF mass spectrometer equipped with the dual-ESI source. The capillary exit voltage was 120 V and gas temperature was 300 °C. All data was recorded in positive mode between 25 m/z and 750 m/z in profile mode. The hardware summation time was 1 second. Peaks were validated using high-accuracy formula confirmation and elution matching from individual reference standards. Quantitation was performed using the MassHunter Quantitative Analysis package (Agilent). An extracted ion chromatograph was generated for analytes using the accurate mass of each compound with a -0.04 to +0.04 ppm m/z extraction window. This was selected to give the best compromise of specificity, sensitivity, and tolerance to slight calibration shifts during the runs. A smoothing window of 15 spectra with a function width of 30 samples was used to improve the reproducibility of the automated “Agile” integrator algorithm for peak detection. Peak areas from the Agile algorithm were exported to Origin 7.0 for determination of standard curves and calculation of concentrations. A concentration vs. time graph was then plotted to determine disappearance of cysteine and production of 5'-deoxyadenosine.

In order to ascertain if HydE co-purifies with any relevant small molecules, 15 μ M of reconstituted protein was precipitated using 1M HCl. The resulting mixture was centrifuged at 13,000 rpm for 15 min at 4 °C to remove precipitated protein and the supernatant was then flash frozen in liquid N₂ and stored at -80 °C until analysis. Supernatant was analyzed using the aforementioned mentioned LCMS protocol. A

similar protocol was followed to ascertain the identities of small molecules that co-purify with spore photoproduct lyase (SPL) using 20 μM as-isolated protein and with pyruvate formate lyase activating enzyme (PFL-AE) using 25 μM as-isolated protein.

Results

Spectroscopic Characterization of HydE

HydE expressed in *E. coli* and purified under anaerobic conditions contains an iron-sulfur cluster, as indicated by spectroscopic characterization. The UV-visible spectral features include a shoulder at ~410 – 412 nm, typical of ligand to metal charge transfer bands due to $[\text{4Fe-4S}]^{2+}$ clusters; reduced intensity of the visible absorbance features in the presence of dithionite is consistent with the reduction of at least some of these clusters to the $[\text{4Fe-4S}]^+$ state. Reconstitution of as-isolated HydE with iron and sulfide yields protein with variable amounts of iron (3.4 – 6.3 Fe/protein), but with UV-vis spectroscopic features that are similar to the as-isolated protein. Rates of nonproductive SAM cleavage to produce dAdo were found to be reproducible despite the range of iron content of the reconstituted protein (data not shown).

Reconstituted HydE exhibits a small nearly isotropic signal with simulated g values of 2.02, 2.00, and 1.97 (0.02 spins/protein), which is increased upon oxidation yielding g values of 2.02, 2.00, and 2.00 (Figure 2); the g -value, lineshape, and increase upon oxidation are all indicative of $[\text{3Fe-4S}]^+$ clusters produced by oxidation of a site-differentiated $[\text{4Fe-4S}]^{2+}$ cluster. The photoreduced enzyme exhibits a strong axial signal indicative of a $[\text{4Fe-4S}]^+$ cluster with simulated g values of 2.03, 1.91, and 1.89 (Figure 2, black and Figure Supplement 2) with 0.37 spins per protein). Evidence for binding of

SAM to the $[4\text{Fe-4S}]^{2+/+}$ cluster present in reconstituted HydE is provided by the new rhombic signal (simulated g values of 2.01, 1.88, and 1.83 observed upon addition of exogenous SAM to the reduced enzyme (Figure 2, blue trace, and supplement). Spin quantitation of the reduced plus SAM signal yields a value of 0.64 spins/protein. This increase relative to the reduced signal suggests that SAM coordination may perturb the redox potential of the $[4\text{Fe-4S}]^{2+/+}$ cluster yielding greater levels of reduction when SAM is present; this behavior is consistent with what has been observed in other radical SAM enzyme systems such as ThiH and HydG(30). Temperature dependent EPR relaxation and power saturation profiles for the reduced plus SAM HydE sample were performed to further probe the FeS cluster content of the reconstituted HydE enzyme. Figure 3A shows the temperature dependent relaxation properties and, as can be clearly seen, a $\geq 98\%$ reduction in signal intensity occurs as the temperature is raised from 13.8 to 30 K, consistent with the relaxation properties of $[4\text{Fe-4S}]^+$ clusters.

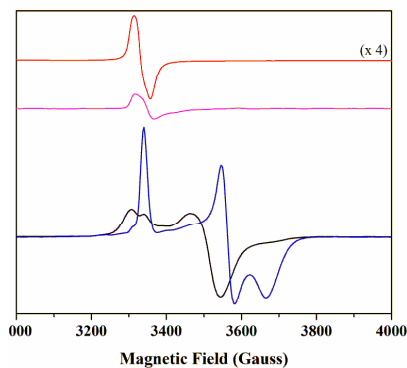


Figure 2. Low temperature (12 K) EPR spectra for reconstituted, active HydE (154 μM protein, 3.4 ± 0.1 Fe/protein). As-reconstituted (magenta), ferricyanide treated (red), photoreduced (black), and photoreduced plus addition of 1 mM AdoMet (blue) spectra are shown with associated g-values. EPR parameters are given in Materials and Methods. The intensity of the oxidized spectrum was manipulated by dividing it by a factor of 4 to put it on scale with the other data in the figure.

Moreover, the sample shows roughly linear dependence of the power saturation profile (Figure 3B), a result that also indicates predominantly $[4\text{Fe-4S}]^+$ content (29). The residual signal intensity present at 60 K in the temperature profile (Figure 3A) is consistent with minor ($\leq 1\%$) $[2\text{Fe-2S}]^+$ content, a result that is not unexpected given the existence of additional cysteine ligands (Cys311, Cys319, and Cys322) present in the primary sequence. An available X-ray crystal structure of HydE from *Thermotoga maritima* reveals that these accessory cysteine ligands coordinate a labile $[2\text{Fe-2S}]$ cluster with variable occupancy that is located 20 \AA from the radical SAM $[4\text{Fe-4S}]$ cluster (31).

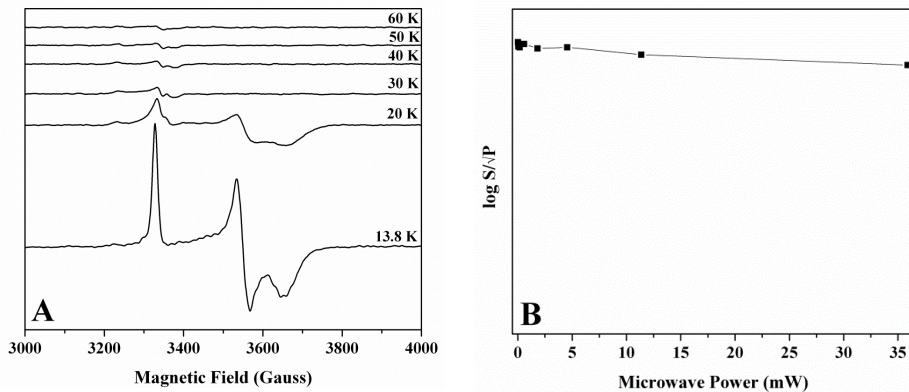


Figure 3. Temperature dependence (A) and power saturation behavior (B) for the photoreduced plus addition of AdoMet sample shown in Figure 2 (blue trace, $154 \mu\text{M}$ protein, $3.4 \pm 0.1 \text{ Fe/protein}$, 1 mM AdoMet). For the temperature dependent studies, microwave power was held constant at 1.8 mW and the temperature was gradually increased to 60 K as denoted in panel A. For the power saturation study, the temperature was held at 12 K while the microwave power was systematically increased from $18 \mu\text{W}$ to 36 mW

Single cysteine to alanine point mutations were shown to have no deleterious effects upon the ability to achieve active hydrogenase in whole cell lysis mixtures, however,

providing strong evidence that the accessory [2Fe-2S] cluster in HydE (when present) plays no role in H-cluster biosynthesis (31).

Effect of Possible Substrates on Rates of HydE-Catalyzed SAM Cleavage

HydE catalyzes the uncoupled cleavage of SAM in the absence of substrate to form 5'-dAdo at a basal rate of 0.56 ± 0.05 mol 5'-dAdo/mol HydE/hour at 37 °C (as measured through HPLC) , which is similar to that reported previously for the enzyme from *T. maritima* (32). Such nonproductive cleavage, as well as the acceleration of SAM cleavage in the presence of substrates, is a common feature of radical SAM enzymes (22, 33, 34). In an effort to identify the substrate of HydE, all twenty amino acids in addition to homocysteine and pyruvate were screened for their ability to stimulate 5'-dAdo production by HydE. Of the 23 molecules tested, only cysteine provided a measurable stimulation of HydE-catalyzed SAM cleavage, with an approximately 50% increase above the measured non productive cleavage rate (Supplement 3). It is interesting that neither homocysteine nor serine stimulated SAM cleavage, despite their close structural relationship to cysteine.

LCMS Analysis of HydE Catalyzed Cysteine Consumption

Due to the ability of cysteine to coordinate FeS clusters and to serve as a precursor for sulfide for FeS cluster assembly, we examined the effect of cysteine on the rates of SAM cleavage for two other radical SAM enzymes . Addition of cysteine to assay mixtures containing either pyruvate formate lyase activating enzyme (PFL-AE) or HydG resulted in no stimulation above basal levels of SAM cleavage (data not shown), suggesting that

the cysteine effect we observe for HydE is specific to HydE. In order to probe whether cysteine serves as a HydE substrate, high performance liquid chromatography coupled with time of flight mass spectrometry (LCMS) was used to quantify 5'-dAdo and cysteine levels over time in assays consisting of HydE, cysteine, SAM, and reductant. The cysteine elution peak was centered at approximately 4.2 minutes. In addition to cysteine, all the other reaction components were observed, with SAM eluting at 6.9 min, HEPES at 4.9 min, and 5' dAdo at 4.0 min . All analytes were observed in the $[M+H]^+$ form, including cysteine (122.026 m/z), SAM (399.141 m/z), 5'-dAdo (252.109 m/z), and HEPES (239.105) (Supplement 1).

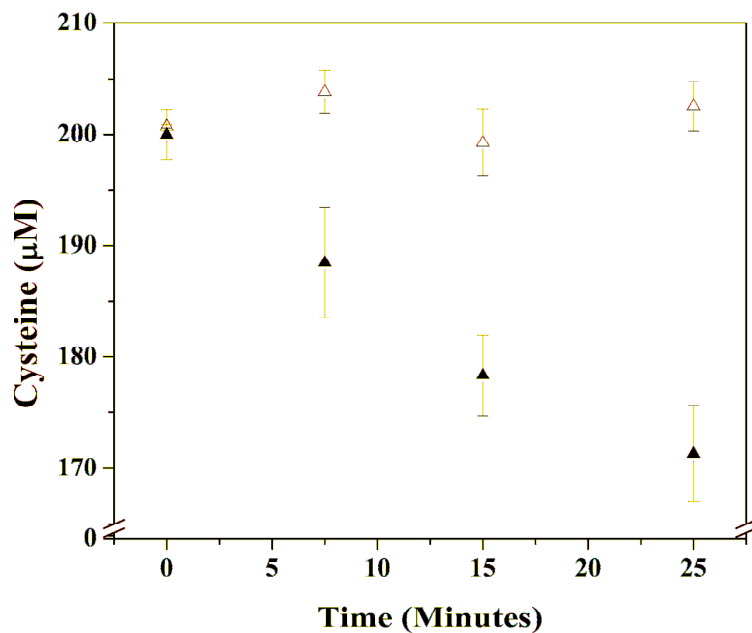


Figure 4. Time-dependent concentration of cysteine in assays lacking (open triangles) and containing (closed triangles) HydE. Assays contained 200 μ M cysteine, 1 mM SAM, 2 mM dithionite, and \pm 25 μ M HydE.

The production of 5'-dAdo as analyzed by LCMS was similar to that determined by HPLC; specifically, HydE catalyzes the uncoupled reductive cleavage of SAM to

produce 5'-dAdo in the absence of cysteine, but the production of 5'-dAdo is enhanced in the presence of cysteine. Quantitation of the concentration levels of both cysteine and 5'-dAdo over time provides clear evidence that as 5'-dAdo is being produced, the amount of cysteine in the assay mixtures is decreasing (Figure 4). Moreover, when the change in cysteine concentration over time is compared to the change in 5'-dAdo concentration over time (after subtracting out the background uncoupled SAM cleavage rate), it becomes clear that the rate of production of 5'-dAdo approximates the rate of cysteine consumption in a nearly 1:1 manner (Figure 6).

EPR and LCMS Analysis of SAM Bound to Purified HydE

The vast majority of characterized radical SAM enzymes utilize SAM as a co-substrate in the catalysis of their varied substrates (35-37). Two notable exceptions to this are SPL and LAM, which utilize SAM as a cofactor. Interestingly, extremely tight binding of methionine and 5'-dAdo has been observed during soaking experiments of HydE crystals, and this observation has been used to suggest that HydE utilizes SAM as a cofactor during catalysis (38).

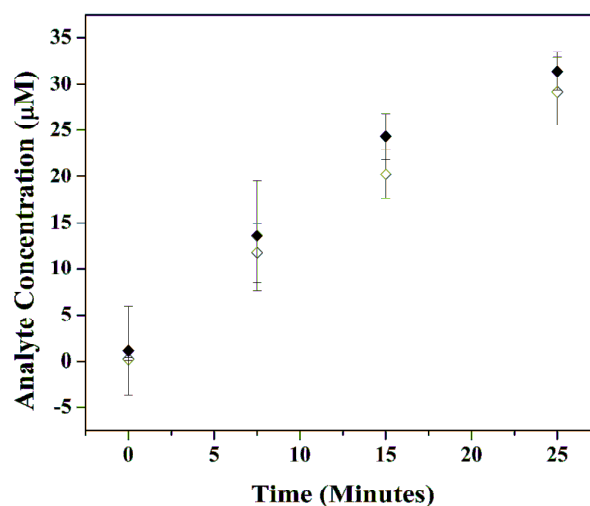
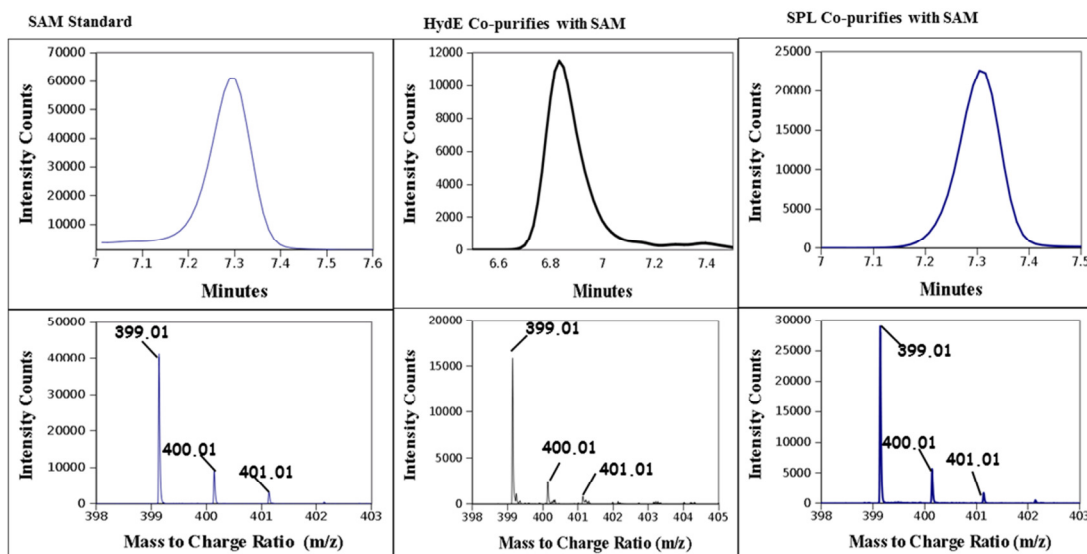


Figure 5. Correlation of the rate of 5'-dAdo production with the rate of cysteine consumption in the complete HydE assay. Assays contained 200 μ M cysteine, 1 mM SAM, 2 mM reductant, and \pm 25 μ M HydE

EPR and LCMS Analysis of SAM Bound to Purified HydE

The vast majority of characterized radical SAM enzymes utilize SAM as a co-substrate in the catalysis of their varied substrates (35-37). Two notable exceptions to this are SPL and LAM, which utilize SAM as a cofactor. Interestingly, extremely tight binding of methionine and 5'-dAdo has been observed during soaking experiments of HydE crystals, and this observation has been used to suggest that HydE utilizes SAM as a cofactor during catalysis (38). More generally, the authors postulate that the role of SAM as either a co-substrate or a cofactor may be delineated through determination of the relative affinities of a given enzyme towards SAM, methionine, and 5'-dAdo. (38). Simulations of the reduced and reduced plus SAM EPR data in Figure 2 revealed that SAM co-purified with HydE. As the simulation results in supplement highlight, a second overlapping signal is present in the reduced signal; this second signal can be reasonably fitted using the parameters used to simulate the reduced plus SAM spectrum

(supplement). These data indicate that SAM has a high affinity for the small molecules. HydE active site, as the stock used to prepare the EPR samples had undergone purification, dialysis, reconstitution, and gel filtration. To investigate this phenomenon more generally, we decided to identify the presence of any small molecules that co-purify with HydE on a prep by prep basis. LCMS analysis of various HydE stocks (2 separate enzyme stocks analyzed) showed that HydE typically co-purifies with SAM and methionine. We were however unable to detect 5'-dAdo in supernatant preparations. As mentioned earlier, SPL and LAM both use SAM as a cofactor, therefore we subjected stocks of these enzymes the same analysis as HydE. Analysis of supernatant preparations clearly show that both these enzymes co-purify with methionine and SAM. Currently we are in the process of quantifying amounts of these small molecules in all three proteins.



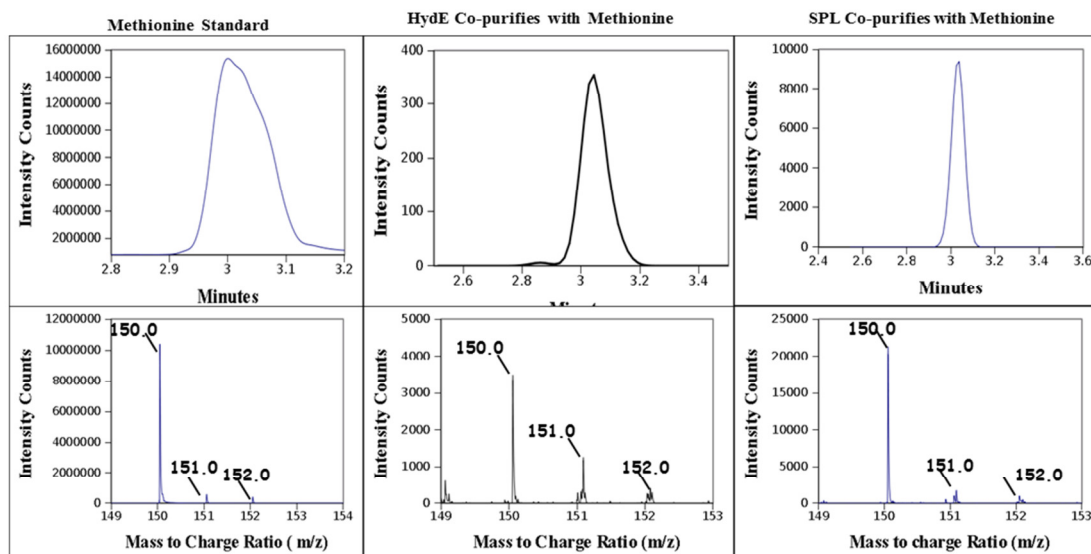


Figure 6: The top figure in every panel is a LC chromatogram and the bottom figure is the corresponding mass spectra. Panel A and B depicts SAM and Methionine standards run under assay conditions. Panel C and D depicts SAM bound to the respective enzymes. Panel E and F depicts methionine bound to the respective enzyme.

Discussion

The biosynthesis of the H-cluster at the active site of the [FeFe]-hydrogenase involves three hydrogenase maturation proteins: HydE, HydF, and HydG. HydE and HydG are radical S-adenosylmethionine (SAM) enzymes while HydF is a GTPase which serves as a scaffold for assembly of the 2Fe subcluster of the H-cluster. HydG exhibits considerable sequence homology to ThiH, a radical SAM enzyme that utilizes tyrosine as a substrate to produce dehydroglycine as a precursor in thiamine biosynthesis, and HydG was ultimately also shown to catalyze the cleavage of tyrosine. Further work demonstrated that this tyrosine cleavage led to the production of the carbon monoxide and cyanide ligands of the H-cluster. In parallel with these *in vitro* studies using purified proteins, the Swartz lab demonstrated that tyrosine, cysteine, and S-adenosylmethionine

stimulated *in vitro* hydrogenase activation in a cell lysate containing all three accessory proteins (HydE, HydF, and HydG), in addition to the purified hydrogenase. The stimulation by SAM could be explained by the fact that HydE and HydG are radical SAM enzymes, and the stimulation by tyrosine could now be explained due to its role as a HydG substrate. The explanation for the stimulation by cysteine has remained more elusive as no specific role for cysteine in H-cluster maturation has yet been revealed.

Herein we report the results of a broad screen designed to identify possible substrates for HydE. Our hypothesis has been that HydE, like HydG, acts on a small common metabolite, most likely an amino acid, to synthesize the dithiolate ligand of the H-cluster. We have thus screened all twenty amino acids, as well as several other common metabolites, by monitoring the rate of HydE-catalyzed reductive SAM cleavage in the presence of these potential substrates. Since radical SAM enzymes routinely catalyze slow SAM cleavage in the absence of substrate, which is enhanced in the presence of substrate, we expected that a positive substrate “hit” would show itself as an increase in the rate of SAM cleavage. In this broad screen, only cysteine enhanced the rate of HydE-catalyzed SAM cleavage (Supplement 3). This result, together with the Swartz result described earlier, begins to point more definitively to cysteine as a substrate of HydE. Since a substrate would be consumed during turnover, we proceeded to develop LCMS techniques to quantify cysteine in our assays, in order to see whether cysteine is consumed. Our data indicates that over 25 minutes the enzyme is able to catalyze 29.1 μ M cysteine. As mentioned earlier, HydE has been characterized as a radical SAM enzyme and therefore uses SAM and produces 5'-deoxyadenosine. Our results indicate over

25minutes HydE catalyze the consumption of 29 μM cysteine while simultaneously generating 33 μM 5'-deoxyadenosine, which indicates an almost 1:1 ratio of cysteine consumption to 5'd'Ado production. This provides compelling evidence that HydE uses SAM as co-substrate similar to the majority of radical SAM enzymes.

We have also conducted a thorough spectroscopic analysis of the as-isolated and reduced HydE and also probed the effects of SAM on the iron sulfur cluster. We have shown that the reduced reconstituted HydE from *Thermotoga maritima* (*T. maritima*) exhibits g-values comparable to those reported herein for *C. acetobutylicum* HydE (22, 32). Further, HydE that was homologously expressed in *C. acetobutylicum* in the presence of HydG and HydF (HydE^{FG}) showed signals typical of [4Fe-4S]⁺ clusters with g-values comparable to those reported herein; a dramatic reduction in [4Fe-4S]⁺ signal intensity was observed in non-reduced samples, collectively leading to the conclusion that HydE binds a single [4Fe-4S]^{2+/+} cluster (17). Although we have some understanding of the role of HydE with cysteine as substrate in H-cluster biosynthesis, the exact mechanism of this enzymes as well as the product of catalysis is still unknown. Therefore our future work will involve teasing out the particular role HydE plays in the formation the dithiolate linked cluster , presumably through utilization of cysteine.

References

1. Peters, J. W. (1999) Structure and mechanism of iron-only hydrogenases, *Current Opinion in Structural Biology* 9, 670-676.
2. Nicolet, Y., Piras, C., Legrand, P., Hatchikian, C. E., and Fontecilla-Camps, J. C. (1999) *Desulfovibrio desulfuricans* iron hydrogenase: The structure shows unusual coordination to an active site Fe binuclear center, *Structure* 7, 13-23.
3. Gordon, J. C., and Kubas, G. J. (2010) Perspectives on how nature employs the principles of organometallic chemistry in dihydrogen activation in hydrogenases, *Organometallics* 29, 4682-4701.
4. Posewitz, M. C., King, P. W., Smolinski, S. L., Zhang, L., Seibert, M., and Ghirardi, M. L. (2004) Discovery of two novel radical *S*-adenosylmethionine proteins required for the assembly of an active [Fe] hydrogenase, *Journal of Biological Chemistry* 279, 25711-25720.
5. King, P. W., Posewitz, M. C., Ghirardi, M. L., and Seibert, M. (2006) Functional studies of [FeFe] hydrogenase maturation in an *Escherichia coli* biosynthetic system, *Journal of Bacteriology* 188, 2163-2172.
6. Frey, P. A., Hegeman, A. D., and Ruzicka, F. J. (2008) The radical SAM superfamily, *Critical Reviews in Biochemistry and Molecular Biology*. 43, 63-88.
7. Vey, J. L., and Drennan, C. L. (2011) Structural insights into radical generation by the radical SAM superfamily, *Chemical Reviews*. 111, 2487-2506.
8. Shepard, E. M., and Broderick, J. B. (2010) *S*-Adenosylmethionine and iron-sulfur clusters in biological radical reactions: The radical SAM superfamily, *Comprehensive Natural Products II: Chemistry and Biochemistry*, pp 625-662,
9. Duschene, K. S., Veneziano, S. E., Silver, S. C., and Broderick, J. B. (2009) Control of radical chemistry in the AdoMet radical enzymes, *Current Opinion in Chemical Biology* 13, 74-83.
10. Roach, P. L. (2011) Radicals from *S*-adenosylmethionine and their application to biosynthesis, *Current Opinion in Chemical Biology* 15, 267-275.
11. Mulder, D. W., Ortillo, D. O., Gardenghi, D. J., Naumov, A. V., Ruebush, S. S., Szilagyi, R. K., Huynh, B., Broderick, J. B., and Peters, J. W. (2009) Activation of HydA(Δ^{EFG}) requires a preformed [4Fe-4S] cluster, *Biochemistry* 48, 6240-6248.

12. Mulder, D. W., Boyd, E. S., Sarma, R., Lange, R. K., Endrizzi, J. A., Broderick, J. B., and Peters, J. W. (2010) Stepwise [FeFe]-hydrogenase H-cluster assembly revealed in the structure of HydA^{ΔEFG}, *Nature* 465, 248-251.
13. Kuchenreuther, J. M., Guo, Y., Wang, H., Myers, W. K., George, S. J., Boyke, C. A., Yoda, Y., Alp, E. E., Zhao, J., Britt, R. D., Swartz, J. R., and Cramer, S. P. (2012) Nuclear resonance vibrational spectroscopy and electron paramagnetic resonance spectroscopy of ⁵⁷Fe-Enriched [FeFe] hydrogenase indicate stepwise assembly of the H-cluster, *Biochemistry* 52, 818-826.
14. Shepard, E. M., Boyd, E. S., Broderick, J. B., and Peters, J. W. (2011) Biosynthesis of complex iron-sulfur enzymes, *Current Opinion in Chemical Biology* 15, 319-327.
15. McGlynn, S. E., Shepard, E. M., Winslow, M. A., Naumov, A. V., Duschene, K. S., Posewitz, M. C., Broderick, W. E., Broderick, J. B., and Peters, J. W. (2008) HydF as a scaffold protein in [FeFe] hydrogenase H-cluster biosynthesis, *FEBS Letters*. 582, 2183-2187.
16. Shepard, E. M., McGlynn, S. E., Bueling, A. L., Grady-Smith, C., George, S. J., Winslow, M. A., Cramer, S. P., Peters, J. W., and Broderick, J. B. (2010) Synthesis of the 2Fe-subcluster of the [FeFe]-hydrogenase H-cluster on the HydF scaffold, *Proceedings of the National Academy of Sciences* 107, 10448-10453.
17. Czech, I., Silakov, A., Lubitz, W., and Happe, T. (2010) The [FeFe]-hydrogenase maturase HydF from *Clostridium acetobutylicum* contains a CO and CN⁻ ligated iron cofactor, *FEBS Letters*. 584, 638-642.
18. Kuchenreuther, J. M., Britt, R. D., and Swartz, J. R. (2012) New insights into [FeFe] hydrogenase activation and maturase function, *PLoS ONE* 7, e45850.
19. McGlynn, S. E., Shepard, E. M., Winslow, M. A., Naumov, A. V., Duschene, K. S., Posewitz, M. C., Broderick, W. E., Broderick, J. B., and Peters, J. W. (2008) HydF as a scaffold protein in [FeFe] hydrogenase H-cluster biosynthesis, *FEBS Letters* 582, 2183-2187.
20. Vallese, F., Berto, P., Ruzzene, M., Cendron, L., Sarno, S., De Rosa, E., Giacometti, G. M., and Costantini, P. (2012) Biochemical analysis of the interactions between the proteins involved in the [FeFe]-hydrogenase maturation process, *Journal of Biological Chemistry* 287, 36544-36555.
21. Kuchenreuther, J. M., Stapleton, J. A., and Swartz, J. R. (2009) Tyrosine, cysteine, and *S*-adenosylmethionine stimulate in vitro [FeFe] hydrogenase activation, *PLoS ONE* 4, e7565.

22. Pilet, E., Nicolet, Y., Mathevon, C., Douki, T., Fontecilla-Camps, J. C., and Fontecave, M. (2009) The role of the maturase HydG in [FeFe]-hydrogenase active site synthesis and assembly, *FEBS Letters*. 583, 506-511.
23. Driesener, R. C., Challand, M. R., McGlynn, S. E., Shepard, E. M., Boyd, E. S., Broderick, J. B., Peters, J. W., and Roach, P. L. (2010) [FeFe]-hydrogenase cyanide ligands derived from S-adenosylmethionine-dependent cleavage of tyrosine, *Angew Chemical International Edition Engl.* 49, 1687-1690.
24. Shepard, E. M., Duffus, B. R., McGlynn, S. E., Challand, M. R., Swanson, K. D., Roach, P. L., Peters, J. W., and Broderick, J. B. (2010) [FeFe]-Hydrogenase maturation: HydG-catalyzed synthesis of carbon monoxide, *Journal of the American Chemical Society* 132, 9247-9249.
25. Kuchenreuther, J. M., George, S. J., Grady-Smith, C. S., Cramer, S. P., and Swartz, J. R. (2011) Cell-free H-cluster synthesis and [FeFe] hydrogenase activation: All five CO and CN⁻ ligands derive from tyrosine, *PLoS ONE* 6, e20346.
26. Bradford, M. M. (1976) A rapid and sensitive method for the quantitation of microgram quantities of protein utilizing the principle of protein-dye binding, *Analytical Biochemistry*. 72, 248-254.
27. Fish, W. W. (1988) Rapid colorimetric micromethod for the quantitation of complexed iron in biological samples, *Methods in Enzymology*. 158, 357-364.
28. Stoll, S., and Schweiger, A. (2006) EasySpin, a comprehensive software package for spectral simulation and analysis in EPR, *Journal of Magnetic Resonance* 178, 42-55.
29. Rupp, H., Rao, K. K., and Hall, D. O. (1978) Electron spin relaxation of iron-sulphur proteins studied by microwave power saturation, *Biochimica et Biophysica Acta (BBA)* 537, 255-269.
30. Shepard, E. M., Duffus, B. R., George, S. J., McGlynn, S. E., Challand, M. R., Swanson, K. D., Roach, P. L., Cramer, S. P., Peters, J. W., and Broderick, J. B. (2010) [FeFe]hydrogenase maturation: HydG-catalyzed synthesis of carbon monoxide, *Journal of the American Chemical Society* 132, 9247-9249.
31. Nicolet, Y., Rubach, J. K., Posewitz, M. C., Amara, P., Mathevon, C., Atta, M., Fontecave, M., and Fontecilla-Camps, J. C. (2008) X-ray structure of the [FeFe]-hydrogenase maturase HydE from *Thermotoga maritima*, *Journal of Biological Chemistry* 283, 18861-18872.

32. Rubach, J. K., Brazzolotto, X., Gaillard, J., and Fontecave, M. (2005) Biochemical characterization of the HydE and HydG iron-only hydrogenase maturation enzymes from *Thermatoga maritima*, *FEBS Letters* 579, 5055-5060.
33. Ollagnier-de Choudens, S., Sanakis, Y., Hewitson, K. S., Roach, P., Münck, E., and Fontecave, M. (2002) Reductive cleavage of *S*-adenosylmethionine by biotin synthase from *Escherichia coli*, *Journal of Biological Chemistry* 277, 13449-13454.
34. Silver, S. C., Chandra, T., Zilinskas, E., Ghose, S., Broderick, W. E., and Broderick, J. B. (2010) Complete stereospecific repair of a synthetic dinucleotide spore photoproduct by spore photoproduct lyase, *Journal of Biological Inorganic Chemistry* 15, 943-955.
35. Shepard, E. M., and Broderick, J. B. (2010) *S*-Adenosylmethionine and iron-sulfur clusters in biological radical reactions: The radical SAM superfamily, *Comprehensive Natural Products II*, pp 625-661
36. Buis, J. M., Cheek, J., Kalliri, E., and Broderick, J. B. (2006) Characterization of an active spore photoproduct lyase, a DNA repair enzyme in the radical *S*-adenosylmethionine superfamily, *Journal of Biological Chemistry* 281, 25994-26003.
37. Coper, N. J., Booker, S. J., Ruzicka, F., Frey, P. A., and Scott, R. A. (2000) Direct FeS cluster involvement in generation of a radical in lysine 2, 3-aminomutase, *Biochemistry* 39, 15668-15673.
38. Nicolet, Y., Amara, P., Mouesca, J.-M., and Fontecilla-Camps, J. C. (2009) Unexpected electron transfer mechanism upon AdoMet cleavage in radical SAM proteins, *Proceedings of the National Academy of Sciences* 106, 14867-14871.
39. Boswell, N.W.B. (2011) Montana State University Bozeman.

MECHANISTIC INSIGHTS INTO HYDE CATALYSIS

Contribution of Authors and Co-Authors

Manuscript in Chapter 4

Author: Shourjo Ghose

Contributions: Protein purification research design, assay optimization, method development, LCMS analysis. Manuscript writing and preparation

Co-author: Eric Shepard

Contributions: Research design, data analysis, manuscript editing

Co-author: John W. Peters

Contributions: Provided valuable insight into and discussions of the [FeFe]-hydrogenase and its maturation. Manuscript editing.

Co-author: Joan B. Broderick

Contributions: Overall conception, direction, and funding of the project. Provided insights into the experimental approach and design. Manuscript writing and preparation.

Manuscript Information Page

Shourjo Ghose, Eric M. Shepard, John W. Peters and Joan B. Broderick
Journal: Biochemistry

Status of the manuscript:

- Prepared for submission to a peer-reviewed journal
- Officially submitted to a peer-reviewed journal
- Accepted by a peer-reviewed journal
- Published in a peer-reviewed journal

MECHANISTIC INSIGHTS INTO HYDE CATALYSIS

Shourjo Ghose, Eric M. Shepard, John W. Peters and Joan B. Broderick

Department of Chemistry and Biochemistry, Montana State University, Bozeman, Montana 59717, United States

Astrobiology Biogeocatalysis Research Center, Montana State University, Bozeman, Montana 59717, United States

Abstract

The biosynthesis and assembly of the active site cluster of the [FeFe]-hydrogenase requires the catalytic action of accessory enzymes HydE, HydG and HydF. We demonstrate here for the first time that HydE catalysis involves hydrogen atom abstraction from the C- β position of the substrate cysteine. High performance liquid chromatographic and mass spectrometric monitoring of deuterium incorporation into 5'-deoxyadenosine upon HydE-catalyzed conversion of cysteine labeled with deuterium at the β position demonstrate the incorporation of deuterium into dAdo. We also show tantalizing preliminary evidence for the role HydF ^{Δ EG} in the H-cluster maturation exceeding that of a scaffold. We believe that HydF ^{Δ EG} plays a dynamic role stabilizing the active conformation of HydE, thereby facilitating and accelerating catalysis.

Introduction

The [FeFe] hydrogenase enzymes catalyze the reversible reduction of protons to hydrogen gas ($2\text{H}^+ + 2\text{e}^- \rightleftharpoons \text{H}_2$) and are a key feature in the H_2 metabolism of many microorganisms [1]. [FeFe] Hydrogenases utilize a complex bridged metal cluster in its active site, referred to as the H-cluster, to catalyze this reaction [2]. The H-cluster is composed of a [4Fe-4S] cubane bridged to a 2Fe bi-nuclear center via a single bridging cysteine. The 2Fe subcluster has been shown to contain five biologically unusual diatomic ligands (CO and CN⁻) as well as a non-protein derived bridging dithiolate [3, 4]. Additionally, crystal structures of the oxidized as well as reduced state of the enzyme

have indicated that the distal Fe ion of the 2Fe center is the site of the proton reduction and H₂ gas production [5, 6].

The biosynthesis of this unique H-cluster requires the catalytic action of maturase proteins, identified as HydE, HydG and HydF [7]. Bioinformatics studies, and biochemical analysis have shown that HydE and HydG belong to the radical *S*-adenosylmethionine (SAM) superfamily of enzymes while HydF is a GTPase[7, 8]. Most members of the radical SAM superfamily contain a three cysteine conserved motif (CX₃CX₂C) that coordinates a [4Fe-4S] catalytic cluster[9]. While three of the 4 Fe ions are ligated by protein derived cysteines, the third unique Fe is coordinated by the amino and carboxyl groups of *S*-adenosylmethionine[10, 11]. In all cases catalysis is initiated by a single electron transfer from a reduced [4Fe-4S]⁺ cluster to SAM resulting in the cleavage of the C-S bond[12]. The consequent 5'-deoxyadenosyl radical (5'-dAdo•) then abstracts an H atom from the substrate to initiate a diverse array of biologically essential chemical reactions[13]. Based on recent spectroscopic and biochemical characterization by the Broderick group as well as others, it proposed that HydE synthesizes the bridging dithiolate (on the 2Fe-2S cluster of HydF), thereby shifting the reactivity to the Fe ions. Thereafter HydG catalyzes the decomposition of tyrosine to produce the 3 carbon monoxide and 2 cyanide ligands. Once the biosynthesis of the cluster is completed on HydF, which is proposed to act as a scaffold, it is translocated to the apo HydA through a cationic channel thereby forming active hydrogenase [14-16].

Herein, we present further evidence implicating cysteine as the substrate for HydE, through the observation of label transfer from deuterated cysteine (deuterated at the C α —

H, C β —H, or thiol C—H) to product 5'-deoxyadenosine. In our study we have utilized specifically deuterium-labeled cysteine and have monitored site specific label transfer to 5'-dAdo via high performance liquid chromatography and mass spectrometry. We have also provided tantalizing preliminary evidence on the role of HydF ^{Δ EG} during the catalytic action of HydE. Our results provide important mechanistic insights into the HydE catalyzed decomposition of cysteine and provide clues towards the identification of a putative product of this catalysis.

Materials and Methods

Protein Expression, Purification, and Reconstitution

HydE was expressed in *E. coli* BL21(DE3) as described previously in chapter 3. Single colonies from streaked plates were used to inoculate 50 mL of phosphate buffered Luria-Bertani (LB) medium, pH 7.5, containing ampicillin. These cultures were grown for 12-15 hours at 37°C and 225 rpm in a thermostatted shaker and were used to inoculate 9-L cultures of 50 mM phosphate buffered (pH 7.5) LB medium supplemented with 5 g/L NaCl, 5 g/L glucose. The 9 L cultures were grown in a thermostatted shaker at 37°C and 225 rpm until an optical density (OD₆₀₀) of 0.5 – 0.6 was reached. The cells were then induced with 1 mM isopropyl thiogalactopyranoside (IPTG) and the medium was supplemented with ferrous ammonium sulfate (FAS, 0.06 g/L). The cultures were grown for an additional 2.5 – 3.0 hours prior to cooling to room temperature and addition of more FAS (0.06 g/L). The cell cultures were then placed under nitrogen at 4°C for an

additional 15 hours. Cells were then harvested by centrifugation and immediately flash frozen in liquid N₂ before being stored at -80°C until further use.

Cell lysis and purification of the proteins were accomplished anaerobically in a Coy anaerobic chamber (Coy Laboratories, Grass Lake, MI). Cell pellets were resuspended in a lysis solution containing 50 mM HEPES pH 7.4, 10 mM imidazole, 500 mM KCl, 5% glycerol, 20 mM MgCl₂, 1 mM phenylmethylsulfonyl fluoride (PMSF), 1% Triton X-100, 0.2 mg/mL lysozyme, 0.03 mg/mL DNase and 0.03 mg/mL RNase. Cells were incubated in the lysis mixture for 1 hr on ice with gentle stirring at which time the mixture was centrifuged for 30 min at 18000 rpm. The supernatant was loaded onto a 5 mL HisTrap Ni²⁺-affinity column or a gravity Ni²⁺ affinity column (GE Healthcare) that was pre-equilibrated with Buffer A (50 mM HEPES pH 7.4, 500 mM KCl, 5% glycerol, 10 mM imidazole). The column was then washed with 10 column volumes of buffer A followed by a step gradient of increasing imidazole in buffer B (50 mM HEPES pH 7.4, 500 mM KCl, 5% glycerol, 500 mM imidazole). The eluting protein fractions were collected and analyzed by sodium dodecyl sulfate polyacrylamide gel electrophoresis (SDS-PAGE) and those determined to be 95% or more pure were pooled. The pooled fractions were then dialyzed against 50 mM HEPES pH 7.4, 500 mM KCl, and 5% glycerol. The dialyzed protein was then placed in O-ring sealed tubes, flash frozen, and stored at -80 °C until further use. Protein concentrations were determined by the method of Bradford using a kit sold by Bio-Rad and bovine serum albumin as a standard [17]. Iron content was determined using the method developed by Fish [18].

Purified HydE was chemically reconstituted under anaerobic conditions in a Coy anaerobic chamber by addition of 5 mM DTT and a ~6-fold excess of FeCl₃ and Na₂S, as described previously [19]. After incubation for 2-3 hours, the protein was centrifuged to remove excess Fe and S and subsequently desalted and buffer exchanged over a G-25 Sephadex column (GE Healthcare) pre-equilibrated in 50 mM HEPES pH 7.4, 500 mM KCl, and 5% glycerol. UV-Vis spectroscopy under anaerobic conditions as well Fe quantitation by the method developed by Fish[18] was used to confirm the iron-sulfur cluster content of the purified, reconstituted protein. The room temperature spectra were taken with a dual beam Varian Cary 50 BIO UV-Vis or Cary 6000i UV-Vis-NIR spectrophotometer at a scan rate of 600 nm/minute. The reconstituted protein was concentrated using a Minicon-B-15 concentrator (Millipore) and then placed in O-ring sealed tubes, flash frozen in liquid N₂, and stored at -80 °C until further use.

Assay Conditions

Assays were carried out in the MBraun box (≤ 1 ppm O₂) using buffers and reagents that were freshly degassed on a Schlenk Line. Assays comprised 25 μ M reconstituted HydE, 2 mM dithionite, 50 mM HEPES, 0.5 M KCl, 5% glycerol, at pH 7.5 and 200 μ M L-cysteine. Cysteine labeled with deuterium at either the C α -H, C β -H, or thiol C-H was used in the assay. To ensure the selective labeling of the solvent exchangeable H atom at the thiol position, lyophilized cysteine was reconstituted into freshly degassed HEPES D₂O buffer and the pD (7.4) confirmed through a pH indicator. All assays with aforementioned cysteine labeled at the thiol position with deuterium were conducted in HEPES D₂O buffer at a pD (7.4). Assays containing all components but SAM were

pre-incubated for 5 minutes at 37 °C and the reaction was initiated by the addition of 1 mM SAM. Aliquots of 50 μ L were taken at different time points and quenched with 3 μ L of 1M HCl. The samples were then centrifuged at 13,000 rpm for 15 min at 4 °C to remove precipitated protein and the supernatant was then flash frozen in liquid N₂ and stored at -80 °C until analysis. To determine the level of cysteine consumed over the reaction period, control assays were performed which were identical to the experimental with the exception that they did not contain SAM. In order to obtain a basal rate of deoxyadenosine production by HydE in the absence of cysteine (uncoupled cleavage), additional control assays were performed as above except lacking cysteine. In order to probe the effect of HydF^{ΔEG} on the catalytic activity of HydE, all the above mentioned assays were repeated in the presence of 5x molar excess of HydF^{ΔEG} and the samples handled in identical fashion. Moreover, In all assays conducted in the absence of HydF^{ΔEG}, the concentration of 5'-deoxyadenosine was calculated by subtracting the amount of 5'-deoxyadenosine produced in the control reaction, without the presence of cysteine (uncoupled cleavage) from that of the experimental. Samples selected for LC-MS were prepared by diluting them 100-fold in 10% methanol, 90% water.

High Performance Liquid Chromatography and Mass Spectrometry Conditions

Samples selected for LC-MS were prepared by diluting them 100-fold in 10% methanol, 90% water in cases except for samples containing D₂O. During a single HPLC run, two consecutive analytical trials were performed for each injected sample, so as to exclude any ambiguity resulting from peak shifts or change in peak area. Aliquots from experimental replicates were run on the HPLC system for a minimum of two times

on different days to eliminate the effects of day to day instrument drifts. All analytes were observed in the $[M+H]^+$ form, and quantitation of deoxyadenosine, SAM, and tyrosine were performed as described below. Due to its ubiquitous presence and high signal quality, the HEPES elution peak was used as a quality control check and as mass accuracy validation. The chromatography system was composed of an Agilent 1290 series UHPLC with binary pump, temperature-controlled auto-sampler and column compartment. The auto-sampler module and reactions were held at 4 °C using the active temperature control option. The separation of the various analytes was performed using normal phase chromatography with a Cogent “Diamond Hydride” HPLC column (MicroSolv, 150 x 2.1mm), held at 50 °C. Solvents consisted of H₂O with 0.1% formic acid in channel “A” and acetonitrile with 0.1% formic acid in channel “B”, and the flow rate was a constant 0.8 mL/min at all times. Prior to sample injection, the column was equilibrated with 100% “B”. Sample injection was performed with the autosampler, and following injection the solvent composition was maintained at 100% B for 2 minutes. A linear gradient was then used from 100% B to 50% B, from 2 min to 6 min. From 6 min to 8.5 min the composition was held at 50% B for elution of strongly-retained compounds. At 8.51 minutes the composition was changed back to 100% B and held until 10.0 minutes for re-equilibration. Due to delays from sample injection, the overall time between samples was approximately 11 minutes. Mass spectra were obtained on an Agilent 6538 Q-TOF mass spectrometer equipped with the dual-ESI source. The capillary exit voltage was 120 V and gas temperature was 300 °C. All data was recorded in positive mode between 25 m/z and 750 m/z in profile mode. The hardware summation

time was 1 second. Peaks were validated using high-accuracy formula confirmation and elution matching from individual reference standards. Quantitation was performed using the MassHunter Quantitative Analysis package (Agilent). An extracted ion chromatograph was generated using the accurate mass of each compound with a -0.04 to +0.04 ppm m/z extraction window. This was selected to give the best compromise of specificity, sensitivity, and tolerance to slight calibration shifts during the runs.

Results

Analysis of HydE-Mediated Deuterium Transfer from Cysteine to dAdo

Previous data from the Broderick group showed cysteine dependent acceleration of HydE catalyzed cleavage of SAM with the corresponding consumption of cysteine (Please refer to Chapter 3). The 1:1 correlation between cysteine consumed and 5'-dAdo generated implicates that HydE is most likely utilizing cysteine as a substrate. In order to gain a mechanistic insight into the HydE-catalyzed reaction, we performed similar assays with cysteine labeled cysteine deuterated at the $C\alpha$ -H, $C\beta$ -H, or thiol C-H. Our primary aim was to determine whether deuterium label became incorporated into the 5'-dAdo resulting from reductive cleavage of SAM during catalysis. Such deuterium transfer would indicate H atom abstraction from cysteine by the 5'-dAdo radical intermediate, thereby providing more direct evidence for the role of cysteine as the substrate of HydE. Analysis of assays conducted with cysteine labeled with deuterium at the α , β and thiol positions indicated that the isotopic distribution of 5'-dAdo were no different than those conducted without cysteine (Figure 1, Table 1). Additionally, when

compared to assays conducted with unlabeled cysteine, analogous amounts of 5'-dAdo were shown to be produced as in experiments conducted with labeled substrate (data not shown). This observed lack of deuterium label incorporation into 5'-dAdo from either the $\alpha\beta$, β and thiol positions, suggested that H atom abstraction was not taking place from any of the aforementioned positions on cysteine.

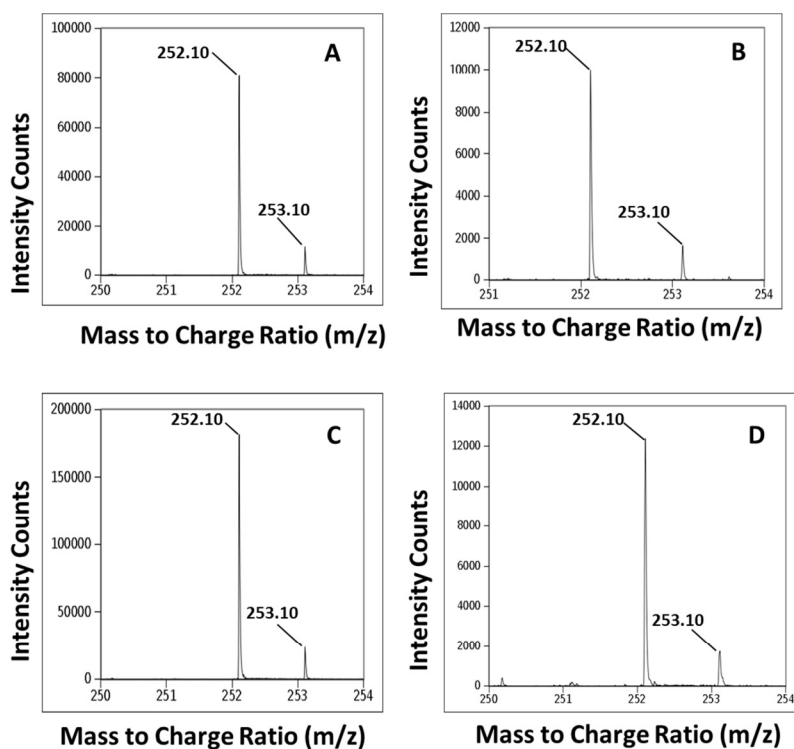


Figure 1: Isotopic distribution of 5-dAdo with deuterium labeled and unlabeled cysteine substrate. (A) Unlabeled cysteine. (B) $[\alpha\beta\text{-D}_2]$ -cysteine. (C) $[\beta\text{-D}]$ Labeled cysteine. (D) Thiol deuterated cysteine. In all cases the observed isotopic distribution was identical

A) Analyte /Assay Substrate	B) Percent Intensity of Secondary to Primary Peak	C) Percent Area of Secondary Peak to Primary Peak
5'-deoxyadenosine Standard	11.3±3.3	10.8±2.1
Deuterium label at β-C of Cysteine	12.2±3.1	10.4±3.5
Deuterium label at α-C of Cysteine	10.4±1.9	12.6±3.4
Deuterium label at Thiol of Cysteine	11.9±2.5	9.8±1.6

Table 4.1: Comparison of the ratios of 5'-dAdo isotopic distribution on assays performed in the presence of HydE only. Column A represents the deuterium labeled substrates used in the assays. Column B represents the ratio of the peak heights. Column C represents the ratio of the peak areas.

Effects of HydF^{ΔEG} on 5'-dAdo Production and Cysteine Consumption

Previously we had calculated the amount of Hyde catalyzed SAM cleavage in the presence of cysteine to have been approximately 80μM dAdo at 25minutes . On the introduction of HydF^{ΔEG} in the assay, however, the rate of 5'-dAdo production was reduced to levels comparable to background uncoupled cleavage (Figure 2). Interestingly, we were also able to observe a slight increase in the levels of cysteine breakdown in assays conducted in the presence of HydF^{ΔEG}. Our observations indicated that at the 25min time point the amount of cysteine turned over by HydE only was 32.8±2.8μM with a corresponding 81.9 ±1.9μM of 5'-deoxyadenosine produced. In contrast, HydE in conjunction with HydF^{ΔEG} was able to consume 41.0±2.6μM cysteine while generating 57.8±2.1 μM 5'-deoxyadenosine. The assays were repeated in the presence of HydF^{EΔG} HydF^{GΔE} and the results obtained were comparable to those with HydF^{ΔEG}(data not shown). Such a phenomenon was not particularly surprising to us, as earlier had biochemical analysis had indicated that HydE and HydF had a strong affinity for each

other[20], indeed bioinformatic analysis on some green algae had shown the genes for HydF and HydE to be fused[21]. The decrease is the molar amount of 5'-dAdo coupled to the increase in cysteine decomposition in assays performed with Hyd^{ΔFEG} spurred us to explore the mechanistic effects of this scaffold enzyme on HydE catalysis. HydE assays similar to those conducted earlier were performed in the presence of HydF^{ΔEG} and deuterated cysteine. Control assays were conducted in the absence of HydF^{ΔEG}. The results provide evidence that in the presence of HydF^{ΔEG} and β-deuterated cysteine some of the deuterium label ends up on 5'-dAdo.

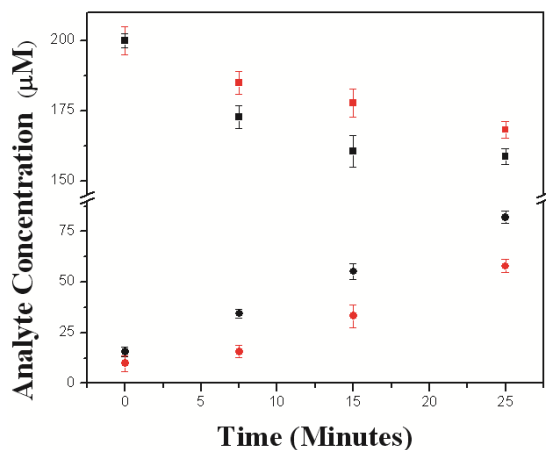


Figure2: The figure compares the decrease in Cysteine concentration and the increase in 5'-deoxyadenosine concentration in the presence of HydE only and HydE with HydF^{ΔEG} over 25min. At the 25min time point HydE only generates 81.9 μM of 5'-deoxyadenosine ● and consume 32.8μM cysteine ■. At the same time point HydE with HydF^{ΔEG} generates 57.8 μM 5'-deoxyadenosine ● and consumes 41.0μM cysteine ■. It must be noted that in both these cases the measurements of 5'-deoxyadenosine produced were calculated without subtracting 5'-dAdo produced due to uncoupled cleavage.

Such a conclusion is validated by the change in the isotopic ratios of the primary (252.10 m/z) and secondary (253.11 m/z) peak (Figure 3, Table 2). In the case where the assay

was conducted with HydE only the ratio of the secondary to the primary peak was calculated to be $12.2 \pm 3.1\%$ (Figure 1C and Figure 3A, Table 1, Table 2).

Analyte /Assay Substrate	Percent Intensity of Secondary to Primary Peak	Percent Area of Secondary Peak to Primary Peak
5'-deoxyadenosine Standard	11.3 ± 3.3	10.8 ± 2.1
Deuterium label at β -C of Cysteine	23.2 ± 2.1	25.0 ± 3.5
Deuterium label at α -C of Cysteine	13.5 ± 4.2	12.4 ± 2.9
Deuterium label at Thiol of Cysteine	12.7 ± 3.8	11.7 ± 3.0

Table 4.2: Comparison of the ratios of 5'-dAdo isotopic distribution on assays performed in the presence of HydE and HydF^{ΔEG}. Column A represents the deuterium labeled substrates used in the assays. Column B represents the ratio of the peak heights. Column C represents the ratio of the peak areas.

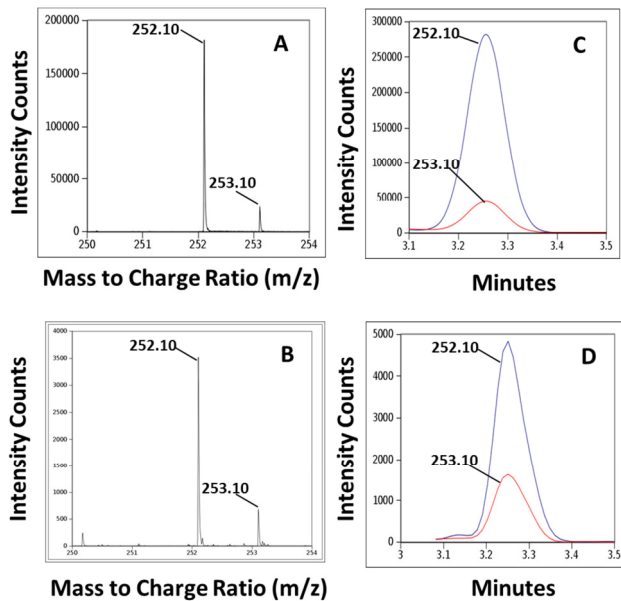


Figure 3: Comparison in isotopic ratios between the primary and secondary peaks of 5'-deoxyadenosine. Panel A represents the mass spectra of 5'-dAdo in the absence of HydF^{ΔEG}. Panel B represents the mass spectra of 5'-dAdo in the presence of HydF^{ΔEG}. Panel C represents the LC chromatogram and peak areas of 5'-dAdo in the absence of HydF^{ΔEG}. Panel D represents the LC chromatogram and peak areas of 5'-dAdo in the presence of HydF^{ΔEG}.

However when the assay was conducted in the presence of HydF^{ΔEG}, we see a substantial increase in the ratio of the secondary to the primary peak which was calculated to be 23.2±2.1% (Fig 3, B, Table 2). Moreover, when the ratios of the peak areas were calculated, it was noticed that ratios in the case of assays performed with HydE only was 10.4±3.5% (Figure 3C, Table 1) and in the case of HydE with HydF^{ΔEG} was calculated to be 25.0±3.5% (Figure 3D, Table 2). This in turn indicates that during catalysis, 5'-dAdo• is able to abstract an H atom from the β carbon of cysteine resulting in a possible decomposition of the substrate. Similar control assays were run with α-D-cysteine as well as assays done in D₂O with the thiol H atom exchanged with deuterium. In no other case was the “D” label traced on to 5'-dAdo.

Discussion

We herein report initial experiments designed to probe potential H-atom abstraction from cysteine during HydE catalysis. In our initial experiments we were unable to detect deuterium incorporation in 5'-dAdo in assays carried out with HydE and [β-D₂]-cysteine. However when HydF^{ΔEG} was included in these assays, deuterium atom incorporation into 5'-dAdo was detected. We did not observe any D atom incorporation to 5'-dAdo when the assays were repeated in the presence of cysteine labeled with deuterium at α carbon or the thiol position. The lack of deuterium incorporation in 5'-dAdo in the absence of HydF^{ΔEG} is perplexing. Additionally, under our assay conditions the addition of HydF^{ΔEG} seems to have a stabilizing effect on HydE as evidenced by increased cysteine turn over and lower nonproductive SAM cleavage. As mentioned above, such an event is not

surprising, as bioinformatic and biochemical characterizations have indicated that HydE and HydF might indeed be interacting with each other in ways which are unique in the H-cluster maturation scheme. [21]. [20]. Taken together, this indicates that HydF could potentially be facilitating HydE catalysis of cysteine either by stabilizing the active conformation of the enzyme or perhaps by shuttling away the products from the active site thereby shifting the equilibrium towards increased cysteine decomposition. We also believe that our data provides insights into the ultimate fate of the products of cysteine degradation by HydE. If HydE is indeed working in conjunction with HydF, the product of cysteine decomposition could potentially be directly and seamlessly incorporated into forming the bridging dithiolate. Our current efforts therefore are directed towards assays with cysteine labeled with ^3H at the β position followed by scintillation counting to determine the ultimate fate of the products of the HydE-catalyzed reaction.

In conclusion, we believe that cysteine is indeed the substrate for HydE and that catalysis is initiated via a single H atom abstraction from the β position of cysteine. Moreover, we have shown evidence that indicates that HydF ^{ΔEG} most likely facilitates this reaction via stabilizing the enzyme in its active form and through mechanisms yet unknown.

References

1. Vignais PM, Billoud B & Meyer J (2001) Classification and phylogeny of hydrogenases. *FEMS Microbiology Reviews* 25, 455-501.
2. Holm RH, Kennepohl P & Solomon EI (1996) Structural and functional aspects of metal sites in biology. *Chemical Reviews* 96, 2239-2314.
3. Peters JW (1999) Structure and mechanism of iron-only hydrogenases. *Current Opinion in Structural Biology* 9, 670-676.
4. Nicolet Y, Piras C, Legrand P, Hatchikian CE & Fontecilla-Camps JC (1999) *Desulfovibrio desulfuricans* iron hydrogenase: The structure shows unusual coordination to an active site Fe binuclear center. *Structure* 7, 13-23.
5. Peters JW, Lanzilotta WN, Lemon BJ & Seefeldt LC (1998) X-ray Crystal structure of the Fe-only hydrogenase (CpI) from *Clostridium pasteurianum* to 1.8 angstrom resolution. *Science* 282, 1853-1858.
6. Nicolet Y, de Lacey AL, Vernede X, Fernandez VM, Hatchikian EC & Fontecilla-Camps JC (2001) Crystallographic and FTIR spectroscopic evidence of changes in Fe coordination upon reduction of the active site of the Fe-only hydrogenase from *Desulfovibrio desulfuricans*. *Journal of the American Chemical Society* 123, 1596-1601.
7. Posewitz MC, King PW, Smolinski SL, Zhang L, Seibert M & Ghirardi ML (2004) Discovery of two novel radical *S*-adenosylmethionine proteins required for the assembly of an active [Fe] hydrogenase. *Journal of Biological Chemistry* 279, 25711-25720.
8. King PW, Posewitz MC, Ghirardi ML & Seibert M (2006) Functional studies of [FeFe] hydrogenase maturation in an *Escherichia coli* biosynthetic system. *Journal of Bacteriology* 188, 2163-2172.
9. Frey PA, Hegeman AD & Ruzicka FJ (2008) The radical SAM superfamily. *Critical Reviews in Biochemistry and Molecular Biology* 43, 63-88.
10. Walsby CJ, Hong W, Broderick WE, Cheek J, Ortillo D, Broderick JB & Hoffman BM (2002) Electron-nuclear double resonance spectroscopic evidence that *S*-adenosylmethionine binds in contact with the catalytically active [4Fe-4S]⁺ cluster of pyruvate formate-lyase activating enzyme. *Journal of the American Chemical Society* 124, 3143-3151.
11. Walsby CJ, Ortillo D, Broderick WE, Broderick JB & Hoffman BM (2002) An anchoring role for FeS clusters: Chelation of the amino acid moiety of *S*-

adenosylmethionine to the unique iron site of the [4Fe-4S] cluster of pyruvate formate-lyase activating enzyme. *Journal of the American Chemical Society* 124, 11270-11271.

12.Chen D, Walsby C, Hoffman BM & Frey PA (2003) Coordination and mechanism of reversible cleavage of S-adenosylmethionine by the [4Fe-4S] center in lysine 2, 3-aminomutase. *Journal of the American Chemical Society* 125, 11788-11789.

13.Peter L R (2011) Radicals from S-adenosylmethionine and their application to biosynthesis. *Current Opinion in Chemical Biology* 15, 267-275.

14.Mulder David W, Shepard Eric M, Meuser Jonathan E, Joshi N, King Paul W, Posewitz Matthew C, Broderick Joan B & Peters John W (2011) Insights into [FeFe]-hydrogenase structure, mechanism, and maturation. *Structure* 19, 1038-1052.

15.Shepard EM & Broderick JB (2010) S-Adenosylmethionine and iron-sulfur clusters in biological radical reactions: The radical SAM superfamily. *Comprehensive Natural Products II: Chemistry and Biochemistry*, pp. 625-662.

16.Shepard EM, Duffus BR, George SJ, McGlynn SE, Challand MR, Swanson KD, Roach PL, Cramer SP, Peters JW & Broderick JB (2010) [FeFe] hydrogenase maturation: HydG-catalyzed synthesis of carbon monoxide. *Journal of the American Chemical Society* 132, 9247-9249.

17.Bradford MM (1976) A rapid and sensitive method for the quantitation of microgram quantities of protein utilizing the principle of protein-dye binding. *Analytical Biochemistry* 72, 248-254.

18.Fish WW (1988) Rapid colorimetric micromethod for the quantitation of complexed iron in biological Samples. *Methods in Enzymology* 158, 357-364.

19.Shepard EM, Duffus BR, McGlynn SE, Challand MR, Swanson KD, Roach PL, Peters JW & Broderick JB (2010) [FeFe]-Hydrogenase maturation: HydG-catalyzed synthesis of carbon monoxide. *Journal of the American Chemical Society* 132, 9247-9249.

20.Vallese F, Berto P, Ruzzene M, Cendron L, Sarno S, De Rosa E, Giacometti GM & Costantini P (2012) Biochemical analysis of the interactions between the proteins involved in the [FeFe] hydrogenase maturation process. *Journal of Biological Chemistry* 287, 36544-36555.

21.Böck A, King PW, Blokesch M & Posewitz MC (2006) Maturation of hydrogenases. *advances. Microbial Physiology* 51, 1-225.

CHAPTER 5

MECHANISTIC INVESTIGATION OF [FeFe]-HYDROGENASE
MATURASE HYDGContribution of Authors and Co-Authors

Manuscript in Chapter 5

Author: Benjamin Duffus

Contributions: Protein purifications. Research design, , HydG characterization and assay optimization,

Co-author: Shourjo Ghose

Contributions: Research design, method development, LCMS analysis.

Co-author: John W. Peters

Contributions: Provided valuable insight into and discussions of the [FeFe]-hydrogenase and its maturation. Manuscript editing.

Co-author: Joan B. Broderick

Contributions: Contributions: Overall conception, direction, and funding of the project. Provided insights into the experimental approach and design. Manuscript writing and preparation.

Manuscript Information Page

Benjamin R. Duffus, Shourjo Ghose, John W. Peters, and Joan B. Broderick*
Journal: Biochemistry

Status of the manuscript:

- Prepared for submission to a peer-reviewed journal
- Officially submitted to a peer-reviewed journal
- Accepted by a peer-reviewed journal
- Published in a peer-reviewed journal

MECHANISTIC INVESTIGATION OF [FeFe]-HYDROGENASE MATURASE HydG

Benjamin R. Duffus, Shourjo Ghose, John W. Peters, and Joan B. Broderick*

Department of Chemistry and Biochemistry, Montana State University, Bozeman, Montana 59717, United States

Astrobiology Biocatalysis Research Center, Montana State University, Bozeman, Montana 59717, United States

Abstract

The unusual active site organometallic H-cluster cofactor in [FeFe]-hydrogenase is biosynthesized by three accessory proteins, two of which are radical AdoMet enzymes (HydE, HydG) and one of which is a GTPase (HydF). We demonstrate here that HydG initiates radical-based tyrosine decomposition through hydrogen abstraction of the phenolic hydrogen atom. The isotopic distributions of 5'-deoxyadenosine (5'-dAdo) were monitored in D₂O with non-labeled tyrosine, as well as in H₂O with deuterium-labeled tyrosine substrates. The observed deuterium atom incorporated in the 5'-dAdo product implicate a mechanism where the dAdo radical interacts with the solvent-exchangeable tyrosine 4-phenol as the principal radical initiation event.

Introduction

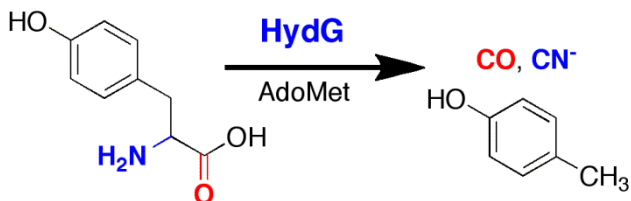
The organometallic active sites of the [NiFe]-hydrogenases and [FeFe]-hydrogenases are unique in their common requirement for coordinated diatomic ligands CO and CN⁻ (1). Each type of hydrogenase has developed evolutionarily distinct methods for controlled synthesis and delivery of these π -accepting ligands that help stabilize low-valent iron species required for the reversible reduction of protons to yield dihydrogen (2). The organometallic H-cluster cofactor from [FeFe]-hydrogenase comprises a [4Fe-4S] cluster bridged by a cysteinyl residue to a 2Fe cluster coordinated by three CO, two CN⁻, and a bridging dithiolate, proposed to be dithiomethylamine(3-5). Only three accessory proteins are necessary for the synthesis of the 2Fe subcluster of the H-cluster, involving two radical S-adenosylmethionine (SAM) enzymes (HydE and HydG) and a

scaffold GTPase (HydF) (6-8). Characterization of HydG has shown that it catalyzes the cleavage of tyrosine to produce *p*-cresol, CN⁻, and CO, resulting in the synthesis of all diatomic ligands observed on the H-cluster (Scheme 1) (9-11). As a theme common to most radical SAM enzyme characterized to date, catalysis is initiated through generation of the 5'-deoxyadenosyl radical(12). This radical is generated via a single electron transfer between the site-differentiated [4Fe-4S] cluster coordinated by a conserved cysteine (CX₃CX₂C) motif and the coordinated SAM molecule(13, 14). Transfer of an electron to SAM results in homolytic bond cleavage of the S—C bond between the sulfonium sulfur and 5'-deoxyadenosyl carbon atoms, resulting in generation of the primary carbon-based 5'-deoxyadenosyl radical(13). This highly reactive primary radical is thereafter quenched via a hydrogen atom abstraction, either from the substrate directly or from the surrounding protein environment (Please refers to figure 2 of Chapter 1).

As biochemical characterization of radical SAM enzyme has increased, depth in understanding the mechanism of generation of the 5'-deoxyadenosyl radical and its interaction with substrates has yielded insight to likely reaction mechanisms. For example, ThiH is a radical SAM enzyme that utilizes tyrosine as its substrate to produce *p*-cresol and dehydroglycine with the latter being utilized in the biosynthesis of thiamine(15, 16). Interestingly phylogenetic analysis has shown that ThiH belongs to a small subfamily of enzyme which includes HydG, an enzyme involved in the maturation scheme of [FeFe]-hydrogenase (10). Biochemical characterization from the Broderick group as well as others has shown that HydG undergoes a radical initiation event with the substrate tyrosine which is very similar to ThiH. Biochemical characterizations of HydG

activity demonstrated that the initial products of tyrosine degradation were dehydroglycine and *p*-cresol (9). Subsequent work with unlabeled as well as ^{13}C , ^{15}N labeled tyrosine confirmed that HydG catalyzed tyrosine cleavage resulted in the synthesis of CN⁻ ligands on the H-cluster(10). Subsequent experiments involving the addition of deoxyhemoglobin in HydG assays with tyrosine revealed that the second turnover product tyrosine cleavage was indeed CO(11). At this point it was evident that HydG decomposition of tyrosine was responsible for all the 5 di-atomic ligands in the H-cluster. This was further confirmed via stopped-flow FTIR spectroscopy of *Clostridium pasteurianum* HydA obtained in the presence of all three maturase enzymes and labeled tyrosine. The resulting FTIR spectra contained characteristic frequencies corresponding to the labeled tyrosine indicating that HydG was indeed responsible for biosynthesizing all five diatomic ligands of the H-cluster(17). As mentioned earlier, HydG belongs to radical SAM super family of enzymes that initiate catalysis via a single H atom abstraction by the 5'-deoxyadenosyl radical from the substrate. Therefore we believe that HydG catalyzed tyrosine decomposition is initiated via a similar mechanism where the reductive cleavage of SAM yields a 5'-dAdo radical which must abstract a hydrogen atom from tyrosine. The resulting tyrosyl radical then presumably undergoes further decomposition resulting in the production of the CN⁻ and CO ligands. To further investigate the aforementioned phenomenon, we have herein used specifically deuterium labeled tyrosine in HydG turnover reactions to identify the likely hydrogen atom abstraction site that initiates the tyrosine decomposition mechanism by HydG. To achieve our objectives, we plan to monitor 5'-deoxyadenosine (dAdo) formation and label

incorporation in to dAdo via liquid chromatography and mass spectrometer. We believe that our results provide insight toward a mechanism where radical-initiated amino acid decomposition results in diatomic ligand synthesis.



Scheme1. Reaction Catalyzed by HydG in [FeFe]-hydrogenase H-Cluster Biosynthesis

Materials and Methods

Growth and Assay Conditions

Clostridium acetobutylicum HydG was heterologously expressed, purified, reconstituted with iron and sulfide (Please refer to chapter 3), (11). Assays for HydG-catalyzed dAdo formation were carried out in an anaerobic chamber (Mbraun , O₂ < 1 ppm) in sealed 1.5 mL eppendorf tubes containing HydG (100 μM) in buffer (50 mM Tris, pH 8.5, 300 mM KCl, 5% glycerol), 5 mM dithionite, 1 mM tyrosine, and 1 mM SAM at 37 °C. Following acid-quench precipitation with 1M HCl (15% v/v) and centrifugation, the supernatant was subjected to HPLC-coupled ESI-MS.

High Performance Liquid Chromatography and Mass Spectrometry Conditions

Samples selected for LC-MS were prepared by diluting them 100-fold in 10% methanol, 90% water in all cases except when noted. During a single HPLC run, two consecutive analytical trials were performed for each injected sample, so as to exclude

any ambiguity resulting from peak shifts or change in peak area as is inherent in the protocols employed. Aliquots from experimental replicates were run on the HPLC system for a minimum of two times on different days to eliminate the effects of day to day instrument drift. All analytes were observed in the $[M+H]^+$ form and quantitation of deoxyadenosine, SAM and tyrosine were performed as described below. Due to its ubiquitous presence and high signal quality, the HEPES elution peak was used as a quality control check and as mass accuracy validation. The chromatography system was composed of an Agilent 1290 series UHPLC with binary pump, temperature-controlled auto-sampler and column compartment. The auto-sampler module and reactions were held at 4 °C using the active temperature control option. The separation of the various analytes was performed using normal phase chromatography with a Cogent “Diamond Hydride” HPLC column (MicroSolv, 150 x 2.1mm), held at 50 °C. Solvents consisted of H₂O with 0.1% formic acid in channel “A” and acetonitrile with 0.1% formic acid in channel “B”, and the flow rate was a constant 0.8 mL/min at all times. Prior to sample injection, the column was equilibrated with 100% “B”. Sample injection was performed with the autosampler, and following injection the solvent composition was maintained at 100% B for 2 minutes. A linear gradient was then used from 100% B to 50% B, from 2 min to 6 min. From 6 min to 8.5 min the composition was held at 50% B for elution of strongly-retained compounds. At 8.51 minutes the composition was changed back to 100% B and held until 10.0 minutes for re-equilibration. Due to delays from sample injection, the overall time between samples was approximately 11 minutes. Mass spectra were obtained on an Agilent 6538 Q-TOF mass spectrometer equipped with the

dual-ESI source. The capillary exit voltage was 120 V and gas temperature was 300 °C. All data was recorded in positive mode between 25 m/z and 750 m/z in profile mode. The hardware summation time was 1 second. Peaks were validated using high-accuracy formula confirmation and elution matching from individual reference standards. Quantitation was performed using the MassHunter Quantitative Analysis package (Agilent). An extracted ion chromatograph was generated using the accurate mass of each compound with a -0.04 to +0.04 ppm m/z extraction window. This was selected to give the best compromise of specificity, sensitivity, and tolerance to slight calibration shifts during the runs.

Results and Discussion

Analysis of HydG assays run in H₂O with specifically isotopically labeled tyrosines (deuterated at the C α —H, C β —H, or ring C—H) showed that no deuterium was incorporated into 5'-dAdo (Figure 1). All experiments yielded isotope distributions similar to 5'-dAdo produced during turnover of unlabeled tyrosine substrate in H₂O. The observed lack of 5'-dAdo deuterium label incorporation from these tyrosine C—D positions suggested that hydrogen atom abstraction likely occurs at a solvent-exchangeable site. To investigate this possibility, assays were carried out in a Tris-D₂O buffer (pD = 8.5) using unlabeled tyrosine, similar to experiments described above in H₂O (D₂O:H₂O = 95:05) and like above were quenched with 1 M HCl (Figure 2). The resultant mass spectrum of the dAdo product was different from that obtained in H₂O assays, with significant amounts of [CH₂D-5']-dAdo, [CHD₂-5']-dAdo, and [CD₃-5']-dAdo produced in addition to non-labeled 5'-dAdo. Under the circumstances where the

5'-dAdo radical presumably abstracts the phenolic H/D atom from the tyrosine, we expect to see a single H/D atom incorporation into 5'-dAdo resulting in an increase of one m/z unit in the case of the labeled tyrosine. In our observed result however we see multiply deuterated species ($\text{CH}_2\text{D}-5'$, $[\text{CHD}_2-5'$, and CD_3-5') of dAdo thereby opening the possibility of multiple abstraction and/or re-abstraction events.

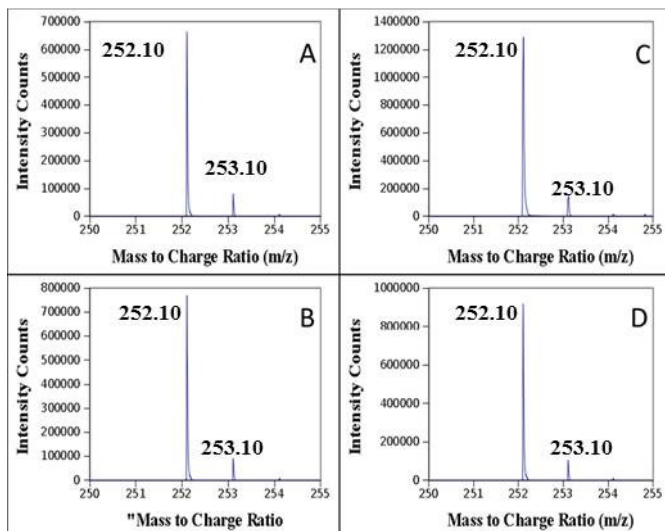


Figure 1. Product 5'-deoxyadenosine mass spectra in H_2O containing buffer with deuterium-labeled Tyr substrates. (A) Unlabeled Tyr. (B) $\text{C}_3\text{-D}_2\text{-Tyr}$. (C) Ring- $\text{D}_4\text{-Tyr}$. (D) $\text{C}_2, \text{Ring-D}_5\text{-Tyr}$.

This result is indeed perplexing and experiments are currently underway to explain this phenomenon. Additionally, the percentage of non-labeled 5'-dAdo was substantial in the observed distribution, however similar percentages of unlabeled 5'-dAdo have been reported for other radical SAM enzymes where hydrogen atom abstraction labeling experiments have been investigated (18, 19). This can most likely attributed to the presence of protic solvent in the assay mixture as well the ability of SAM to undergo uncoupled cleavage in the presence of HydG and tyrosine(10). It should be noted that

the protic enzyme denaturant HCl did not impact the observed distributions performed in D₂O, since similar distributions were observed among samples that were not treated with HCl (data not shown). To confirm that label incorporation was associated with the catalytic reaction using tyrosine as a substrate, the experiment was repeated in the absence of tyrosine in D₂O (data not shown). The overall quantity of detected 5'-dAdo product was significantly less than in the presence of substrate, representative of baseline level nonproductive SAM cleavage by HydG (Table 1 row 2). We can also attribute the presence of a small amount mono deuterated 5'-dAdo (Table 1 row 2) to a certain percentage of the generated dAdo radical being quenched by exchangeable amino acid residues on the protein or D₂O solvent. Similarly, attempts to utilize phenylalanine rather than tyrosine as a substrate resulted in little to no stimulation of 5'-dAdo production, and the dAdo produced had an isotope distribution similar to that observed with tyrosine as a substrate (Fig 2C, Table 1 row 3).

To investigate possible effects of pD on the extent of deuterium incorporated into dAdo, the assay was performed in a different buffer (50 mM HEPES, 500 mM KCl, 5% glycerol pD = 7.4). As with the results in the higher pD Tris buffer described above, the isotopic distribution for 5'-dAdo is reflective of significant deuterium label incorporation. However, in Hepes pD 7.4 the deuterated 5'-dAdo was almost exclusively mono-labeled, with negligible bis- and tris-labeled product observed (Figure 2D, Table 1 row 3). Taken together our observations with specifically deuterated tyrosine substrate do indicate that the initial H atom abstraction by the dAdo radical does indeed take place from the phenolic hydrogen. Our hypothesis is given further credence

with the lack of any observed label incorporation in experiments conducted in H₂O with the C α -H, C β -H and ring deuterated substrates. As the analog phenylalanine does not stimulate 5'-dAdo production with intact enzyme, nor does it produce a different 5'-dAdo isotope distribution from the absence of the tyrosine substrate, initial abstraction cannot occur at the C α -amino group. These results stand out in stark contrast with experiments done in D₂O and tyrosine where we observe a majority of mono deuterated product as well a substantial amount of bis- and tris-labeled product.

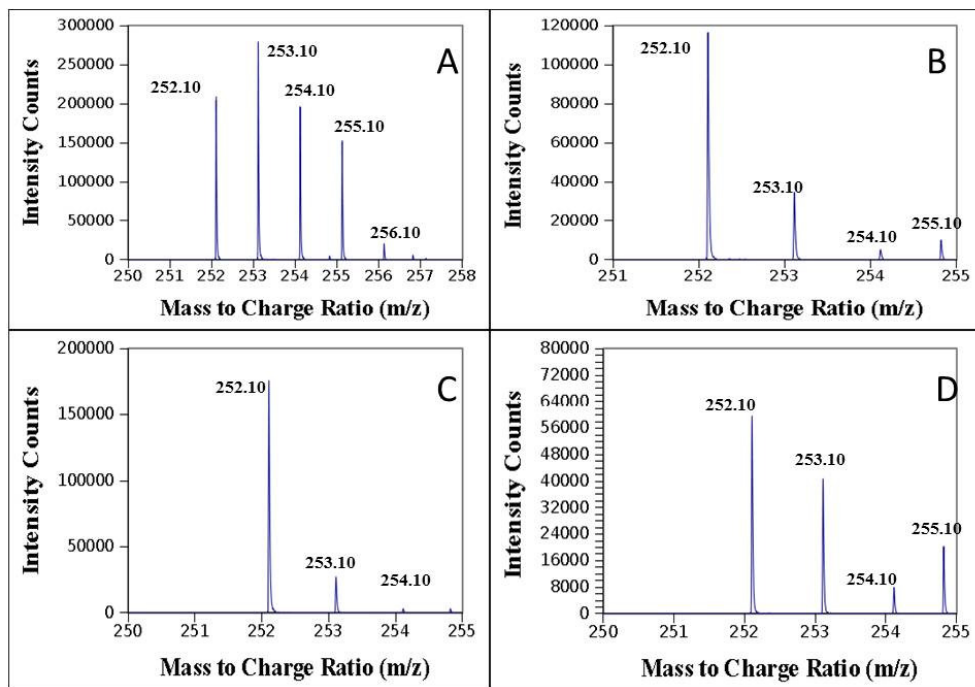


Figure 2. Product 5'-deoxyadenosine mass spectra in D₂O buffer with natural abundance substrates in Tris-D₂O (pD = 8.5) (A) Tyr. (B) No Tyr. (C) Phe. (D) Tyr in HEPES-D₂O (pD = 7.4)

Analyte/Substrate	Percent Labeling of Analytes by Peak Height			
	— CH ₃	— CH ₂ D	— CHD ₂	— CD ₃
dAdo				
Tyr	27.8	33.2	21.8	17.2
No Substrate	84.2	15.8	0.0	0.0
Phe	84.6	14.5	0.9	0.0
HEPES-D ₂ O	63.5	30.9	3.9	1.7

Table 5.1. dAdo Deuterium Distribution with Intact HydG

Multiple deuterium labels detected in the 5'-dAdo product is potentially intriguing with respect to the H atom abstraction process, as it implicates multiple abstraction and/or re-abstraction events by the d-Ado radical as part of the turnover process. Interestingly, SAM has been previously shown to serve as a co-substrate in the HydG reaction, where the extent of SAM cleavage relative to the amount of *p*-cresol, CO and CN⁻ produced was suggestive of dAdo radical consumption by substrate (10). It has been shown earlier that the tyrosine decomposition mechanism yielding CO and CN⁻ is unique, requiring activity of two discrete, site-differentiated [4Fe-4S] clusters (11-13) Therefore, To investigate the nature of the abstraction/re-abstraction in the consumption of SAM by HydG, similar label transfer experiments were performed using a truncated version of HydG, lacking 88 amino acid residues in the C-terminal region that binds the accessory CX₂CX₂₂C Fe-S cluster. Experiments were performed under similar conditions (50 mM Tris, 300 mM KCl, 5% glycerol, pD = 8.5) as described for the intact enzyme noted above (D₂O:H₂O = 88:12). In contrast to the intact enzyme, the dAdo isotope distribution from truncated enzyme was comprised of exclusively unlabeled and mono-labeled product (Figure 3, Table 2). Under comparable conditions, bis- and tris-labeled

products were found to be non-existent. Initial characterization of the C-terminal truncated HydG has shown that very little product formation is observed, suggesting that the C-terminal region serves an important stabilizing role in facilitating the reaction (20, 21). Consistent with the initial reports, the C-terminal truncated HydG shows a decreased amount of 5'-dAdo produced, at approximately 30 % of levels detected with the full enzyme (data not shown).

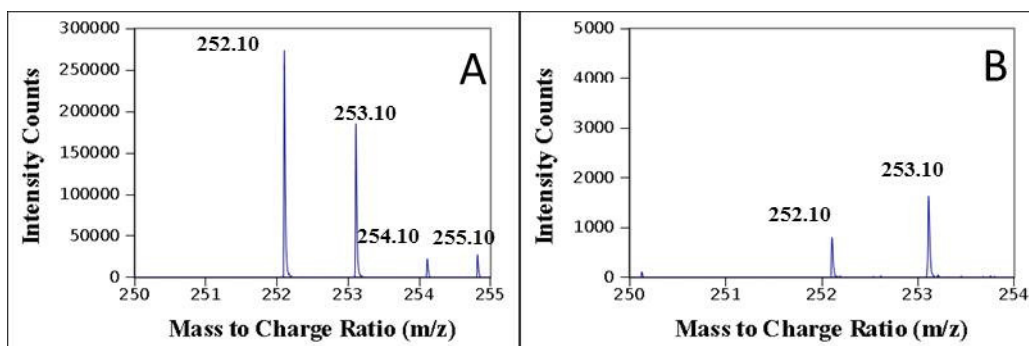


Figure 3. Mass spectra of 5'-deoxyadenosine product from C-terminal truncated HydG in Tris-D₂O (pD = 8.5) buffer. (A) Tyr. (B) No Tyrosine

Analyte/Substrate	Percent Labeling of Analytes by Peak Height			
	—CH ₃	—CH ₂ D	—CHD ₂	—CD ₃
dAdo				
Tyr	75.2	24.8	0.0	0.0
No Substrate	52.3	47.6	0.0	0.0

Table 5.2. dAdo Deuterium Distribution with C-terminal Truncated HydG in tris-D₂O.

Considering that the truncation is a substantial perturbation to the enzyme, differences in tyrosine or SAM binding to HydG can be expected to be significantly poorer, and could result in differences in the extent of deuterium label transfer. Together with the decreased overall amount of product 5'-dAdo formed, the observation of a single

deuterium label incorporated into dAdo from the truncated enzyme is consistent with a single, initial hydrogen abstraction occurring as the principal initiation event on the tyrosine substrate.

Conclusions

HydG-catalyzed tyrosine decomposition is a unique, radical-based reaction where the synthesized diatomic ligand products are delivered to HydF, and eventually delivered to HydA as the assembled 2Fe subcluster. The cumulative data supports abstraction of the tyrosine 4-phenol hydrogen atom by the 5'-dAdo radical following reductive cleavage of SAM. Additionally we propose that a subsequent re-abstraction by the phenoxide radical results in multiple deuterium atoms observed in the product 5'-dAdo. The identity of the substrate radical initiation site (from 5'-dAdo product analysis) is significant, as it provides potential insight into the putative oxidized glycine intermediate that yields CO and CN⁻.

References

1. Mulder, David W., Shepard, Eric M., Meuser, Jonathan E., Joshi, N., King, Paul W., Posewitz, Matthew C., Broderick, Joan B., and Peters, John W. (2011) Insights into [FeFe]-hydrogenase structure, mechanism, and maturation, *Structure* 19, 1038-1052.
2. Swanson, K. D., Duffus, B. R., Beard, T. E., Peters, J. W., and Broderick, J. B. (2011) Cyanide and carbon monoxide ligand formation in hydrogenase biosynthesis, *European Journal of Inorganic Chemistry* 7, 935-947.
3. Peters, J. W., Lanzilotta, W. N., Lemon, B. J., and Seefeldt, L. C. (1998) X-ray Crystal structure of the Fe-only hydrogenase (CpI) from *Clostridium pasteurianum* to 1.8 angstrom resolution, *Science* 282, 1853-1858.
4. Nicolet, Y., Piras, C., Legrand, P., Hatchikian, C. E., and Fontecilla-Camps, J. C. (1999) *Desulfovibrio desulfuricans* iron hydrogenase: the structure shows unusual coordination to an active site Fe binuclear center, *Structure* 7, 13-23.
5. Silakov, A., Wenk, B., Reijerse, E., and Lubitz, W. (2009) 14N HYSCORE investigation of the H-cluster of [FeFe] hydrogenase: evidence for a nitrogen in the dithiol bridge, *Physical Chemistry Chemical Physics* 11, 6592-6599.
6. King, P. W., Posewitz, M. C., Ghirardi, M. L., and Seibert, M. (2006) Functional studies of [FeFe] hydrogenase maturation in an *Escherichia coli* biosynthetic system, *Journal of Bacteriology* 188, 2163-2172.
7. Posewitz, M. C., King, P. W., Smolinski, S. L., Zhang, L., Seibert, M., and Ghirardi, M. L. (2004) Discovery of two novel radical *S*-adenosylmethionine proteins required for the assembly of an Active [Fe] Hydrogenase, *Journal of Biological Chemistry* 279, 25711-25720.
8. Mulder, D. W., Boyd, E. S., Sarma, R., Lange, R. K., Endrizzi, J. A., Broderick, J. B., and Peters, J. W. (2010) Stepwise [FeFe] hydrogenase H-cluster assembly revealed in the structure of $\text{HydA}^{\Delta\text{EFG}}$, *Nature* 465, 248-251.
9. Pilet, E., Nicolet, Y., Mathevon, C., Douki, T., Fontecilla-Camps, J. C., and Fontecave, M. (2009) The role of the maturase HydG in [FeFe] hydrogenase active site synthesis and assembly, *FEBS Letters*. 583, 506-511.
10. Driesener, R. C., Challand, M. R., McGlynn, S. E., Shepard, E. M., Boyd, E. S., Broderick, J. B., Peters, J. W., and Roach, P. L. (2010) [FeFe] hydrogenase cyanide ligands derived From *S*-adenosylmethionine-dependent cleavage of tyrosine, *Angewandte Chemie International Edition* 49, 1687-1690.

11. Shepard, E. M., Duffus, B. R., George, S. J., McGlynn, S. E., Challand, M. R., Swanson, K. D., Roach, P. L., Cramer, S. P., Peters, J. W., and Broderick, J. B. (2010) [FeFe] hydrogenase maturation: HydG-catalyzed synthesis of carbon monoxide, *Journal of the American Chemical Society* 132, 9247-9249.
12. Frey, P. A., Hegeman, A. D., and Ruzicka, F. J. (2008) The radical SAM superfamily, *Critical Reviews in Biochemistry and Molecular Biology* 43, 63-88.
13. Chen, D., Walsby, C., Hoffman, B. M., and Frey, P. A. (2003) Coordination and mechanism of reversible cleavage of S-adenosylmethionine by the [4Fe-4S] center in lysine 2, 3-aminomutase, *Journal of the American Chemical Society* 125, 11788-11789.
14. Walsby, C. J., Ortillo, D., Broderick, W. E., Broderick, J. B., and Hoffman, B. M. (2002) An anchoring role for FeS clusters: Chelation of the amino acid moiety of S-adenosylmethionine to the unique iron site of the [4Fe-4S] cluster of pyruvate formate-lyase activating enzyme, *Journal of the American Chemical Society* 124, 11270-11271.
15. Begley, T. P., Downs, D. M., Ealick, S. E., McLafferty, F. W., Van Loon, A. P., Taylor, S., Campobasso, N., Chiu, H.-J., Kinsland, C., and Reddick, J. J. (1999) Thiamin biosynthesis in prokaryotes, *Archives of Microbiology* 171, 293-300.
16. Begley, T. P. (2006) Cofactor biosynthesis: An organic chemist's treasure trove, *Natural Product Reports* 23, 15-25.
17. Kuchenreuther, J. M., George, S. J., Grady-Smith, C. S., Cramer, S. P., and Swartz, J. R. (2011) Cell-free H-cluster synthesis and [FeFe] hydrogenase activation: All five CO and CN⁻ ligands derive from tyrosine, *PLoS ONE* 6, e20346.
18. Wecksler, S. R., Stoll, S., Iavarone, A. T., Imsand, E. M., Tran, H., Britt, R. D., and Klinman, J. P. (2010) Interaction of PqqE and PqqD in the pyrroloquinoline quinone (PQQ) biosynthetic pathway links PqqD to the radical SAM superfamily, *Chemical Communications* 46, 7031-7033.
19. Wiig, J. A., Hu, Y., Lee, C. C., and Ribbe, M. W. (2012) Radical SAM-dependent carbon insertion into the nitrogenase M-cluster, *Science* 337, 1672-1675.
20. Nicolet, Y., Martin, L., Tron, C., and Fontecilla-Camps, J. C. (2010) A glycyl free radical as the precursor in the synthesis of carbon monoxide and cyanide by the [FeFe]-hydrogenase maturase HydG, *FEBS Letters* 584, 4197-4202.
21. Tron, C., Cherrier, M. V., Amara, P., Martin, L., Fauth, F., Fraga, E., Correard, M., Fontecave, M., Nicolet, Y., and Fontecilla-Camps, J. C. (2011) Further characterization

of the [FeFe] hydrogenase maturase HydG, *European Journal of Inorganic Chemistry* 2011, 1121-1127.

CHAPTER 6

GENERAL CONCLUSIONS AND FUTURE DIRECTIONS

The primary goals of the research described in this dissertation were threefold. The first objective was to understand the solution phase dynamics of SPL in the presence of damaged DNA substrate and SAM. SPL is a non-photoactivatable DNA repair enzyme found in spore forming members of the *Bacillus* and *Clostridium* species(1, 2). The catalytic action of this enzyme has direct implications on the remarkable UV resistance of bacterial spores, which are the causative agents of a variety of diseases. To that end, understanding the mechanism of action of this enzyme, specifically the dynamic interactions of the enzyme with its substrate which leads to recognition and binding, would provide us with invaluable insight into UV resistance of bacterial spores.

Some of the primary outstanding issues concerning the repair of SPTpT by SPL are the events involved with substrate recognition and binding. The issue was made more complicated due to the lack of a substrate-bound structure that would potentially provide insight into the varied regions of the protein interacting with the substrate. In order to gain an understanding of the solution phase dynamics of SPL upon substrate binding, we utilized the minimal dinucleotide substrate SPTpT(2, 3), which was synthesized in our lab. The work described in Chapter 2 employed hydrogen deuterium exchange as monitored via high performance liquid chromatography and mass spectrometry, a technique seldom utilized in bioinorganic chemistry to probe structural changes in enzymes containing oxygen sensitive metal clusters. We characterized the interactions of SPL with SAM, SPL with SPTpT, and SPL with SPTpT and SAM, both under aerobic

and anaerobic conditions. We probed the effects of the anaerobic environment in order to obtain an understanding of the role of the oxygen-sensitive 4Fe-4S catalytic cluster on binding. Our results indicate that the protein undergoes a significant global conformational change on binding to SAM and a further perturbation takes place when it is concurrently bound to SAM and SPTpT. We were also able to show that the presence of the catalytic cluster does indeed accentuate the degree of structural dynamism when the enzyme is bound to its cofactor and substrate. Our results were corroborated by recently published crystal structures of SPL with SAM and SP dinucleoside substrate. The ligand bound structure indicated that significant conformational change occurs in the active site region on substrate binding including a β hairpin region which experiences a movement of 2 Å. It has also been proposed that this region might be involved in base flipping interactions commonly observed in DNA repair enzymes such as DNA photolyases. In addition, it has been shown in previous radical SAM enzymes that the binding of SAM and its correct orientation in the active site is dependent on multiple interactions such as hydrogen bonding, hydrophobic interactions and salt bridges, in addition to coordination of the unique iron of the [4Fe-4S] cluster. In the case of SPL binding SAM, the amino group of the methionyl moiety of SAM has been shown to interact with Ser142 and Asp143 and the carboxylate moiety with Lys174 and Ser195, while the adenine and ribose groups are held in place via hydrogen bonding interactions with Tyr96, Tyr98, Ala234 and Ala273. It is likely therefore that these interactions upon SAM binding contribute to the observed changes in H/D exchange in our experiments.

The study presented herein provides the first insight into the dynamics of SPL binding with substrate while utilizing un-reconstituted enzyme and the physiologically relevant SP-dinucleotide substrate. Our analysis has provided insight into conformational change brought about by SAM and SP binding while utilizing methodologies which are high throughput in nature and commensurate with the anaerobic nature of radical SAM enzymes. We believe that the techniques utilized by us can prove invaluable in probing the enzyme-ligand interactions of other radical SAM enzymes whose structures are yet to be elucidated.

The subsequent topics of investigation concerns the hydrogenase maturase enzymes, HydE and HydG, involved in the bio-synthesis and assembly of the [FeFe]-hydrogenase active site H cluster(4, 5). The second objective of my research was the biochemical characterization of HydE, with the ultimate goal identifying the substrate and elucidating the mechanism of catalysis. The initial approach towards identifying a putative substrate involved assaying for enhanced SAM cleavage by HydE in the presence of all twenty amino acids and some common metabolites. This initial screening, carried out by my predecessor on the project, indicated that the presence of cysteine along with HydE and SAM resulted in enhanced SAM cleavage as monitored by 5'-dAdo production. This observation was consistent with published studies showing that addition of cysteine and tyrosine to cell lysates of the maturase enzymes resulted in stimulation of [FeFe]-hydrogenase activity. Consequently, based on the data obtained from our screening assays we decided to further probe the role of cysteine in HydE catalysis via LC-MS. Our subsequent investigations provided confirmation that cysteine increased the rate of

HydE catalyzed 5'-dAdo production and further, that cysteine was consumed in a 1:1 stoichiometry to the 5-dAdo produced. This implied that for every molecule of SAM cleaved by HydE to produce 5'-dAdo, one molecule of cysteine was being consumed. As mentioned earlier in this dissertation, it is proposed that the 2Fe-2S cluster on HydF (which acts as a scaffold in the maturation scheme) gets modified by the actions of HydE and HydG(6-8). Moreover, bioinformatic studies have shown in certain cases the *hyde* and *hydf* genes (9) are fused, and recent biochemical characterization has also indicated a strong binding interaction between the two enzymes(10). Therefore we hypothesized that the presence of HydF might affect HydE catalysis. In order to probe the effects of HydF Δ EG on HydE, we conducted assays in the presence of both these enzymes and deuterium labeled cysteine. Our results indicate that the presence of HydF Δ EG decreases levels of nonproductive 5'-dAdo formation, with a concomitant increase in the amount of cysteine consumed over time. Additionally, assays conducted in the presence of cysteine labeled with deuterium at specific positions point to a mechanism in which the HydE-generated 5'-dAdo \bullet abstracts an H atom from the β carbon of cysteine to initiate catalysis. Taken together, these results provide an initial but critical window into the catalytic action of HydE in the maturation scheme of [Fe-Fe]-Hydrogenase.

Our third and final line of research involved investigation of the mechanism of tyrosine cleavage by the maturase enzyme HydG. HydG synthesizes the CO and CN-ligands of the H-cluster via the decomposition of tyrosine(11, 12). Our primary objective in the current work was to gain insight into the mechanism of HydG-catalyzed tyrosine

cleavage by identifying the specific site of the H-atom abstraction by the 5'-dAdo• intermediate. To that end we performed assays with tyrosine labeled with deuterium in different positions, and traced the label transfer via LC-MS. Our analysis indicated that during the HydG catalyzed decomposition of tyrosine, the 5'-dAdo• radical abstracts an H atom from the phenolic position which is subsequently detected on 5'-dAdo via LC-MS.

The work presented in this dissertation has provided insights into the structural as well as mechanistic parameters of three radical SAM enzymes. We have demonstrated that the substrate for HydE is cysteine and that catalysis is initiated via single H atom abstraction from the β -carbon. We have also obtained similar insights into the mechanism of tyrosine decomposition by HydG where catalysis takes place via an H atom abstraction from the phenolic position. The insights obtained from the H/D exchange studies with SPL has not only provided us with information about global conformational events in the enzyme on ligand binding, it has also provided us with sensitive and rapid methodology to probe structural perturbation in anaerobic proteins.

References

1. Chandor, A., Douki, T., Gasparutto, D., Gambarelli, S., Sanakis, Y., Nicolet, Y., Ollagnier-de-Choudens, S., Atta, M., and Fontecave, M. (2007) Characterization of the DNA repair spore photoproduct lyase enzyme from *Clostridium acetobutylicum*: A radical-SAM enzyme, *Comptes Rendus Chimie* 10, 756-765.
2. Chandra, T., Silver, S. C., Zilinskas, E., Shepard, E. M., Broderick, W. E., and Broderick, J. B. (2009) Spore Photoproduct Lyase Catalyzes Specific Repair of the 5R but Not the 5S Spore Photoproduct, *Journal of the American Chemical Society* 131, 2420-2421.
3. Silver, S. C., Chandra, T., Zilinskas, E., Ghose, S., Broderick, W. E., and Broderick, J. B. (2010) Complete stereospecific repair of a synthetic dinucleotide spore photoproduct by spore photoproduct lyase, *J Biol Inorg Chem* 15, 943-955.
4. Shepard, E. M., Boyd, E. S., Broderick, J. B., and Peters, J. W. (2011) Biosynthesis of complex iron-sulfur enzymes, *Curr Opin Chem Biol* 15, 319-327.
5. McGlynn, S. E., Mulder, D. W., Shepard, E. M., Broderick, J. B., and Peters, J. W. (2009) Hydrogenase cluster biosynthesis: organometallic chemistry nature's way, *Dalton Transactions*, 4274-4285.
6. Czech, I., Silakov, A., Lubitz, W., and Happe, T. (2010) The [FeFe]-hydrogenase maturase HydF from *Clostridium acetobutylicum* contains a CO and CN- ligated iron cofactor, *FEBS Lett.* 584, 638-642.
7. Joshi, N., Shepard, E. M., Byer, A. S., Swanson, K. D., Broderick, J. B., and Peters, J. W. (2012) Iron-sulfur cluster coordination in the [FeFe]-hydrogenase H cluster biosynthetic factor HydF, *FEBS letters*, 22, 3939-3943.
8. Shepard, E. M., McGlynn, S. E., Bueling, A. L., Grady-Smith, C., George, S. J., Winslow, M. A., Cramer, S. P., Peters, J. W., and Broderick, J. B. (2010) Synthesis of the 2Fe-subcluster of the [FeFe]-hydrogenase H-cluster on the HydF scaffold, *Proc. Natl. Acad. Sci. U.S.A.* 107, 10448-10453.
9. Böck, A., King, P. W., Blokesch, M., and Posewitz, M. C. (2006) Maturation of hydrogenases, *Advances in microbial physiology* 51, 1-225.
10. Vallese, F., Berto, P., Ruzzene, M., Cendron, L., Sarno, S., De Rosa, E., Giacometti, G. M., and Costantini, P. (2012) Biochemical Analysis of the Interactions between the Proteins Involved in the [FeFe]-Hydrogenase Maturation Process, *Journal of Biological Chemistry* 287, 36544-36555.
11. Shepard, E. M., Duffus, B. R., George, S. J., McGlynn, S. E., Challand, M. R., Swanson, K. D., Roach, P. L., Cramer, S. P., Peters, J. W., and Broderick, J. B. (2010)

[FeFe]-Hydrogenase Maturation: HydG-Catalyzed Synthesis of Carbon Monoxide,
Journal of the American Chemical Society 132, 9247-9249.

12. Swanson, K. D., Duffus, B. R., Beard, T. E., Peters, J. W., and Broderick, J. B.
(2011) Cyanide and Carbon Monoxide Ligand Formation in Hydrogenase Biosynthesis,
European Journal of Inorganic Chemistry 2011, 935-947.

REFERENCES CITED

1. Lu, Y., Berry, S. M., and Pfister, T. D. (2001) Engineering novel metalloproteins: design of metal-binding sites into native protein scaffolds, *Chemical Reviews* 101, 3047-3080.
2. Barker, P. D. (2003) Designing redox metalloproteins from bottom-up and top-down perspectives, *Current Opinion in Structural Biology* 13, 490-499.
3. Lill, R. (2009) Function and biogenesis of iron-sulphur proteins, *Nature* 460, 831-838.
4. Beinert, H. (2000) Iron-sulfur proteins: ancient structures, still full of surprises, *Journal of Biological Inorganic Chemistry* 5, 2-15.
5. Meyer, J. (2008) Iron-sulfur protein folds, iron-sulfur chemistry, and evolution, *Journal of Biological Inorganic Chemistry* 13, 157-170.
6. Sands, R. H., and Beinert, H. (1960) Studies on mitochondria and submitochondrial particles by paramagnetic resonance (EPR) spectroscopy, *Biochemical and Biophysical Research Communications* 3, 47-52.
7. Tagawa, K., and Arnon, D. I. (1962) Ferredoxins as electron carriers in photosynthesis and in the biological production and consumption of hydrogen gas. *Nature* 195, 537 - 543
8. Mortenson, L., Valentine, R., and Carnahan, J. (1962) An electron transport factor from *Clostridium pasteurianum*, *Biochemical and Biophysical Research Communications* 7, 448.
9. Beinert, H. (1997) Iron-Sulfur Clusters: Nature's Modular, Multipurpose Structures, *Science* 277, 653-659.
10. Beinert, H., Meyer, J., and Lill, R. (2004) Iron-sulfur proteins, *Encyclopedia of Biological Chemistry* 2, 482-489.
11. Rees, D. C. (2002), Great metalloclusters in enzymology, *Annual Review of Biochemistry* 71, 221-246.
12. Rao, P. V., and Holm, R. (2004) Synthetic analogues of the active sites of iron-sulfur proteins, *Chemical Reviews* 104, 527-560.
13. Moulis, J. M., Davaise, V., Golinelli, M. P., Meyer, J., and Quinkal, I. (1996) The coordination sphere of iron-sulfur clusters: lessons from site-directed mutagenesis experiments, *Journal of Biological Inorganic Chemistry* 1, 2-14.

14. Sellers, V. M., Johnson, M. K., and Dailey, H. A. (1996) Function of the [2Fe-2S] cluster in mammalian ferrochelatase: a possible role as a nitric oxide sensor, *Biochemistry* 35, 2699-2704.
15. Sazanov, L. A., and Hinchliffe, P. (2006) Structure of the Hydrophilic Domain of Respiratory Complex I from *Thermus thermophilus*, *Science* 311, 1430-1436.
16. Johnson, D. C., Dean, D. R., Smith, A. D., and Johnson, M. K. (2005) Structure, function, and formation of biological iron-sulfur clusters, *Annual Reviews of Biochemistry*. 74, 247-281.
17. Johnson, M. K. (1998) Iron-sulfur proteins: new roles for old clusters, *Current Opinion in Chemical Biology* 2, 173-181.
18. Wächtershäuser, G. (2006) From volcanic origins of chemoautotrophic life to bacteria, archaea and eukarya, *philosophical transactions of the Royal Society: Biological Sciences* 361, 1787-1808.
19. Kopp, R. E., Kirschvink, J. L., Hilburn, I. A., and Nash, C. Z. (2005) The paleoproterozoic snowball Earth: A climate disaster triggered by the evolution of oxygenic photosynthesis, *Proceedings of the National Academy of Sciences* 102, 11131-11136.
20. Glaser, T., Hedman, B., Hodgson, K. O., and Solomon, E. I. (2000) Ligand K-edge X-ray absorption spectroscopy: a direct probe of ligand-metal covalency, *Accounts of Chemical Research* 33, 859-868.
21. Brzóška, K., Meczynska, S., and Kruszewski, M. (2006) Iron-sulfur cluster proteins: electron transfer and beyond, *Acta Biochim Pol.* 53, 685.
22. Thauer, R. K., and Schönheit, P. (1982) Iron-Sulfur complexes of ferredoxin as a storage form of iron in *Clostridium pasteurianum*, iron-sulfur proteins, *Archives of Microbiology* 3, 285-288
23. Golinelli, M. P., Chatelet, C., Duin, E. C., Johnson, M. K., and Meyer, J. (1998) Extensive ligand rearrangements around the [2Fe-2S] cluster of *Clostridium pasteurianum* ferredoxin, *Biochemistry* 37, 10429-10437.
24. Cunningham, R. P., Asahara, H., Bank, J. F., Scholes, C. P., Salerno, J. C., Surerus, K., Munck, E., McCracken, J., Peisach, J., and Emptage, M. H. (1989) Endonuclease III is an iron-sulfur protein, *Biochemistry* 28, 4450-4455.

25. Kuo, C. F., McRee, D. E., Fisher, C. L., O'Handley, S. F., Cunningham, R. P., and Tainer, J. A. (1992) Atomic structure of the DNA repair [4Fe-4S] enzyme endonuclease III, *Science* 258, 434.
26. Fleischhacker, A. S., and Kiley, P. J. (2011) Iron-containing transcription factors and their roles as sensors, *Current Opinion in Chemical Biology* 15, 335-341.
27. Beinert, H. (2010) Catalysis and Gene Regulation, *Metals in Biology* 29, 45-51.
28. Smith, J. L., Zaluzec, E. J., Wery, J. P., Niu, L., Switzer, R. L., Zalkin, H., and Satow, Y. (1994) Structure of the allosteric regulatory enzyme of purine biosynthesis, *Science* 264, 1427.
29. Wu, C. K., Dailey, H. A., Rose, J. P., Burden, A., Sellers, V. M., and Wang, B. C. (2001) The 2.0 Å structure of human ferrochelatase, the terminal enzyme of heme biosynthesis, *Nature Structural & Molecular Biology* 8, 156-160.
30. Frey, P. A., Hegeman, A. D., and Ruzicka, F. J. (2008) The radical SAM superfamily, *Critical Reviews in Biochemistry and Molecular Biology* 43, 63-88.
31. Sofia, H. J., Chen, G., Hetzler, B. G., Reyes-Spindola, J. F., and Miller, N. E. (2001) Radical SAM, a novel protein superfamily linking unresolved steps in familiar biosynthetic pathways with radical mechanisms: functional characterization using new analysis and information visualization methods, *Nucleic Acids Research* 29, 1097-1106.
32. Shepard, E. M., and Broderick, J. B. (2010) *S*-Adenosylmethionine and iron-sulfur clusters in biological radical reactions: The radical SAM superfamily, *Comprehensive Natural Products II*, 625-661.
33. Duschene, K. S., Veneziano, S. E., Silver, S. C., and Broderick, J. B. (2009) Control of radical chemistry in the AdoMet radical enzymes, *Current Opinion in Chemical Biology* 13, 74-83.
34. Chirpich, T. P., Zappia, V., Costilow, R. N., and Barker, H. A. (1970) Lysine 2,3-aminomutase, *Journal of Biological Chemistry* 245, 1778-1789.
35. Cheek, J., and Broderick, J. B. (2002) Direct H atom abstraction from spore photoproduct C-6 initiates DNA repair in the reaction catalyzed by spore photoproduct lyase: Evidence for a reversibly generated adenosyl radical intermediate, *Journal of the American Chemical Society* 124, 2860-2861.
36. Peter L, R. (2011) Radicals from *S*-adenosylmethionine and their application to biosynthesis, *Current Opinion in Chemical Biology* 15, 267-275.

37. Walsby, C. J., Ortillo, D., Broderick, W. E., Broderick, J. B., and Hoffman, B. M. (2002) An anchoring role for FeS clusters: Chelation of the amino acid moiety of *S*-adenosylmethionine to the unique iron site of the [4Fe-4S] cluster of pyruvate formate-lyase activating enzyme, *Journal of the American Chemical Society* 124, 11270-11271.
38. Vey, J. L., and Drennan, C. L. (2011) Structural insights into radical generation by the radical SAM superfamily, *Chemical Reviews* 111, 2487-2506.
39. Berkovitch, F., Nicolet, Y., Wan, J. T., Jarrett, J. T., and Drennan, C. L. (2004) Crystal structure of biotin synthase, an *S*-Adenosylmethionine-dependent radical enzyme, *Science* 303, 76-79.
40. Chen, D., Walsby, C., Hoffman, B. M., and Frey, P. A. (2003) Coordination and mechanism of reversible cleavage of *S*-adenosylmethionine by the [4Fe-4S] center in lysine 2, 3-aminomutase, *Journal of the American Chemical Society* 125, 11788-11789.
41. Vey, J. L., Yang, J., Li, M., Broderick, W. E., Broderick, J. B., and Drennan, C. L. (2008) Structural basis for glycyl radical formation by pyruvate formate-lyase activating enzyme, *Proceedings of the National Academy of Sciences* 105, 16137-16141.
42. Magnusson, O. T., Reed, G. H., and Frey, P. A. (2001) Characterization of an allylic analogue of the 5'-deoxyadenosyl radical: An intermediate in the reaction of lysine 2, 3-aminomutase, *Biochemistry* 40, 7773-7782.
43. Booker, S. J. (2009) Anaerobic functionalization of unactivated C-H bonds, *Current Opinion in Chemical Biology* 13, 58-73.
44. Moss, M., and Frey, P. (1990) Activation of lysine 2, 3-aminomutase by *S*-adenosylmethionine, *Journal of Biological Chemistry* 265, 18112-18115.
45. Nicolet, Y., Amara, P., Mouesca, J.-M., and Fontecilla-Camps, J. C. (2009) Unexpected electron transfer mechanism upon AdoMet cleavage in radical SAM proteins, *Proceedings of the National Academy of Sciences* 106, 14867-14871.
46. Hiscox, M. J., Driesener, R. C., and Roach, P. L. (2012) Enzyme catalyzed formation of radicals from *S*-adenosylmethionine and inhibition of enzyme activity by the cleavage products, *Biochimica et Biophysica Acta (BBA) - Proteins and Proteomics* 1824, 1165-1177.
47. Zhang, Y., Zhu, X., Torelli, A. T., Lee, M., Dzikovski, B., Koralewski, R. M., Wang, E., Freed, J., Krebs, C., and Ealick, S. E. (2010) Diphthamide biosynthesis requires an organic radical generated by an iron-sulphur enzyme, *Nature* 465, 891-896.

48. Zhu, X., Dzikovski, B., Su, X., Torelli, A. T., Zhang, Y., Ealick, S. E., Freed, J. H., and Lin, H. (2011) Mechanistic understanding of *Pyrococcus horikoshii* Dph2, a [4Fe-4S] enzyme required for diphthamide biosynthesis, *Molecular BioSystems* 7, 74-81.
49. Dowling, D. P., Vey, J. L., Croft, A. K., and Drennan, C. L. (2012) Structural diversity in the AdoMet radical enzyme superfamily, *Biochimica et Biophysica Acta (BBA)-Proteins & Proteomics* 11, 1178-1195
50. Donnellan Jr, J. E., and Stafford, R. S. (1968) The ultraviolet photochemistry and photobiology of vegetative cells and spores of *Bacillus megaterium*, *Biophysical Journal* 8, 17-28.
51. Nicholson, W. L., Munakata, N., Horneck, G., Melosh, H. J., and Setlow, P. (2000) Resistance of *Bacillus* endospores to extreme terrestrial and extraterrestrial environments, *Microbiology and Molecular Biology Reviews* 64, 548-572.
52. Pedraza-Reyes, M., Gutiérrez-Corona, F., and Nicholson, W. L. (1994) Temporal regulation and forespore-specific expression of the spore photoproduct lyase gene by sigma-G RNA polymerase during *Bacillus subtilis* sporulation, *Journal of Bacteriology* 176, 3983-3991.
53. Rebeil, R., Sun, Y., Chooback, L., Pedraza-Reyes, M., Kinsland, C., Begley, T. P., and Nicholson, W. L. (1998) Spore photoproduct lyase from *Bacillus subtilis* spores is a novel iron-sulfur DNA repair enzyme which shares features with proteins such as class III anaerobic ribonucleotide reductases and pyruvate-formate lyases, *Journal of Bacteriology* 180, 4879-4885.
54. Fajardo-Cavazos, P., Rebeil, R., and Nicholson, W. L. (2005) Essential cysteine residues in *Bacillus subtilis* spore photoproduct lyase identified by alanine scanning mutagenesis, *Current Microbiology* 51, 331-335.
55. Buis, J. M., Cheek, J., Kalliri, E., and Broderick, J. B. (2006) Characterization of an active spore photoproduct lyase, a DNA repair enzyme in the radical S-adenosylmethionine superfamily, *Journal of Biological Chemistry* 281, 25994-26003.
56. Silver, S. C., Chandra, T., Zilinskas, E., Ghose, S., Broderick, W. E., and Broderick, J. B. (2010) Complete stereospecific repair of a synthetic dinucleotide spore photoproduct by spore photoproduct lyase, *Journal of Biological Inorganic Chemistry* 15, 943-955.
57. Chandor, A., Douki, T., Gasparutto, D., Gambarelli, S., Sanakis, Y., Nicolet, Y., Ollagnier-de-Choudens, S., Atta, M., and Fontecave, M. (2007) Characterization of the DNA repair spore photoproduct lyase enzyme from *Clostridium acetobutylicum*: A radical-SAM enzyme, *Comptes Rendus Chimie* 10, 756-765.

58. Rebeil, R., and Nicholson, W. L. (2001) The subunit structure and catalytic mechanism of the *Bacillus subtilis* DNA repair enzyme spore photoproduct lyase, *Proceedings of the National Academy of Sciences* 98, 9038-9043.
59. Pieck, J. C., Hennecke, U., Pierik, A. J., Friedel, M. G., and Carell, T. (2006) Characterization of a new thermophilic spore photoproduct lyase from *Geobacillus stearothermophilus* (SpIG) with defined lesion containing DNA substrates, *Journal of Biological Chemistry* 281, 36317-36326.
60. Chandor, A., Berteau, O., Douki, T., Gasparutto, D., Sanakis, Y., Ollagnier-de-Choudens, S., Atta, M., and Fontecave, M. (2006) Dinucleotide spore photoproduct, a minimal substrate of the DNA repair spore photoproduct lyase enzyme from *Bacillus subtilis*, *Journal of Biological Chemistry* 281, 26922-26931.
61. Gambarelli, S., Luttringer, F., Padovani, D., Mulliez, E., and Fontecave, M. (2005) Activation of the anaerobic ribonucleotide reductase by *S*-Adenosylmethionine, *Chemistry BioChemistry* 6, 1960-1962.
62. Friedberg, E. C., and Hanawalt, P. C. (1988) DNA repair 532.
63. Branzei, D., and Foiani, M. (2005) The DNA damage response during DNA replication, *Current Opinion in Cell Biology* 17, 568-575.
64. Cox, M. M., Goodman, M. F., Kreuzer, K. N., Sherratt, D. J., Sandler, S. J., and Marians, K. J. (2000) The importance of repairing stalled replication forks, *Nature* 404, 37-41.
65. Bjedov, I., Tenaillon, O., Gérard, B., Souza, V., Denamur, E., Radman, M., Taddei, F., and Matic, I. (2003) Stress-induced mutagenesis in bacteria, *Science* 300, 1404-1409.
66. De Mott, M. S., and Dedon, P. C. (2010) Chemistry of inflammation and DNA damage: Biological impact of reactive nitrogen species, *The Chemical Biology of DNA Damage*, 423, 21-51.
67. Nohmi, T. (2006) Environmental stress and lesion-bypass DNA polymerases, *Annual Review of Microbiology* 60, 231-253.
68. Rogerio, M. (1997) Iron homeostasis, oxidative stress, and DNA damage, *Free Radical Biology and Medicine* 23, 783-792.
69. Lindahl, T., and Wood, R. D. (1999) Quality control by DNA repair, *Science* 286, 1897-1905.

70. Budzowska, M., and Kanaar, R. (2009) Mechanisms of dealing with DNA damage-induced replication problems, *Cell Biochemistry and Biophysics* 53, 17-31.
71. Eker, A., Quayle, C., Chaves, I., and van der Horst, G. (2009) DNA repair in mammalian cells, *Cellular and Molecular Life Sciences* 66, 968-980.
72. Ravanat, K. (2001) Direct and indirect effects of UV radiation, *Journal of Photochemistry and Photobiology*, 74, 231-245
73. Cadet, J., Sage, E., and Douki, T. (2005) Ultraviolet radiation-mediated damage to cellular DNA, *Mutation Research, Fundamental and Molecular Mechanisms of Mutagenesis* 571, 3-17.
74. Iwai, S. (2008) Pyrimidine Dimers: UV-Induced DNA Damage, *Modified Nucleosides*, pp 97-131.
75. Douki, T., and Cadet, J. (2001) Individual determination of the yield of the main UV-induced dimeric pyrimidine photoproducts in DNA suggests a high mutagenicity of CC photolesions, *Biochemistry* 40, 2495-2501.
76. Sancar, A. (1996) DNA excision repair, *Annual Review of Biochemistry* 65, 43-81.
77. Sancar, A. (2003) Structure and function of DNA photolyase and cryptochrome blue-light photoreceptors, *Chemical Reviews* 34, 143-169.
78. Sancar, A. (1994) Structure and function of DNA photolyase, *Biochemistry* 33, 2-9.
79. Tremblay, M., Toussaint, M., D'Amours, A., and Conconi, A. (2009) Nucleotide excision repair and photolyase repair of UV photoproducts in nucleosomes: assessing the existence of nucleosome and non-nucleosome rDNA chromatin in vivo, *Biochemistry and Cell Biology* 87, 337-346.
80. Wang, T. C., and Rupert, C. S. (1977) Transitory germinative excision repair in *Bacillus subtilis*, *Journal of Bacteriology* 129, 1313-1319.
81. Li, J., Bhat, A., and Xiao, W. (2011) Regulation of nucleotide excision repair through ubiquitination, *Acta Biochimica et Biophysica Sinica* 43, 919-929
82. Menoni, H., Shukla, M. S., Gerson, V., Dimitrov, S., and Angelov, D. (2011) Base excision repair in dinucleosomes, *Nucleic Acids Research*. 4, 203-209
83. Brettel, K., and Byrdin, M. (2010) Reaction mechanisms of DNA photolyase, *Current Opinion in Structural Biology* 20, 693-701.

- 84.Sancar, A. (2008) Structure and function of photolyase and in-vivo enzymology, *Journal of Biological Chemistry* 283, 32153-32157.
- 85.Eker, A. P. M., Dekker, R. H., and Berends, W. (1981) Photoreactivating enzyme from *Streptomyces grieseus*. On the nature of the chromomophore cofactor in streptomyces grieseus photoreactivating enzymes, *Photochemistry and Photobiology* 33, 65-72.
- 86.Eker, A. P. M., Hessels, J. K. C., and van de Velde, J. (1988) Photoreactivating enzyme from the green alga *Scenedesmus acutus*. Evidence for the presence of two different flavin chromophores, *Biochemistry* 27, 1758-1765.
- 87.Jorns, M. S., Sancar, G. B., and Sancar, A. (1984) Identification of a neutral flavin radical and characterization of a second chromophore in *Escherichia coli* DNA photolyase, *Biochemistry* 23, 2673-2679.
- 88.Donnellan, J. E., and Setlow, R. B. (1965) Thymine photoproducts but not thymine dimers found in ultraviolet-irradiated bacterial spores, *Science* 149, 308-310.
- 89.Setlow, P. (2001) Resistance of spores of *Bacillus* species to ultraviolet light, *Environmental and Molecular Mutagenesis* 38, 97-104.
- 90.Setlow, P. (2007) I will survive: DNA protection in bacterial spores, *Trends In Microbiol* 15, 172-180.
- 91.Magill, N. G., Loshon, C. A., and Setlow, P. (1990) Small, acid-soluble, spore proteins and their genes from two species of *Sporosarcina*, *FEMS Microbiology Letters* 72, 293-297.
- 92.Mason, J. M., and Setlow, P. (1986) Essential role of small, acid-soluble spore proteins in resistance of *Bacillus subtilis* spores to UV light, *Journal of Bacteriology* 167, 174-178.
- 93.Moeller, R., Setlow, P., Reitz, G., and Nicholson, W. L. (2009) Roles of small, acid-soluble spore proteins and core water content in survival of *Bacillus subtilis* spores exposed to environmental solar UV radiation, *Applied Environmental Microbiology* 75, 5202-5208.
- 94.Lee, K. S., Bumbaca, D., Kosman, J., Setlow, P., and Jedrzejewski, M. J. (2008) Structure of a protein-DNA complex essential for DNA protection in spores of *Bacillus* species, *Proceedings of the National Academy of Sciences* 105, 2806-2811.

95. Mohr, S. C., Sokolov, N. V., He, C. M., and Setlow, P. (1991) Binding of small acid-soluble spore proteins from *Bacillus subtilis* changes the conformation of DNA from B to A, *Proceedings of the National Academy of Sciences* 88, 77-81.
96. Fairhead, H., Setlow, B., and Setlow, P. (1993) Prevention of DNA damage in spores and in vitro by small, acid-soluble proteins from *Bacillus* species, *Journal of Bacteriology* 175, 1367-1374.
97. Setlow, P. (1988) Small, Acid-Soluble Spore Proteins of *Bacillus* Species: Structure, synthesis, genetics, function, and degradation, *Annual Review of Microbiology* 42, 319-338.
98. Tovar-Rojo, F., and Setlow, P. (1991) Effects of mutant small, acid-soluble spore proteins from *Bacillus subtilis* on DNA in vivo and in vitro, *Journal of Bacteriology* 173, 4827-4835.
99. Nicholson, W. L., Setlow, B., and Setlow, P. (1991) Ultraviolet irradiation of DNA complexed with alpha/beta-type small, acid-soluble proteins from spores of *Bacillus* or *Clostridium* species makes spore photoproduct but not thymine dimers, *Proceedings of the National Academy of Sciences* 88, 8288-8292.
100. Jones, S., van Heyningen, P., Berman, H. M., and Thornton, J. M. (1999) Protein-DNA interactions: A structural analysis, *Journal of Molecular Biology* 287, 877-896.
101. Kundu, L. M., Linne, U., Marahiel, M., and Carell, T. (2004) RNA is more UV resistant than DNA: The formation of UV-induced DNA lesions is strongly sequence and conformation dependent, *Chemistry – A European Journal* 10, 5697-5705.
102. Griffith, J., Makhov, A., Santiago-Lara, L., and Setlow, P. (1994) Electron microscopic studies of the interaction between a *Bacillus subtilis* alpha/beta-type small, acid-soluble spore protein with DNA: Protein binding is cooperative, stiffens the DNA, and induces negative supercoiling, *Proceedings of the National Academy of Sciences* 91, 8224-8228.
103. Setlow, B., and Setlow, P. (1987) Thymine-containing dimers as well as spore photoproducts are found in ultraviolet-irradiated *Bacillus subtilis* spores that lack small acid-soluble proteins, *Proceedings of the National Academy of Sciences* 84, 421-423.
104. Fairhead, H., Setlow, B., Waites, W. M., and Setlow, P. (1994) Small, acid-soluble proteins bound to DNA protect *Bacillus subtilis* spores from being killed by freeze-drying, *Applied Environmental Microbiology* 60, 2647-2649.

105. Setlow, B., and Setlow, P. (1993) Binding of small, acid-soluble spore proteins to DNA plays a significant role in the resistance of *Bacillus subtilis* spores to hydrogen peroxide, *Applied Environmental Microbiology* 59, 3418-3423.
106. Varghese, A. J. (1970) 5-Thyminy-5,6-dihydrothymine from DNA irradiated with ultraviolet light, *Biochemical and Biophysical Research Communications* 38, 484-490.
107. Lin, G., and Li, L. (2010) Elucidation of spore-photoproduct formation by isotope labeling, *Angew Chemical International Edition English* 49, 9926-9929.
108. Fairhead, H., and Setlow, P. (1992) Binding of DNA to alpha/beta-type small, acid-soluble proteins from spores of *Bacillus* or *Clostridium* species prevents formation of cytosine dimers, cytosine-thymine dimers, and bipyrimidine photoadducts after UV irradiation, *Journal of Bacteriology* 174, 2874-2880.
109. Fajardo-Cavazos, P., Salazar, C., and Nicholson, W. L. (1993) Molecular cloning and characterization of the *Bacillus subtilis* spore photoproduct lyase (spl) gene, which is involved in repair of UV radiation-induced DNA damage during spore germination, *Journal of Bacteriology* 175, 1735-1744.
110. Slieman, T. A., Rebeil, R., and Nicholson, W. L. Spore photoproduct (SP) lyase from *Bacillus subtilis* specifically binds to and cleaves SP (5-Thyminy-5,6-Dihydrothymine) but not cyclobutane pyrimidine dimers in UV-irradiated DNA, *American Society for Microbiology*. 571, 249-246.
111. Kim, S. J., Lester, C., and Begley, T. P. (1995) Synthesis of the dinucleotide spore photoproduct, *The Journal of Organic Chemistry* 60, 6256-6257.
112. Nicewonger, R., and Begley, T. P. (1997) Synthesis of the spore photoproduct, *Tetrahedron Letters* 38, 935-936.
113. Friedel, M. G., Berteau, O., Pieck, J. C., Atta, M., Ollagnier-de-Choudens, S., Fontecave, M., and Carell, T. (2006) The spore photoproduct lyase repairs the 5*S*- and not the 5*R*-configured spore photoproduct DNA lesion, *Chemical Communications* 4, 445-447.
114. Chandra, T., Silver, S. C., Zilinskas, E., Shepard, E. M., Broderick, W. E., and Broderick, J. B. (2009) Spore photoproduct lyase catalyzes specific repair of the 5*R* but not the 5*S* spore photoproduct, *Journal of the American Chemical Society* 131, 2420-2421.
115. Heil, K., Kneutinger, A. C., Schneider, S., Lischke, U., and Carell, T. (2011) crystal structures and repair studies reveal the identity and the base-pairing properties of the UV-

- induced spore photoproduct DNA lesion, *Chemistry – A European Journal* 17, 9651-9657.
116. Lin, G., Chen, C.-H., Pink, M., Pu, J., and Li, L. (2011) Chemical synthesis, crystal structure and enzymatic evaluation of a dinucleotide spore photoproduct analogue containing a formacetal linker, *Chemistry – A European Journal* 17, 9658-9668.
117. Mehl, R. A., and Begley, T. P. (1999) Mechanistic studies on the repair of a novel DNA photolesion: The spore photoproduct, *Organic Letters* 1, 1065-1066.
118. Yang, L., Lin, G., Liu, D., Dria, K. J., Telser, J., and Li, L. (2011) Probing the reaction mechanism of spore photoproduct lyase (SPL) via diastereoselectively labeled dinucleotide SP TpT substrates, *Journal of the American Chemical Society* 133, 10434-10447.
119. Chandor-Proust, A., Berteau, O., Douki, T., Gasparutto, D., Ollagnier-de-Choudens, S., Fontecave, M., and Atta, M. (2008) DNA repair and free radicals, new insights into the mechanism of spore photoproduct lyase revealed by single amino acid substitution, *Journal of Biological Chemistry* 283, 36361-36368.
120. Cadet, J., Anselmino, C., Douki, T., and Voituriez, L. (1992) New trends in photobiology: Photochemistry of nucleic acids in cells, *Journal of Photochemistry and Photobiology* 15, 277-298.
121. Douki, T., and Cadet, J. (2003) Formation of the spore photoproduct and other dimeric lesions between adjacent pyrimidines in UVC-irradiated dry DNA, *Photochemical & Photobiological Sciences* 2, 433-436.
122. Butenandt, J., Burgdorf, L. T., and Carell, T. (1999) Synthesis of DNA lesions and DNA-lesion-containing oligonucleotides for DNA-repair studies, *Synthesis* 5, 1085-1105.
123. Burckstummer, E., and Carell, T. (2008) Synthesis and properties of DNA containing a spore photoproduct analog, *Chemical Communications*.12, 4037-4039.
124. Mantel, C., Chandor, A., Gasparutto, D., Douki, T., Atta, M., Fontecave, M., Bayle, P.-A., Mouesca, J.-M., and Bardet, M. (2008) Combined NMR and DFT studies for the absolute configuration elucidation of the spore photoproduct, a UV-induced DNA lesion, *Journal of the American Chemical Society* 130, 16978-16984.
125. Husain, I., Sancar, G. B., Holbrook, S. R., and Sancar, A. (1987) Mechanism of damage recognition by *Escherichia coli* DNA photolyase, *Journal of Biological Chemistry* 262, 13188-13197.

126. Mees, A., Klar, T., Gnau, P., Hennecke, U., Eker, A. P. M., Carell, T., and Essen, L.-O. (2004) Crystal structure of a photolyase bound to a CPD-like DNA lesion after in situ repair, *Science* 306, 1789-1793.
127. Wei, Y. (2006) Poor base stacking at DNA lesions may initiate recognition by many repair proteins, *DNA Repair* 5, 654-666.
128. Benjdia, A., Heil, K., Barends, T. R. M., Carell, T., and Schlichting, I. (2012) Structural insights into recognition and repair of UV-DNA damage by Spore Photoproduct Lyase, a radical SAM enzyme, *Nucleic Acids Research* 18, 9308-9318
129. Slupphaug, G., Mol, C. D., Kavli, B., Arvai, A. S., Krokan, H. E., and Tainer, J. A. (1996) A nucleotide-flipping mechanism from the structure of human uracil-DNA glycosylase bound to DNA, *Nature* 384, 87-92.
130. McCullough, A. K., Dodson, M. L., Schärer, O. D., and Lloyd, R. S. (1997) The role of base flipping in damage recognition and catalysis by T4 endonuclease V, *Journal of Biological Chemistry* 272, 27210-27217.
131. Lawrence, C. C., and Stubbe, J. (1998) The function of adenosylcobalamin in the mechanism of ribonucleoside triphosphate reductase from *Lactobacillus leichmannii*, *Current Opinion in Chemical Biology* 2, 650-655.
132. Vignais, P. M., Billoud, B., and Meyer, J. (2001) Classification and phylogeny of hydrogenases, *FEMS Microbiology Reviews* 25, 455-501.
133. Peters, J. W., Lanzilotta, W. N., Lemon, B. J., and Seefeldt, L. C. (1998) X-ray crystal structure of the Fe-only hydrogenase (CpI) from *Clostridium pasteurianum* to 1.8 angstrom resolution, *Science* 282, 1853-1858.
134. Shepard, E. M., Boyd, E. S., Broderick, J. B., and Peters, J. W. (2011) Biosynthesis of complex iron-sulfur enzymes, *Current Opinion in Chemical Biology* 15, 319-327.
135. Nicolet, Y., Lemon, B. J., Fontecilla-Camps, J. C., and Peters, J. W. (2000) A novel FeS cluster in Fe-only hydrogenases, *Trends in Biochemical Sciences* 25, 138-143.
136. Mulder, David W., Shepard, Eric M., Meuser, Jonathan E., Joshi, N., King, Paul W., Posewitz, Matthew C., Broderick, Joan B., and Peters, John W. (2011) Insights into [FeFe] hydrogenase structure, mechanism, and maturation, *Structure* 19, 1038-1052.
137. Silakov, A., Wenk, B., Reijerse, E., and Lubitz, W. (2009) 14N HYSORE investigation of the H-cluster of [FeFe] hydrogenase: Evidence for a nitrogen in the dithiol bridge, *Physical Chemistry Chemical Physics* 11, 6592-6599.

138. Pandey, A. S., Harris, T. V., Giles, L. J., Peters, J. W., and Szilagy, R. K. (2008) Dithiomethylether as a ligand in the hydrogenase H-cluster, *Journal of the American Chemical Society* 130, 4533-4540.
139. Ryde, U., Greco, C., and De Gioia, L. (2010) Quantum refinement of [FeFe] hydrogenase indicates a dithiomethylamine ligand, *Journal of the American Chemical Society* 132, 4512-4513.
140. Mulder, D. W., Boyd, E. S., Sarma, R., Lange, R. K., Endrizzi, J. A., Broderick, J. B., and Peters, J. W. (2010) Stepwise [FeFe] hydrogenase H-cluster assembly revealed in the structure of HydA^{ΔEFG}, *Nature* 465, 248-251.
141. McGlynn, S., Ruebush, S., Naumov, A., Nagy, L., Dubini, A., King, P., Broderick, J., Posewitz, M., and Peters, J. (2007) In vitro activation of [FeFe] hydrogenase: New insights into hydrogenase maturation, *Journal of Biological Inorganic Chemistry* 12, 443-447.
142. McGlynn, S. E., Mulder, D. W., Shepard, E. M., Broderick, J. B., and Peters, J. W. (2009). Hydrogenase cluster biosynthesis: Organometallic chemistry nature's way, *Dalton Transactions* 22, 4274-4285.
143. Posewitz, M. C., King, P. W., Smolinski, S. L., Zhang, L., Seibert, M., and Ghirardi, M. L. (2004) Discovery of two novel radical S-Adenosylmethionine proteins required for the assembly of an active [Fe] hydrogenase, *Journal of Biological Chemistry* 279, 25711-25720.
144. Meyer, J. (2007) [FeFe] hydrogenases and their evolution: A genomic perspective, *Cellular and Molecular Life Sciences* 64, 1063-1084.
145. King, P. W., Posewitz, M. C., Ghirardi, M. L., and Seibert, M. (2006) Functional studies of [FeFe] hydrogenase maturation in an *Escherichia coli* biosynthetic system, *Journal of Bacteriology* 188, 2163-2172.
146. Peters, J. W., Szilagy, R. K., Naumov, A., and Douglas, T. (2006) A radical solution for the biosynthesis of the H-cluster of hydrogenase, *FEBS Letters* 580, 363-367.
147. McGlynn, S. E., Shepard, E. M., Winslow, M. A., Naumov, A. V., Duschene, K. S., Posewitz, M. C., Broderick, W. E., Broderick, J. B., and Peters, J. W. (2008) HydF as a scaffold protein in [FeFe] hydrogenase H-cluster biosynthesis, *FEBS Letters* 582, 2183-2187.
148. Shepard, E. M., McGlynn, S. E., Bueling, A. L., Grady-Smith, C., George, S. J., Winslow, M. A., Cramer, S. P., Peters, J. W., and Broderick, J. B. (2010) Synthesis of the

2Fe-subcluster of the [FeFe]-hydrogenase H-cluster on the HydF scaffold, Proceedings of the National Academy of Sciences 107, 10448-10453.

149.Czech, I., Silakov, A., Lubitz, W., and Happe, T. (2010) The [FeFe]-hydrogenase maturase HydF from *Clostridium acetobutylicum* contains a CO and CN⁻ ligated iron cofactor, FEBS Letters 584, 638-642.

150.Pilet, E., Nicolet, Y., Mathevon, C., Douki, T., Fontecilla-Camps, J. C., and Fontecave, M. (2009) The role of the maturase HydG in [FeFe]-hydrogenase active site synthesis and assembly, FEBS Letters. 583, 506-511.

151.Driesener, R. C., Challand, M. R., McGlynn, S. E., Shepard, E. M., Boyd, E. S., Broderick, J. B., Peters, J. W., and Roach, P. L. (2010) [FeFe] hydrogenase cyanide ligands derived from *S*-adenosylmethionine-dependent cleavage of tyrosine, *Angewandte Chemie International Edition* 49, 1687-1690.

152.Shepard, E. M., Duffus, B. R., George, S. J., McGlynn, S. E., Challand, M. R., Swanson, K. D., Roach, P. L., Cramer, S. P., Peters, J. W., and Broderick, J. B. (2010) [FeFe] hydrogenase maturation: HydG-catalyzed synthesis of carbon monoxide, *Journal of the American Chemical Society* 132, 9247-9249.

153.Tron, C., Cherrier, M. V., Amara, P., Martin, L., Fauth, F., Fraga, E., Correard, M., Fontecave, M., Nicolet, Y., and Fontecilla-Camps, J. C. (2011) Further characterization of the [FeFe] hydrogenase maturase HydG, *European Journal of Inorganic Chemistry* 2011, 1121-1127.

154.Kuchenreuther, J. M., George, S. J., Grady-Smith, C. S., Cramer, S. P., and Swartz, J. R. (2011) Cell-free H-cluster synthesis and [FeFe] hydrogenase activation: All Five CO and CN⁻ ligands derive from tyrosine, *PLoS ONE* 6, e20346.

155.Joshi, N., Shepard, E. M., Byer, A. S., Swanson, K. D., Broderick, J. B., and Peters, J. W. (2012) Iron-sulfur cluster coordination in the [FeFe]-hydrogenase H cluster biosynthetic factor HydF, FEBS Letters 22, 3939-3943

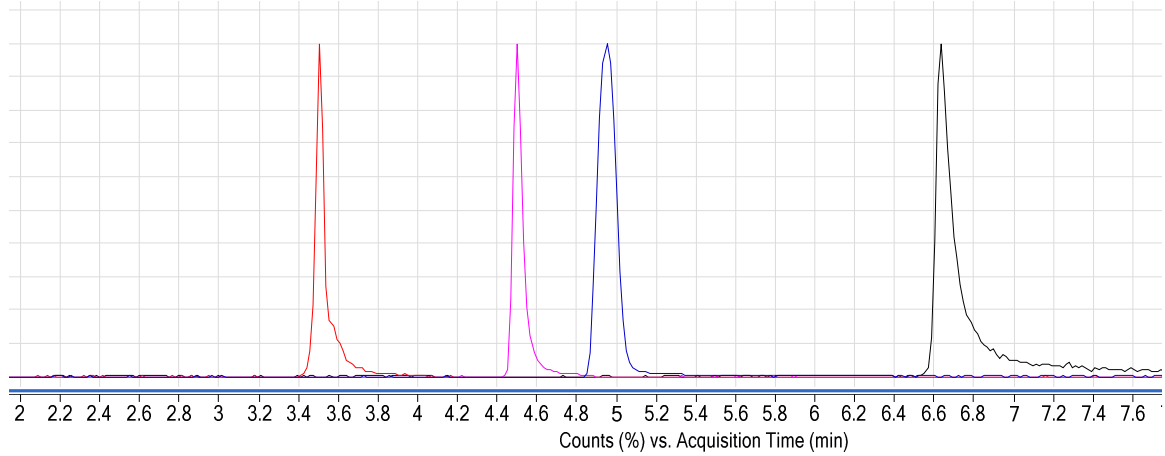
156.Nicolet, Y., Rubach, J. K., Posewitz, M. C., Amara, P., Mathevon, C., Atta, M., Fontecave, M., and Fontecilla-Camps, J. C. (2008) X-ray structure of the [FeFe] hydrogenase maturase HydE from *Thermotoga maritima*, *Journal of Biological Chemistry* 283, 18861-18872.

157.Rubach, J. K., Brazzolotto, X., Gaillard, J., and Fontecave, M. (2005) Biochemical characterization of the HydE and HydG iron-only hydrogenase maturation enzymes from *Thermotoga maritima*, FEBS Letters 579, 5055-5060.

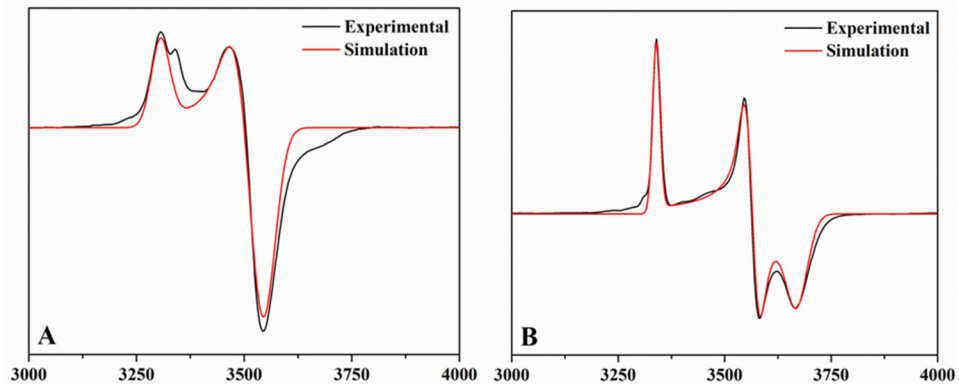
158. Jameson, G. N., Coper, M. M., Hernández, H. L., Johnson, M. K., and Huynh, B. H. (2004) Role of the [2Fe-2S] cluster in recombinant *Escherichia coli* biotin synthase, *Biochemistry* 43, 2022-2031.
159. Kuchenreuther, J. M., Britt, R. D., and Swartz, J. R. (2012) New insights into [FeFe] hydrogenase activation and maturase function, *PLoS ONE* 7, e45850.
160. Kuchenreuther, J. M., Stapleton, J. A., and Swartz, J. R. (2009) tyrosine, cysteine, and *S*-adenosyl methionine stimulate in vitro [FeFe] hydrogenase activation, *PLoS ONE* 4, e7565.
161. Boswell, N.W.B. (2011) Montana State University Bozeman.

APPENDIX A

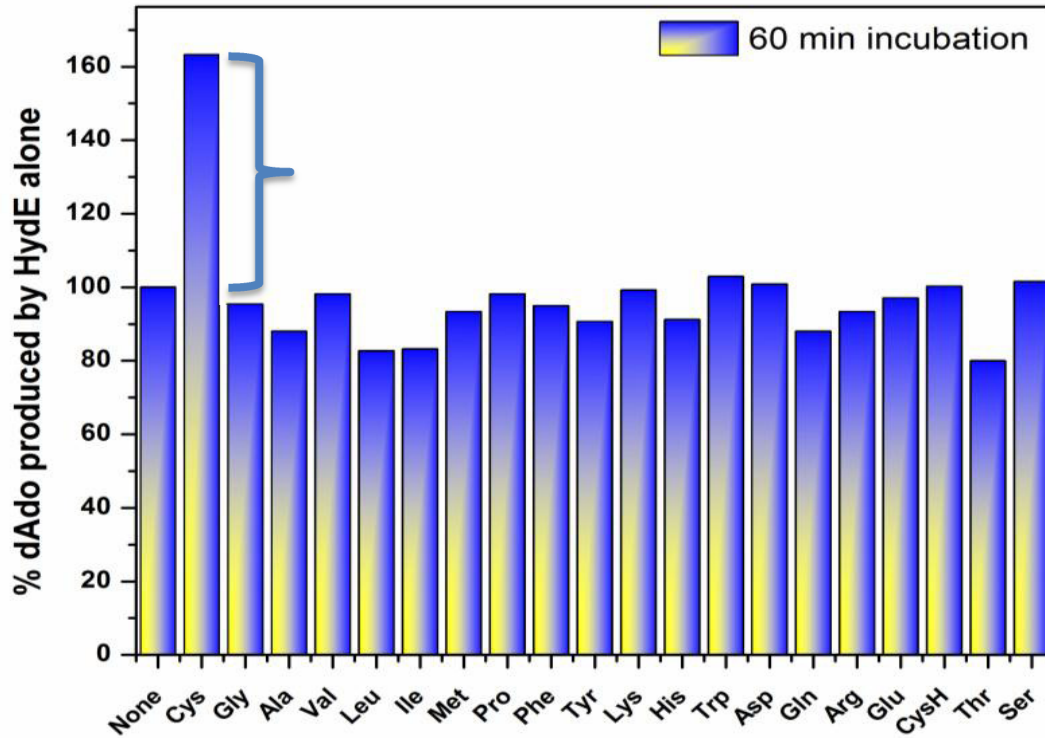
SUPPLEMENTAL INFORMATION FOR CHAPTER 3



Supplement 1: The figure illustrates the chromatographic separation of the primary components in the assay mixture. 5'-deoxyadenosine is the least retained at 4.0min followed by cysteine at 4.6min. The buffer component HEPES elutes at 5.0min followed by the reaction co-factor SAM at 6.7min.



Supplement 2: The figure illustrates the EPR simulation and experimental spectra indicating the presence of SAM in the reconstituted HydE



Supplement 3: The figure illustrates the 5'-dAdo production as a response to incubation with different amino acids and small molecules. The stimulatory effects on SAM cleavage as a response to cysteine is clearly visible resulting in a 50% increase in the rate of SAM cleavage. (This figure is taken from reference 39 in chapter 3)